University of Alberta

Activation of Delayed and Fluid Petroleum Coke for the Adsorption and Removal of Naphthenic Acids from Oil Sands Tailings Pond Water

by

Christina Caroline Small

A thesis submitted to the Faculty of Graduate Studies and Research
in partial fulfillment of the requirements for the degree of

Master of Science
in
Geoenvironmental Engineering

Civil and Environmental Engineering

Spring 2011
Edmonton, Alberta

Examining Committee

Dr. Zaher Hashisho, Department of Civil and Environmental Engineering

Dr. Selma Guigard, Department of Civil and Environmental Engineering

Dr. Natalia Semagina, Department of Chemical and Materials Engineering

Dedication

I would like to dedicate this thesis to my family. Thank you for supporting my move across the country in order for me to further my education.

ABSTRACT

Oil sands companies produce substantial quantities of tailings known to contain high concentrations of dissolved organic by-products. The use of petroleum coke was proposed as a potential adsorbent for organic contaminant removal from tailings pond water. Physical activation was used to create a greater surface area and porosity within the delayed and fluid coke. Increased temperature (900^{o}C), steam rate (0.5 mL/min), and activated time (6 h) led to high iodine numbers of 670 and 620 mg/g for activated delayed and fluid cokes, respectively. For both best activated cokes, the micropore to mesopore ratio was approximately 50:50. When 5 g/L of activated delayed and fluid cokes were added to the tailings water, 91% of the dissolved organic carbon and 92% of the naphthenic acids were removed. Such analyses indicate that an oil sands waste by-product can be used to treat tailings pond water to remove toxic and corrosive organic contaminants.

Acknowledgements

Firstly, I would like to express my deepest gratitude to my two supervisors Dr. Zaher Hashisho and Dr. Ania C. Ulrich for their consistent guidance and unwavering support throughout my course work and research. To this day they continue to challenge me and introduce me to new academic and research experiences, which has been crucial to my development within the engineering field. Their expertise and knowledge was essential for the accomplishment of this work. It has been a privilege to have worked with you both.

I would also like to acknowledge financial support from the Natural Science and Engineering Research Council (NSERC), and Suncor Energy Inc. for the industrial scholarship that supported me throughout my studies. I would like to thank the Oil Sands Tailings Research Facility (OSTRF) for their funding, support, and resources available during my research.

I would also like to thank Suncor Energy Inc. and Syncrude Canada Ltd. for providing process-affected water as well as delayed and fluid coke samples. These materials were essential for the study.

I extend my appreciation to the technicians within the Civil and Environmental Engineering Department at the University of Alberta: Jela Burkus, Maria Demeter, and Steve Gamble. Their assistance, advice, suggestions, availability, and support aided the success of my many experiments.

Finally I would like to thank the National Institute for Nanotechnology (NINT) for allowing me access to various instruments necessary for my characterization experiments.

Table of Contents

List of Tables

List of Figures

List of Abbreviations and Nomenclature

Al	Aluminum
BET	Brunauer, Emmett, and Teller Theory
Br	Bromide
BTEX	Benzene, toluene, ethylbenzene, and xylene
Ca	Calcium
$CaCO_3$	Calcium Carbonate
CH_4	Methane Gas
Cl^-	Chloride
CO_2	Carbon Dioxide Gas
CO	Carbon Monoxide Gas
COD	Chemical Oxygen Demand
Cu	Copper
DOC	Dissolved Organic Carbon
EC_{20}	Effective Concentration, 20%
F	Fluoride
FTIR	Fourier Transform Infrared
GAC	Granular Activated Carbon
HCl	Hydrochloric Acid
H_3PO_4	Phosphoric Acid
H_2SO_4	Sulphuric Acid
K_2CO_3	Potassium Carbonate
KOH	Potassium Hydroxide
K_2S	Potassium Sulphide
Li	Lithium
Mg	Magnesium
Mn	Manganese
Mo	Molybdenum
N_2	Nitrogen Gas
NAs	Naphthenic Acids
Na	Sodium

NaOH	Sodium Hydroxide
NH_4^+	Ammonium
Ni	Nickel
O_2	Oxygen Gas
OD	Outside Diameter
OSNAs	Oil Sands Naphthenic Acids
P/ P_o	Equilibrium Pressure/ Saturation Pressure
PA	Process-Affected
Pb	Lead
PO_4^{3-}	Phosphate
SEM	Scanning Electron Micrograph
SO_4^{2-}	Sulphate
TGA	Thermogravimetric Analysis
TOC	Total Organic Carbon
V	Vanadium
$ZnCl_2$	Zinc Chloride

CHAPTER 1: INTRODUCTION

1.1 Introduction

1.1.1 The Oil Sands Industry

The oils sands industry in north-eastern Alberta, Canada resides in Fort McMurray, where companies (such as Syncrude Canada Ltd. and Suncor Energy Inc.), cumulatively produce over 1.1 million barrels of synthetic crude oil per day (Paslawski et al., 2009). The extraction and upgrading of bitumen (an unconventional fossil fuel) requires a large quantity of water, resulting in a sizable amount of wet waste. Currently, there is more than 4×10^8 m^3 of slurry waste (composed of sand, fine clays, water, bitumen, and inorganic and organic compounds) stored in tailings ponds throughout the Athabasca oil sands region (Paslawski et al., 2009). This large volume of waste presents an issue for land reclamation and environmental protection.

During bitumen upgrading (occurring after the separation and extraction procedures), a petroleum coke by-product is generated through either delayed or fluid coking processes (Furimsky, 1998). Over 5 million tonnes of delayed and fluid petroleum coke is cumulatively generated per year between Syncrude Canada Ltd. and Suncor Energy Inc. (Fedorak and Coy, 2006). Approximately two thirds of the petroleum coke produced throughout the region is stockpiled and stored on-site (Etsell and Jang, 2006; Ityokumbul, 1994). Due to the minimal use and understanding of the material, it is considered to be a waste by-product requiring proper disposal to minimize potential environmental impacts.

Another by-product of the bitumen extraction and refining processes are organic acids, where 80% of the organic acids are composed of oil sands naphthenic acids, which become concentrated within the recycled process water (Allen, 2008). Naphthenic acids naturally reside within ores (originating from depositional and post-depositional environments), and are released during the oil sands extraction processes due to digestion with water under alkaline pHs (Clemente et al., 2003). Naphthenic acids represent a group of organic acids with differing structural chemical compositions. The generalized empirical structure is as follows: $C_nH_{2n+z}O_2$, incorporating differing degrees of saturation and aromaticity (typically containing carboxylic acids and nitrogen and sulphur components) (Mohamed et al., 2008). Due to the range of variability among oil sands naphthenic acids, they have yet to be successfully classified individually. These oil sands naphthenic acids have been found to be one of the main contributors of acute toxicity within the tailings pond water, even at low concentrations (Allen, 2008). As the concentration of the naphthenic acids increase within the process water, the future water re-use may become inhibited due to the nature of the contaminants. More specifically, the naturally occurring naphthenic acids do not readily breakdown and their corrosive and accumulative nature may decrease the efficiency of oil production and refining (Mohamed et al., 2008; Meredith et al., 2000).

As the oil sands mining operations expand throughout western Canada, the amount of dry and wet wastes (including petroleum coke and the naphthenic acid organic fraction) will develop as well. Consequently, an understanding of the characteristics and nature of the wastes may allow for the potential recycling of process-water while providing a necessary means of use for the delayed and fluid petroleum cokes.

1.1.2 Adsorption by Carbonaceous Media

Granular activated carbon (GAC) is a well-known material used for the adsorption of organics. The carbonaceous substances used are typically made from wood, coal, lignin, coconut shells, and sugar; once activated, these materials reveal high surface areas and an array of functional groups (Karanfil and Kilduff, 1999). The high surface area allows for the increased efficiency of adsorption, and the particular functional groups permit the attraction of organic material (including organic acids). Once activated, the unpaired electrons on the surfaces and edges of the GAC alter the polarity and surface acidity of the structure, allowing for hydrophobic interactions with the organic substances (Karanfil and Kilduff, 1999). This leads to the solubility of the organic material, permitting the adsorption and removal of particular organics from the solution of interest (Karanfil et al., 1996). This process is ideal for the remediation of contaminated industrial wastewater, due to the production of less toxic by-products. Current research has demonstrated that GAC has the capacity to adsorb naphthenic acids produced in the oil sands industry, as seen through the use of fluorescence spectrophotometry (Mohamed et al., 2008).

The petroleum coke by-product produced by the oil sands industry may be an effective alternative to GAC in the adsorption of organic acids; more specifically, oil sands naphthenic acids. Once activated, this available waste by-product (mainly composed of carbon) may have high adsorptive capacities, ten times higher than that of petroleum coke in raw form (Shawwa et al., 2001). This indicates that the oil sands coke can be used for adsorption purposes in both its raw and activated form.

The full potential of the adsorption of naphthenic acids onto oil sands delayed and fluid coke has yet to be demonstrated. Due to the differing mining, processing and upgrading techniques used throughout the Athabasca oil sands region, it can be expected that the delayed and fluid petroleum coke by-products differ in nature. As a result, further understanding of the structural and behavioural characteristics of the cokes is necessary in order to determine the potential adsorption capacity of the oil sands naphthenic acids.

1.2 Research Objectives

The goal of the research is to observe whether activated delayed and fluid petroleum coke have the ability to adsorb organics (more specifically, oil sands naphthenic acids) within process-affected mine tailings water. This will be investigated through the use of the delayed and fluid cokes both as is and activated. In doing so, the following objectives can be described:

1. Characterization of the structural properties of raw and activated delayed and fluid coke
2. Characterization of the adsorption capacity of organic acids onto raw and activated delayed and fluid coke
3. Characterization of the leaching potential of metals and inorganic by-products from raw and activated delayed and fluid coke

These objectives will be explored through the use of 24 h batch tests on the process-affected water after interacting with raw and activated delayed and fluid coke. Petroleum coke structural and behavioural characterization will be explored through the use of thermogravimetric analysis (TGA), X-ray diffraction (XRD), iodine and methylene blue adsorption, N_2 adsorption isotherms, and scanning electron micrographs (SEMs). Leaching potential and adsorption capacity of inorganic and organic by-products will be observed through the following tests and procedures: pH, electrical conductivity (EC), total alkalinity, ion chromatography (IC), inductively coupled plasma mass spectrometry (ICPMS), dissolved organic carbon (DOC) content, fluorescence spectrometry, and Fourier transform infra-red spectrometry (FT-IR). Microtox^{TM} toxicity tests will provide a bigger picture understanding of the competing inorganic and organic adsorption processes relating their affects to water quality.

This research is significant because it will utilize the readily available petroleum coke waste by-product to physically treat the contaminated tailings pond water. The removal of corrosive organic by-products will allow for an extended use of the recycled water, reducing the need for imported fresh water sources. The elimination of toxic naphthenic acids will aid in the efficient remediation of the tailings ponds during mine closure, permitting the addition of aquatic life. Overall, this treatment technology will assist in sustainable development within the Athabasca region.

1.3 Thesis Outline

This thesis consists of five chapters, each of which will contribute to the overall main objectives of the research. An overall general theoretical review of the field of study and research conducted in this area completed thus far is presented in chapter 2. Chapter 3 concentrates on the activation and characterization of the delayed and fluid petroleum coke. The leaching potential and adsorption capacity are addressed in chapter 4. Chapter 5 will present the final conclusions as well as the engineering significance of the adsorption of naphthenic acids to the oil sands coke.

1.4 Chapter 1 References

Allen, E.W. 2008. Process water treatment in Canada's oil sands industry: 1. target pollutants and treatment objectives. *Journal of Environmental Engineering and Science*; 7: 123-138.

Clemente, J.S, Prasad, N.G.N., MacKinnon, M.D., and Fedorak, P.M. 2003. A statistical comparison of naphthenic acids characterized by gas chromatography-mass spectrometry. *Chemosphere*; 50:1265-1274.

Etsell, T.H., and Jang, H. 2006. Mineralogy and phase transition of oil sands coke ash. *Fuel*; 85: 1526-1534.

Fedorak, P.M., and Coy, D.L. 2006. Oil sands cokes affect microbial activities. *Fuel*; 85: 1642-1651.

Furimsky, E. 1998. Gasification of oil sand coke: review. *Fuel Processing Technology*; 56: 263- 290.

Ityokumbul, M.T. 1994. Experimental evaluation of molten caustic leaching of an oil sand coke residue. *The Canadian Journal of Chemical Engineering*; 72: 370-374.

Karanfil, T., and Kilduff, J.E. 1999. Role of granular activated carbon surface chemistry on the adsorption of organic compounds. 1. Priority pollutants. *Environmental Science and Technology*; 33: 3217-3224.

Karanfil, T., Kilduff, J.E., Schlautman, M.A., and Weber, W.J. 1996. Adsorption of organic macromolecules by granular activated carbon. 1. Influence of molecular properties under anoxic solution conditions. *Environmental Science and Technology*; 30: 2187-2194.

Meredith, W., Kelland, S.J., and Hones, D.M. 2000. Influence of biodegradation on crude oil acidity and carboxylic acid composition. *Organic Geochemistry*; 31: 1059-1073.

Mohamed, M.H., Wilson, L.D., Headley, J.V., and Peru, K.M. 2008. Screening of oil sands naphthenic acids by UV- VIS adsorption and fluorescence emission spectrophotometry. *Journal of Environmental Science and Health Part A*; 43: 1700- 1705.

Paslawski, J.C., Headley, J.V., Hill, G.A., and Nemati, M. 2009. Biodegradation kinetics of trans-4-methyl-1-cyclohexane carboxylic acid. *Biodegradation*; 20: 125-133.

Shawwa, A.R., and Smith, D.W., and Sego, D.C. 2001. Color and chlorinated organics removal from pulp mills wastewater using activated petroleum coke. *Water Resources*; 35: 745-749.

CHAPTER 2: THEORETICAL BACKGROUND AND LITERATURE REVIEW

2.1 Theoretical Background

2.1.1 Adsorption

The forces of attraction, physical in nature, produce an interaction among ions and compounds leading to the process of adsorption (Gregg and Sing, 1982). More specifically, van der Walls forces (fluctuating attractive and repulsive forces) are responsible for the weakly held bonds or electrostatic interactions that result in the physical 'sticking' (or adsorption) of components. Materials capable of being adsorbed are termed adsorbates; whereas an adsorbent refers to a solid capable of performing adsorption. Molecules and atoms can be fixed through the formation of weak bonds forming on the surfaces and edges of an adsorbent (Martin-Gullón and Menéndez-Diaz, 2006). Physisorption occurs whenever an adsorbate is brought in contact with the surface of an adsorbate, leading to the enrichment of the material (Sing et al., 1985). These forces and reactions lead to a change in equilibrium of a surrounding system. The following Equation (2-1) expresses the relationship between adsorption and desorption for an adsorbate-adsorbent system:

$$X + M_{Surface} \leftrightarrow XM_{Surface} \quad \text{(Kim and Sohn, 2005)} \qquad \textbf{(2-1)}$$

2.1.1.1 Energy and Surface Area

The enthalpy (ΔH) of adsorption is dependent upon the following conditions: the surface area available for adsorption; the nature of the adsorbate and adsorbent; the surface reactivity; and, the temperature and pressure occurring at the time of adsorption (Bansal and Goyal, 2005). If there are vacant sites on the adsorbent and the rate of contact between the adsorbent and adsorbate is high; adsorption will occur. In contrast, desorption will occur if there is sufficient energy for the adsorbate to form an alternative bond within a system. This energy represents the internal heat of the system required for adsorption/ or desorption to occur between particles. The change in energy is due to the change in state created by the addition of the adsorbate (Gregg and Sing, 1982). The reverse applies under the specific conditions allowing for desorption of an adsorbate on the surface of the adsorbent. The exothermic process of adsorption can be described by the Equation (2-2) (where T represents the temperature in the system); the result is a negative change in free energy (ΔG) and a decrease in entropy (ΔS) (Mark and Mattson, 1971).

$$\Delta H = \Delta G + T\Delta S \qquad \textbf{(2-2)}$$

The potential energy between two atoms is a function of distance; therefore, with increasing distance from the surface (due to a higher number of molecules and/ or atoms on the adsorbent), the rate of adsorption will decrease (Gregg and Sing, 1982; Bansal and Goyal, 2005). As a result, optimal adsorption will only occur if there is sufficient contact with the surface and edges of an adsorbent, where attractive forces are strongest. Under the right circumstances, a solid will be able to selectively adsorb or desorb atoms and compounds (corresponding to the liquid or gas phase) on its surface until a state of equilibrium is reached. This occurs when the rate of adsorption equals that of desorption; occurring at a new constant temperature and pressure (Bansal and Goyal, 2005). The energy for adsorption differs from one face to another on a solid as these surfaces contain imperfections due to heterogeneities within the crystalline structure (Gregg and Sing, 1982). These imperfections allow for different physical and chemical reactions to occur at the surface which can either promote or inhibit adsorption. More specifically, the imperfections result from the variability in surface functional groups, as well as the pore network throughout an adsorbent.

Chemically, the type and number of surface functional groups on the adsorbent will affect the rate of adsorption and the interactions between the adsorbent and adsorbate. These surface groups are produced when unsaturated carbon atoms on the edge of basal planes possess unpaired electrons which ultimately favour the binding to heteroatoms (Martin-Gullón and Menéndez-Diaz, 2006). These functional groups can be acidic (for example, carboxylic acid and phenol groups), basic in nature (for example, chromene groups) as well as either hydrophilic or hydrophobic. Carbons that have undergone incomplete carbonization (heating at lower temperatures) will produce functional groups that are rich in oxygen (Choma et al., 1991). As a result, the heating of materials that are chemically dominated by carbon will alter the surface acidity as well as the associated polarity, modifying the attraction between the adsorbent and the adsorbate. Chemical modifications are typically completed in order to alter the arrangement and presence of functional groups, enhancing adsorption (Yang, 2003). These changes promote the development of adsorbents used to preferentially adsorb either acidic or basic species. Though the functional group sites account for a small portion of the total surface area, the changes in the chemical nature may alter the adsorbents adsorption capacity (Martin-Gullón and Menéndez-Diaz, 2006).

The principal physical property governing adsorption is the porous structure of a material (Martin-Gullón and Menéndez-Diaz, 2006). Porous solids typically have an internal surface area that is orders of magnitudes greater than that of their external surfaces (Gregg and Sing, 1982). Pores can be completely isolated from their neighbours (closed pores), only open at one end (blind pores), open at two ends (through pores), or be a continuous channel reaching the external surface of the adsorbent material (Rouquerol et al., 1994). The International Union of Pure and Applied Chemistry (IUPAC) initially classified pores within the context of physisorption: micropores (< 2 nm), mesopores (2 to 50 nm), and macropores (>50 nm) (Sing et al, 1985). This classification is mostly based on the mechanisms occurring within the pores during N_2 adsorption at 77 K and 1 atm (Zdravkov et al, 2007). Typically, the pores themselves can either be cylindrical in shape, blind, ink-bottle shaped, funnel shaped or slit-shaped, where the shape and size distribution affects the accessibility of the adsorbate into the internal surface area (Gregg and Sing, 1982; Rouquerol et al., 1994). The voids that make up the internal pore system create an internal surface area ideal for adsorption due to the enhanced surface for molecules and atoms to bind to. A greater number of micropores will provide a larger surface area, allowing a greater adsorption capacity. However, the surface area available depends upon the structure of the adsorbent and the number of exposed pores accessible to the adsorbate. As a result, mesopores and macropores are important components of the porous solids because they serve as passages for the adsorbate to the micropores (Martin-Gullón and Menéndez-Diaz, 2006).

2.1.1.2 Isotherms

Adsorption isotherms are typically used in order to describe the quantity of an adsorbate sorbed onto an adsorbent with respect to its concentration in solution when measured at a constant temperature (Langmuir, 1997). As a result, this relationship describes the partitioning of a species (or components) between a solid, aqueous and gas phase within the environment by relating the known concentrations. The different adsorption reactions can be described by several different models where results are commonly obtained from laboratory batch tests. Adsorption isotherms are not always linear; however, they do involve increasing trends, where as the concentration of an adsorbate increases in solution, the adsorption capacity of the adsorbent increases as well (Langmuir, 1997). This relationship is shown in the following Figure 2-1. Here, the slope of the linear part of the curve (indicating an increasing trend) within the figure corresponds to the distribution coefficient (K_d), representing the ratio of adsorbed species to solute concentrations (Appelo and Postma, 2007).

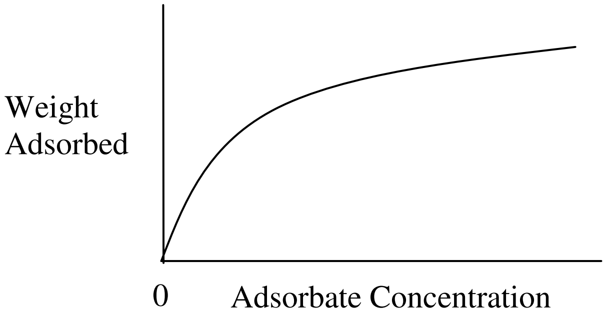

Figure 2-1: General Adsorption Isotherm (adapted from Langmuir, 1997)

Various models have been developed to characterize the partitioning of an adsorbate onto an adsorbate surface. These models simplify the many reactions occurring between adsorbent material and its surrounding environment, representing a limitation of the technique. Langmuir derived the following Equation (2-3) to describe adsorption relationships (most commonly used for gases):

$$W = \frac{aC_g}{1+bC_g} \qquad \textbf{(2-3)}$$

where W represents the amount of gas per unit mass of adsorbent (kg/kg); a and b are constants to be determined through experimentations; and C_g is the equilibrium concentration of the gas of interest (g/m^3) (Davis and Masten, 2004). The equation represents the fractional coverage of the adsorbate on the surface of the adsorbent. This method is commonly used to describe the adsorption onto a surface due to monolayer coverage, adsorption site equivalence and adsorption site independence (Kim and Sohn, 2005). As a result, the Langmuir theory suggests that there are no intermolecular interactions within a homogeneous layer (Choma et al., 1991). Consequently, though the Langmuir adsorption isotherm may be appropriate for the estimation of ideal cases, it may not be valid for estimating the specific adsorption interactions within the environment where adsorption may be heterogeneous in nature.

An alternative model is the Freundlich model represented by the following Equation (2-4):

$$\frac{x}{m} = KC^n \qquad \textbf{(2-4)}$$

where x is the weight of the adsorbate (mg); m is the weight of the adsorbent (g); K and n are constants; and, C is the aqueous concentration (g/L) (Langmuir, 1997). This equation has been suggested to better fit the process of adsorption since it assumes that most surfaces are heterogeneous (Kim and Sohn, 2005). Within the equation, the exponential term can allow for the consideration of decreasing adsorption with increasing adsorbate concentration; or a variation in energy between the adsorbent and the adsorbate (Mark and Mattson, 1971). This model has been previously used to describe the adsorption of colour and chlorinated organics onto activated petroleum coke from pulp mills wastewater (Shawwa et al., 2001).

2.1.2 Characterization of Carbon Properties

The unique characterization of raw and activated carbon includes the determination of surface area and pore size. This allows for an understanding of the process of adsorption between different materials. These methods are generally preformed on activated carbons since they are common and efficient adsorbents. Activation is typically preferred as it enhances the pore structure of heavily enriched carbon materials, generating a greater adsorption capacity (Kumar et al., 2006). As a result, assessing the characteristics of activated and non-activated carbon materials provides a greater understanding of the potential adsorbent-adsorbate interactions on a micro-/ mesopore scale.

2.1.2.1 BET Theory and Nitrogen Adsorption

The adsorption capacity is typically determined through adsorption isotherms from gas adsorption measurements (Martin-Gullón and Menéndez-Diaz, 2006). The development of the Brunauer, Emmett and Teller (BET) theory allowed for the determination of the specific surface area of an adsorbent, as well as the approximate heat of adsorption by assuming that the Langmuir isotherm can be applied to every adsorption layer on an adsorbate (Choma et al., 1991). As a result, the theory assumes a homogeneous surface with no lateral interactions among molecules. More specifically, there exists uniform adsorption energy across the surface sites, where adsorption is also analogous among layers. This presents a limitation of the technique since all adsorption reactions occurring on every layer may not be adequately represented by the ideal case of homogeneous layer coverage. The isotherms are determined through the adsorption of N_2 at 77 K or CO_2 at 273 K. In some cases, the effect of diffusion may occur for nitrogen when the kinetic energy is low, restricting accessibility of nitrogen to all of the pores (Martin-Gullón and Menéndez-Diaz, 2006). In such instances, the adsorption of CO_2 is often used. The following Equations (2-5 and 2-6) were provided by Martin-Gullón and Menéndez-Diaz (2006) to represent the BET equation:

$$\frac{p/p^0}{n(p^0-p)} = \frac{1}{nC} + \frac{C-1}{n_m}\frac{p}{p^0} \qquad \textbf{(2-5)}$$

$$\text{, and } C = \exp\left(\frac{q_1-q_L}{RT}\right) \qquad \textbf{(2-6)}$$

For this equation, p is the pressure in equilibrium with the adsorbate and p^0 is the saturated vapour pressure of the adsorbate (which is known depending on the gas used for the adsorption). Within this equation the width of the pores, cracks and capillaries of the adsorbent limits the maximum number of adsorbed layers, even at saturation pressure (Brunauer et al., 1938). The BET theory can be used to provide surface areas of micro- and mesoporous adsorbents. The BET surface area for carbons typically ranges from 500- 1500 m^2/g (Martin-Gullón and Menéndez-Diaz, 2006).

2.1.2.2 Iodine Number

The determination of the iodine number is based upon assessing the amount of iodine adsorbed by a carbonaceous material per gram of carbon (ASTM, 2006). The iodine utilized in this test is in the form of I_2, where the outcome of the iodine number can be related to the surface area of pores between 10 and 28 Å in diameter (Yang, 2003). The results of this testing can be related to porosity as well as surface area; however, the produced values do not directly measure the ability of a carbon material to adsorb other species (ASTM, 2006). At the same time, enhanced pore structures indicated by high iodine numbers will imply a greater adsorption capacity. In contrast, low iodine numbers will suggest poor pore development during the carbonization and activation stage (Kumar et al., 2006). As a result, low iodine numbers may signify the need for the activation of non-activated carbons in order to develop an enhanced pore structure ideal for increased adsorption. These relationships obtained from liquid phase adsorption of iodine can account for trends occurring on the specific surface as well as within the pore volume. Studies have indicated that the results of iodine numbers and BET surface areas are correlated when surface areas are less than 1000 m^2/g. If a material has a larger surface area than 1000 m^2/g with narrow micropores (<10

Å), the iodine number may give rise to lower values due to a poor accessibility of iodine to existing micropores (Budinova et al., 2006). Consequently, BET surface area (nitrogen adsorption) should be investigated in order to determine the actual pore size distribution within a carbon material (Budinova et al., 2006). Iodine number can also be affected by the amount of volatiles, water and/ or sulphur initially present within an adsorbent; inhibiting the amount of iodine adsorbed (ASTM, 2006). Such aspects should be kept in mind when determining the iodine number in order to accurately interpret the results.

2.1.2.3 Methylene Blue

The methylene blue molecule is larger in size than an iodine molecule and may provide an indication of the mesopores existing within a carbon material. Mesoporosity is desirable for liquid-phase applications whereas, microporosity is typically used in gas-phase applications (Yang, 2003). As a result, the adsorption of methylene blue has been used to characterize adsorbents used for waste water and organic contaminant treatment (Potgieter, 1991; Shawwa et al., 2001; and Hameed et al., 2007).

Methylene blue adsorption is used for the determination of surface areas in both activated carbons and in soils (typically clays). The literature describes two different methods of determining the adsorption of methylene blue by various adsorbents. The titration method measures the adsorption of methylene blue onto clays by observing whether or not a drop of pH altered slurry (methylene blue/ clay mixture) produces a light blue halo (ASTM, 2009). The calculated methylene blue index can indicate the specific surface area of the clay soil. Only the reactive portions of a soil can react with the methylene blue (leading to its adsorption), presenting a limitation of this method (Sivapullaiah et al., 2008).

Alternatively, the methylene blue batch test method has been used to describe the adsorption properties of activated carbons. The results of the test are typically described as the amount of methylene blue adsorbed per weight of carbon. However, this test has differed throughout the literature owing to the absence of a standardized method. Potgieter (1991) conducted methylene blue batch tests using a methylene blue solution of 25 mg/L mixed with distilled water on activated carbon. The solutions were mixed for approximately 72 hours before the filtrate was analyzed at 630 nm (the position of maximum absorbance) with a Spectronic 20 spectrophotometer (Potgieter, 1991).

This method was altered by Shawwa et al. (1999) who used a methylene blue solution of 800 mg/L, where the absorbance of the filtrate was conducted at 620 nm by a UV-VIS spectrometer. Sample procedures followed ASTM D3860-98 (1999), where sample contact time was 24 h. Sample pH was not specified. The absorbance found was compared to a previously prepared calibration chart made up of a series of methylene blue dilutions. These results were expressed as grams of methylene blue adsorbed per 100 g of activated petroleum coke.

Hameed et al. (2007) found that samples undergoing a batch test should be mixed for 24 h in order for the solid-solution mixture to reach equilibrium; at this point, adsorption could be calculated using the following Equation (2-7):

$$q_e = \frac{(C_o - C_e)V}{W} \qquad \textbf{(2-7)}$$

where C_o is the initial concentration, C_e is the concentration at equilibrium, V is the volume of the solution, and W is the mass of the dry adsorbent (Hameed et al., 2007).

This method was investigated further by Yasin et al. (2007) who researched the effect of contact time, pH, and adsorbent dosage with a 500 mg/L solution of methylene blue. The results suggest that the percentage of methylene blue removal increased with increasing contact time, pH, and dosage. The maximum contact time required for equilibrium with activated carbon as an adsorbent was found to be 180 minutes due to the strong initial attractive forces between the adsorbent and the adsorbate (Yasin et al., 2007). However, the presence of hydrogen ions can compete with the methylene blue molecules for adsorption sites at a lower pH levels. Consequently, higher pH levels will allow for a greater adsorption of methylene blue (Yasin et al., 2007).

2.2 Literature Review

This section presents an overview of the main components associated with this research, as well as a review of the activation process and its application to petroleum coke.

2.2.1 Process-Affected (PA) Water

The Athabasca oil sands deposit, located in Fort McMurray, Alberta is known to contain over 174 billion barrels of bitumen; an unconventional fossil fuel (Allen, 2008a; CAPP, 2009). During oil processing, fresh and recycled water are used to separate bitumen from the surrounding sand and clay fractions though Clark hot water extraction procedures (Allen, 2008a). The resulting process-affected (PA) water contains a range of pollutants of varying concentrations (Vlasopoulos et al., 2006). The composition of the PA water differs among companies across the Athabasca region due to the unique geology of the mining area as well as the distribution of the ore (Beir et al., 2007). However, the overall trend is the production of highly saline water containing sizable amounts of coarse and fine sediments, dissolved inorganic and organic by-products, and fractions of unrecoverable bitumen. Four cubic meters of unusable slurry waste is produced for every 3 m^3 of recycled and fresh water used to extract bitumen from 1 m^3 of oil sands (Quagraine et al., 2005). The amount of net fresh water required averages about 4 barrels per barrel of oil produced, where 2 to 3 barrels of fresh water are taken from the nearby Athabasca River (CAPP, 2009). The slurry waste along with the contaminated PA water is stored on site within manufactured tailings ponds due to the zero discharge policy adapted by companies in the Athabasca oil sands region. These engineered dam and dyke systems are designed to contain and settle the water and other by-products of the mining and extraction processes, allowing for oil sands producers to recycle 80 to 95% of the water used (CAPP, 2009).

Dewatering of the tailings ponds through densification procedures permits the partial settling of sediments and the release of water, allowing for further recycling of PA water throughout the operations (Quagraine et al., 2005). With further contamination of by-products from the extraction procedures, additional clean water is required. This increases the demand for imported fresh water resources. Within the Athabasca region, the main water sources come from the Athabasca River, groundwater, run-off, and connate water (Allen, 2008a). The key issues within the Athabasca region are whether the water withdrawal can support the oil sands industry within the future, as well as the effect of possible contamination of water resources on the surrounding communities. Consequently, the development of strategies to remediate the PA water is necessary to increase the efficiency of water recycling as well as to mitigate potential environmental impacts.

The use of spray freezing on oil sands wastewater was investigated by Gao et al. (2004) as a PA wastewater treatment option, where partial freezing was completed at -10 and -24°C and run-off was collected. Results indicated the effective reduction of: conductivity (78%), colour, total organic carbon (77%), and chemical oxygen demand (70%) (Gao et al., 2004). However, limitations of the technique include the increase of pH in all ice samples, evaporation causing water loss, and aeration during wastewater spraying causing oxidation of volatile organic compounds (Gao et al., 2004).

Emerging technologies for oil sands wastewater treatment have been outlined by Allen (2008b) including: adsorption, micro- and ultrafiltration, nanofiltration, reverse osmosis, electrodialysis, biological treatment, advanced oxidation, and treatment wetlands. However, the utilization of these technologies is dependent upon the target contaminants of interest (for example, organics, heavy metals, or salts). Consequently, a thorough understanding of the target pollutants within the PA water is required in order to design and develop optimal treatment techniques and methodologies. Of the various technologies, the use of adsorbents may be the most feasible technique due to the wide range of available materials (activated carbon, clays, natural organic matter, zeolites, and synthetic polymers), as well as their ability to remove a wide range of pollutants specific to oil sands PA water (Allen, 2008b). The use of natural and widely available materials as adsorbents is desirable for wastewater treatment as they are considered to have a low environmental impact as well as a minimal production of waste (Allen, 2008b).

Vlasopoulos et al. (2006) conducted a life cycle analysis on the environmental impact of 20 process water treatment technologies produced during oil and gas extraction. The analysis indicated that the following combination of technologies offers low environmental impacts, representing feasible options for the oil sands industry: dissolved air flotation, absorption, dual media filtration and reverse osmosis (Vlasopoulos et al., 2006). These results indicate that there may not be one direct solution for the treatment of PA water, and a combination of treatments may offer the most effective results.

2.2.2 Oil Sands Naphthenic Acids (OSNAs)

One of the major contaminants within oil sands PA water ranging from 50 to 100 mg/L is the dissolved organic material comprised of the following components: organic acids, aromatic compounds, and bitumen (Allen, 2008a; Whitby, 2010). These waste by-products of the oil extraction process become concentrated during PA water recycling, and contribute to the poor water quality of the tailings ponds (colour, toxicity, total organic carbon, etc.). Eighty percent of the organic acid fraction is comprised of oil sands naphthenic acids; a term referring collectively to all of the carboxylic acids founds within crude oil (Allen, 2008a; Brient et al., 1995). Oil sands naphthenic acids (OSNAs) naturally reside in ores within the Athabasca oil sands region, originating from depositional and post depositional environments; these organic acids are released during oil sands extraction via aqueous digestion procedures (Clemente et al., 2003). Consequently, the concentration and composition of OSNAs can be expected to differ across the Athabasca oil sands region depending on the geology of the area in which the ores are mined. OSNAs represent a class of complex mixtures of alkyl-substituted acyclic and cycloaliphatic carboxylic acids (Yen et al., 2004). These organic acids can also be represented by the general chemical formula $C_nH_{2n+Z}O_2$, where the structure varies depending on the number of hydrogen atoms lost as linear hydrocarbon chains are gained. More specifically, *n* represents the carbon number and *Z* is either zero or a negative even number, indicating the number of cyclic rings in a specific homologous series (Yen et al., 2004; Hao et al., 2005; Janfada et al., 2006; Scott et al., 2008; and, Mohamed et al.; 2008). The ring structures within OSNAs typically contain 5 or 6 carbon atoms existing in various combinations (Holowenko et al., 2002). Therefore, there resides a large range of OSNAs with different functional groups and levels of aromaticity, resulting in some species that are more toxic than others. Figure 2-2 shows examples of basic acyclic, monocyclic, bicyclic, and tricyclic naphthenic acids.

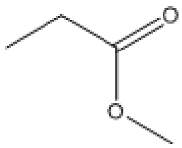

Acyclic Naphthenic Acid
Length ≥ 5.77 Å

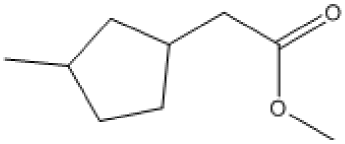

Monocyclic Naphthenic Acid
Length ≥ 8.82 Å

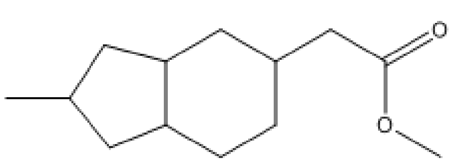

Bicyclic Naphthenic Acid
Length ≥ 13.39 Å

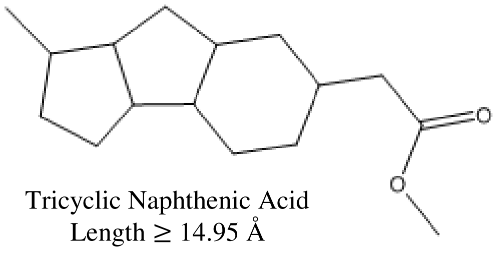

Tricyclic Naphthenic Acid
Length ≥ 14.95 Å

Figure 2-2: Examples of aromatic and acyclic naphthenic acid structures, where Z=0,-2,-4, and -6. The side chain is typically an aliphatic group.

Lately, the term ‘naphthenic acid’ has been considered to be ambiguous due to the range of organic compounds being considered as part of the group of polar organic carboxylic acids (Grewer et al., 2010). The presence of pyrroles, thiophenes, and phenols in some OSNAs add to the complexity and uncertainty surrounding the unique class of compounds (Whitby, 2010). Consequently, the OSNAs found within the Athabasca oil sands region cannot be considered as classical and pure naphthenic acids, but rather complex naphthenic acid mixtures. This represents a large challenge in the characterization and quantification of OSNAs (Grewer et al., 2010).

Naphthenic acids have been referred to as the primary source of toxicity within oil sands tailing pond water (Hao et al., 2005; Allen, 2008a; Scott et al., 2008; Whitby, 2010; Grewer et al., 2010). Research has suggested that microbial activity can reduce the toxicity of OSNAs within aging tailings pond waters (Holowenko et al., 2002; Clemente et al., 2003). Decreasing toxicity has also been observed with increasing time and degradation of OSNAs producing carbon numbers of C_{22+}, where molecular structures are dominated by carbon numbers 13 to 16 (Allen, 2008a). At the same time, the literature indicates that storage of OSNAs within tailings ponds has not been effective in decreasing concentrations below 20 mg/L, even after decades of storage (Martin et al., 2008). Natural biodegradation of OSNAs within oils have also been found to release high concentrations of carboxylic acids increasing the total acid number (TAN) (Meredith et al., 2000). As a result, it is still unknown which specific components within OSNAs are responsible for the toxicity itself, nor how long it will take for the OSNAs to completely degrade. Researchers suggest that the toxicity may be attributed to only a part of the OSNA group (Holowenko et al., 2002).

Consequently, there are large gaps in the knowledge surrounding the unique characterization of OSNAs. Natural concentrations of OSNAs found within the Athabasca river (running through the oil sands deposits) was determined to range from 0.1 to 0.9 mg/L (Clemente and Fedorak, 2005). In contrast, OSNA concentrations have been measured to be between 40 and 120 mg/L within tailings pond waters stored within the Athabasca region (Janfada et al., 2006). Consequently, the high concentration of OSNAs within the tailings ponds is not in equilibrium with the surrounding environment, and any potential leaching and mobilization of OSNAs may result in a large environmental impact.

The solubility of OSNAs in water is affected by pH (greatest above neutral), where preferential sorption is likely to occur within the environment, depending on the functional groups present (Janfada et al., 2006). This situation favours the mobility of OSNAs in surface waters contaminated with petroleum, allowing for uptake by plants and animals (Clemente and Fedorak, 2005).

Research has demonstrated that OSNAs are acutely and chronically toxic to a variety of organisms including the following: fish, amphibians, zooplankton, mammals (rats and guinea pigs), as well as bacteria (including *Vibrio fischeri*) (Whitby, 2010). More specifically, OSNAs have been confirmed to be toxic to fish at concentrations exceeding 2.5 to 5 mg/L (Clemente and Fedork, 2005; Whitby, 2010). This represents a problem for the oil sands industry when considering mine closure and tailings pond reclamation. Studies have shown that the treatment of tailings pond water for the removal of OSNAs has led to the reduction of acute lethality towards rainbow trout and water fleas (Rogers et al., 2002).

OSNAs are also corrosive to the oil processing and refining infrastructure. Corrosion occurs through the formation of hydrogen gas at typical operating temperatures (200 to 400^{o}C), causing chelation of metal ions in the presence of carboxylic acid groups (Clemente and Fedorak, 2005). The rate and amount of corrosion is dependent upon the following factors: temperature, availability of carboxylic acid groups, molecular composition of the present metal compounds, and increasing alkyl chain length (to a maximum of three methylene side groups) on the available OSNA (Brient et al., 1995; Clemente and Fedorak, 2005; Whitby, 2010). New studies indicate that increasing corrosivity is not related to increasing TAN number during the processing of heavy degraded oils (Whitby, 2010).

Innovative and feasible methods aiming at the reduction in OSNAs within tailings ponds are necessary in order to reduce toxicity and corrosivity of the PA water. This would lead to increased recycling of the PA water, as well as efficient remediation of the tailings ponds during mine closure.

2.2.3 Petroleum Coke

The process of ‘coking’ is utilized to convert heavy petroleum residues into gas oil, or gasoline; where after processing, a percentage of the products remain- becoming refinery waste (Onder and Bagdoyan, 1994). The term ‘coke’ refers to any carbonaceous solid produced during hydrocarbon processing. Consequently, petroleum coke is a by-product of the upgrading of bitumen to synthetic crude oil. Petroleum coke can be produced through either dealkylation or dehydrogenation reactions during thermal cracking. Dealkylation involves the transformation of asphaltenes and resins to straight chain compounds through elevated temperatures. The resulting products are highly amorphous with large concentrations of impurities (Onder and Bagdoyan, 1994). On the other hand, dehydrogenation reactions use subsequent polymerization or condensation of free radicals to form high carbon-to-hydrogen ratios and larger molecular weight compounds. The final coke product has a more crystalline appearance due to the abundance of aromatics (Onder and Bagdoyan, 1994). These procedures are mainly used to break down (or ‘crack’) complex hydrocarbons into smaller units, also referred to as carbon rejection or carbonization (Scott and Fedorak, 2004). The specific hydrocarbon composition of petroleum is variable depending on the geographical location of the oilfield as well as the depth of the well (Scott and Fedorak, 2004). Consequently, it can be expected that the petroleum coke composition will also vary between, as well as within companies. Operational parameters (including coke drum pressures, recycle ratio, steam addition, and temperature) can also affect the yield and chemical/ structural composition of the produced petroleum coke (Onder and Bagdoyan, 1994).

Coking can be separated into delayed coking techniques and fluid coking techniques. Delayed coking includes rapid heating in a furnace under specific temperature and pressure conditions correlating to the materials thermal cracking temperature; typically, resulting in a coke with a sponge-like structure (Onder and Bagdoyan, 1994). The feedstock is then immediately transferred to a coking drum before any deposition or separation of liquids and solids can take place (Scott and Fedorak, 2004). The remaining solids are referred to as 'delayed coke'. Fluid coking involves the spraying of residual oil through steam injection onto hot coke particles (serving as a heat source and a reaction media), resulting in the instantaneous conversion to coke with thermal cracking (Onder and Bagdoyan, 1994; Scott and Fedorak, 2004). Though coke is re-used throughout the process, a large majority of the produced fluid coke is still considered to be an undesirable waste.

The coking processes are highly dependent upon their thermal treatments. Delayed coking generally occurs at a temperature range of 415 to 450^{o}C, whereas fluid coking uses higher temperatures ranging from 480 to 565^{o}C (Fedorak and Coy, 2006). This heating not only affects how the oil is separated from the waste fractions, but also produces different compositions of gases within the coke products depending on the degree of volatilization. As a result, the volatiles measured within the delayed and fluid cokes can range from 7 to 13% and 4 to 6%, respectively (Fedorak and Coy, 2006). Coke composition is also affected by the composition of the bitumen sent for refining. Consequently, petroleum coke in the Athabasca region has higher ash content due to the fine clays entrapped within the bitumen feedstock (Fedorak and Coy, 2006). With these factors in mind, it can be assumed that the resulting characteristics and chemical compositions of the delayed and fluid cokes differ. As waste by-products, the petroleum cokes also contain varying levels of concentrated impurities. Table 2-1 contains the chemical and physical characteristics of fluid (Syncrude Canada Ltd.) and delayed (Suncor Energy Inc.) petroleum coke found within the Athabasca oil sands region.

Table 2-1: Physical and chemical characteristics of fluid (Syncrude Canada Ltd.) and delayed coke (Suncor Energy Inc.) as found throughout the literature.

		Fluid Coke	Delayed Coke	Reference
Physical Characteristics	**Shape**	Spherical, uniform	large lumps, non-uniform	Fedorak and Coy, 2006
	Size	Medium to fine sand size	Well-graded sandy gravel to large chunks	Scott and Fedorak, 2004
	Specific Gravity	1.5-1.7	1.2-1.4	Fedorak and Coy, 2006
Ultimate Analysis	**Carbon**	78.5%	82.3%	Chen, 2010
	Nitrogen	1.8%	1.6%	Chen, 2010
	Hydrogen	1.9%	3.7%	Chen, 2010
	Sulphur	7.2%	6.8%	Chen, 2010
Elemental Concentration	**Vanadium**	1690 mg/kg	-	Ityokumbul, 1994
	Nickel	680 mg/kg	-	Ityokumbul, 1994
Ash Composition	**V_2O_5**	4.9%	4.4%	Jang and Etsell, 2009
	NiO	-	1.2%	Jang and Etsell, 2009
Proximate Analysis	**Volatiles**	7.1%[1]	11.9%[2]	[1]Di Panfilo and Egiebor, 1996; [2]Shawwa et al., 2001
	Moisture	1.8[1]	1.8[2]	[1]Di Panfilo and Egiebor, 1996; [2]Shawwa et al., 2001

-, not available

Syncrude Canada Ltd. and Suncor Energy Inc. cumulatively produce over 6000 tonnes of petroleum coke per day (Furimsky, 1998). This results in a cumulative production of over 5 million tonnes of petroleum coke per year, where estimates indicate 1 billion m^3 of total coke production throughout the entire lifetime of the oil sands operations in Alberta (Fedorak and Coy, 2006). Petroleum cokes typically have a high sulphur content ranging from 2 to 7%, where treatment is necessary before or after fuel consumption (Furimsky, 1998). Due to the associated costs, most of this petroleum is stockpiled on-site leading to the minimal use of the material. Suncor Energy Inc. uses a portion of their delayed coke in boilers in order to generate steam and electricity after hydrotreatment to remove sulphur (Scott and Fedorak, 2004). Still, it is unknown whether outdoor storage of the petroleum coke has an impact on the health of the surrounding environment. The literature has hypothesized that the material is benign (Fedorak and Coy, 2006). A previous study has shown that Syncrude coke is non-leachable with respect to regulated elements and volatile organics, especially under low pHs where high rates of leaching may be of concern (Furimsky, 1998). Recent studies have measured significant amounts of Ni on cokes from upgraders attributed to airborne contaminants (Kelly et al., 2010). The atmospheric deposition of As, Pb, and Hg from emissions by Suncor Energy Inc. and Syncrude Canada Ltd. has also increased by approximately a 3-fold between 2001 and 2008 (Kelly et al., 2010). The presence of these contaminants within the large coke stockpiles may affect the environment with respect to leaching, mobility, bioaccumulation, and toxicity. However, there is no further research within this area.

Though the use of petroleum coke is limited, storage of the coke material is important as it may represent a valuable fuel commodity in the future. The literature indicates that petroleum coke has a calorific value equal to that of medium grade coal of approximately 37 MJ/kg (Lee and Choi, 2000). Until this becomes an economically viable option for the oil sands industry, alternative uses of the petroleum coke should be investigated. An alternative application has included the use of petroleum coke for adsorption purposes. This may be a viable option due to the high carbon content within the material ranging from 78 to 82% by wt. (Table 2-1). With activation, delayed coke has been shown to develop a large surface area and porosity, where adsorptive capacities are 10 times that of raw coke (Shawwa et al., 2001). As a result, this product may be useful to the oil sands industry with respect to tailings pond wastewater treatment.

2.2.4 Activated Carbon

Activated carbon has been classically used to adsorb organic contaminants (Stavropoulos and Zabaniotou, 2009). Though anciently used to prolong drinking water supplies, the First World War marks the starting point of activated carbon development and production as an adsorbent for water and vapour/ gas phase treatment (Menendez-Diaz and Martin-Gullon, 2006). The term 'activated carbon' refers to a range of amorphous carbon-based materials that have been structurally altered to exhibit an extended porosity and intra-particulate surface area (Bansal et al., 1988). As a result, activated carbons can originate from a variety of organic precursors, high in carbon content (for example, coal, coconut shells, bamboo, wood, peat, etc.). The resulting products are excellent adsorbents and have been typically used to purify, decolourize, deodorize, dechlorinate, detoxicate, filter, modify salt content, separate, and concentrate to allow for recovery (Bansal et al., 1988). Due to its wide availability, it is a feasible and effective option for industries interested in contaminant/ pollution control, remediation, and recycling. However, the selection of an activated carbon is important since the qualities can differ among products making some activated carbons better suited for specific applications (Hassler, 1941). The method of activation (whether physical or chemical) will affect the number of pores as well as their shape, size and distribution. Granular activated carbon (GAC), a common form of activated carbon, has a characteristic non-graphitic and non-graphitizable carbon structure that is highly disordered (Menendez-Diaz and Martin-Gullon, 2006). This allows for the existence of an extensive porous structure throughout the material. The structure can also be described as stacks of randomly cross-linked aromatic sheets (Bansal et al, 1988).

Studies have shown that activated carbon has the ability to remove dissolved organic carbon and naphthenic acids from oil sands PA water (Hall and Tollefson, 1979; Shawwa et al., 2001; Allen, 2008b). However, these studies have produced mixed results, where activated carbon was not effective at removing other target pollutants (such as aliphatic hydrocarbons, BTEX compounds, and emulsified oils) (Allen, 2008b). Other experiments using UV-VIS absorbance and fluorescence spectrophotometry have indicated that GAC is effective in adsorbing naphthenic acids at pH =9 (Mohamed et al., 2008). However, it is not known whether the naphthenic acids removed were of the toxic form. Nevertheless, these results indicate that the use of activated carbon adsorption should be developed as a treatment technology for the oil sands industry. The application of readily available carbon-based materials to the oil sands companies within the Athabasca region should be investigated in order to minimize costs and increase the efficiency of the reclamation technique.

2.2.5 Activation

Preparation of activated carbon involves the alteration of a raw carbonaceous material into one that contains a higher surface area due to the development of an enhanced porosity. The process of activation typically consists of two steps: carbonization and activation. The first step is a carbonization stage where any non-carbon elements within a substance are volatilized through pyrolytic decomposition (Bansal and Goyal, 2005). More specifically, a carbon substance is heated in the absence of oxygen in order to drive off non-carbon elements (such as oxygen, nitrogen, and hydrogen), creating a charcoal-like material. This process has also been explained as the thermal decomposition and volatilization of hydrates and carbonates at temperatures less than the carbonaceous material's melting point (Bansal et al., 1988). Chemically, the remaining carbons re-arrange themselves into random, cross-linked, aromatic sheets; primarily developing irregular pores (Bansal and Goyal, 2005). This is typically completed within stationary, rotary, or fluidized bed ovens (Shawwa et al., 1999). As a result, the efficiency of the carbonization stage is dependent upon the following: the nature of the carbonaceous material, the heating temperature, the rate of heating and the atmosphere during the heating process. Figure 2-3 shows a scanning electron micrograph (SEM) of non-activated and activated coke, indicating the development of pores through carbonization and activation sequences.

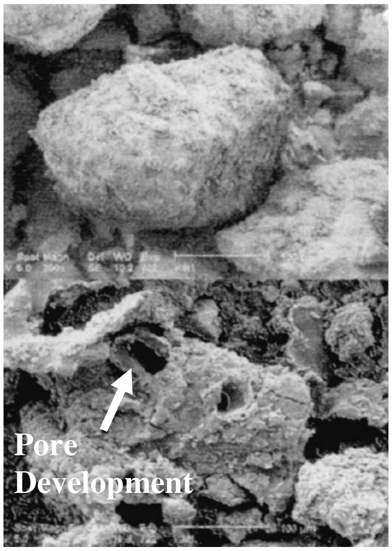

Figure 2-3: SEM of non-activated and activated coke indicating the development of surface area (adapted from Lee and Choi, 2000).

Ultimately, the temperature is a defining parameter that will impact the type of char created. During carbonization, the carbonaceous material undergoes a softening period before it begins to harden and shrink (Bansal et al., 1988). The softening period will depend upon the rate of heating. A low rate of heating may result in denser or harder chars. At the same time, low temperature heating can lead to less volatilization and shrinking (Bansal et al., 1988). This would result in a greater yield in char, since shrinking may lead to a decrease in the overall pore volume. A lower rate of heating also assists in the formation of micropores, where density and hardness are greater (Martin-Gullón and Menéndez-Diaz, 2006). In contrast, if temperatures are too high, burn-out can occur between the walls of adjacent pores, increasing the number of macro-pores (Bansal et al., 1988). Consequently, higher temperatures favour the production of meso- and macro-pores, leading to a lower density char. If the chosen carbonization temperature is too high, the carbon can crystallize into graphite, increasing the difficulty of the activation stage (Shawwa et al., 1999). In the past, carbonization was typically completed at temperatures less then 500^{o}C (Hassler, 1941). Since then, it has been suggested that carbonization be conducted in an inert atmosphere at low heating rates and temperatures ranging from 400-600^{o}C (Choma et al., 1991). Alternatively, Shawwa et al. (1999), suggest a carbonization range at higher temperatures ranging from 500-800^{o}C. These temperature rates would depend on the type of carbon used, as well as the heating time. During thermal decomposition, carbon dioxide and water vapour are produced. These components can react with the carbon structure if they are not removed through the fast flow of an inert gas (Shawwa et al., 1999). As a result, the atmosphere during carbonization also plays an important role in controlling the type of char produced.

The pores generated within the carbonization stage can typically be filled with the decomposed products which can be removed during the activation stage (Bansal and Goyal, 2005). During this process, the activation agent removes any decomposed products and disorganized carbons, further developing a microporous structure (Bansal et al., 1988). This cleans out the passages between the pores, while enhancing the pore volume of a material. However, the effectiveness of the activation stage is highly dependent upon the following: the type of carbonaceous material used; the temperature and atmosphere chosen for the carbonization stage; the temperature and atmosphere chosen for the activation stage; and, the activating agent chosen for activation. Activation can also be defined as a combustion process resulting in preferential etching, producing an active carbon containing: a greater surface area and porosity, as well as a chemically reactive surface (Mattson and Mark, 1971). The loss of material through activation typically ranges between 20 to 50%; the burn-off can be used as an indicator of microporosity development (Buitrón et al., 2000). For an active carbon matrix, heteroatoms (such as oxygen) exist in the form of single atoms and/ or functional groups located at the edges of basal planes. These groups influence the adsorptive properties as well as the reactivity of the carbon (Karanfil and Kilduff, 1999). It is the high surface areas and reactivity of the surfaces that have made active carbons effective adsorbents.

The type of carbonaceous material used will ultimately define the final porous nature of the activated product produced. For example, some carbons may produce an activated product that is dominated with micropores ideal for gas adsorption. However, the pore size distribution within the activated carbon may not be preferred for waste-water treatment due to the possible adsorbate-adsorbent interactions (Mattson and Mark, 1971). Carbonaceous materials that have been used to produce activated carbon include wood, coal, lignin, coconut shells, sugar, sawdust, petroleum coke, peat, etc. (Mattson and Mark, 1971; Karanfil and Kilduff, 1999). Due to the different chemical make-up of these materials, they may individually require different activation parameters (such as temperature and atmosphere).

There are two modes of activation: physical activation and chemical activation. Both methods involve the degradation of decomposed non-carbon products in order to enhance surface area. This is completed through increasing the number of pores within a carbon substance. Both activation techniques involve the use of different activating agents. These activating agents directly interact with the carbon atoms to form the unique activated carbon structure (Bansal et al., 1988).

Physical activation is typically completed in an oven or furnace where the heat and the activating agent can be applied simultaneously under temperatures ranging from 800 to 1000^{o}C. External heating is utilized in order to drive the typical endothermic reactions (Bansal et al., 1988). The activating agents used are oxidizing agents such as steam (H_2O), CO_2, air, or a mixture of the agents. The rate of reactivity is as follows: $O_2 > H_2O > CO_2$; making CO_2 the least reactive agent (Martin-Gullón and Menéndez-Diaz, 2006). Physical activation with an oxygen atmosphere is an exothermic reaction which can result in excessive burning- difficult to control. For these reasons oxygen is not typically used (Bansal et al., 1988). Consequently, steam is typically used as an activating agent for the physical activation of carbons. Bansal et al. (1988) defined the following reactions (Equations 2-8 to 2-11) to describe the behaviour of the different activating agents during physical activation:

$$\mathrm{C} + \mathbf{H_2O} \leftrightarrow \mathrm{CO} + \mathrm{H_2}\ [-29\ \mathrm{kcal}] \qquad \mathbf{(2\text{-}8)}$$

$$\mathrm{C} + \mathbf{CO_2} \leftrightarrow 2\mathrm{CO}\ [-39\ \mathrm{kcal}] \qquad \mathbf{(2\text{-}9)}$$

$$\mathrm{C} + \mathbf{O_2} \leftrightarrow \mathrm{CO_2}\ [+92.4\ \mathrm{kcal}] \qquad \mathbf{(2\text{-}10)}$$

$$\mathrm{C} + \mathbf{O_2} \leftrightarrow 2\mathrm{CO}\ [+53.96\ \mathrm{kcal}] \qquad \mathbf{(2\text{-}11)}$$

A higher temperature is required for activation with CO_2 than with H_2O since the process is more endothermic as identified by the heat of reaction.

In contrast, chemical activation uses a concentrated dehydrating reagent as an activating agent. This is mixed with the carbonaceous material before drying and heating in an oven (or furnace). Common activating agents observed throughout the literature include the following: H_3PO_4, K_2CO_3, H_2SO_4, KOH, $ZnCl_2$, and K_2S (Bansal et al., 1988; Choma et al., 1991; Yang, R., 2003). Different chemical agents can yield different overall carbon pore structures. For example, activation with KOH results in a more microporous structure than $ZnCl_2$ which is known to generate a mesoporous structure (Yang, 2003). These activating agents dehydrate the starting carbonaceous material while influencing pyrolytic decomposition in the absence of oxygen (Bansal et al., 1988). Activating agents can be harmful to the environment if used in large quantities; however, agents such as KOH are beneficial as the dehydration inhibits the production of tar (Guo et al., 2005). During chemical activation, oxidation primarily occurs within the decomposed products found within the pores, and secondly, within the carbon residing on the pore walls. The result is a highly developed pore structure. For this method, carbonization and activation occur simultaneously at temperatures ranging from 500 to 900^{o}C (Yang, 2003). The temperatures required for chemical activation are lower than required for physical activation, allowing for a better development of pore structure (Bansal et al., 1988). Lower temperatures also prevent the potential for burn-out to occur between the pores, which would lead to the production of a macroporous material.

The impregnation ratio (ratio of activating agent to starting material) controls the resulting pore diameter within the carbon. For example, the greater initial degree of impregnation, the greater the increase in pore diameter observed in the final carbon product (Bansal et al., 1988). More specifically, pore development will be controlled by the amount of saturation by the activating agent. Yang (2003), suggests the use of KOH at a ratio of 3:1 in order to obtain a large microporosity of pores mainly at 2 nm in diameter. The process of chemical activation is completed when 50% of the carbon structure has been burnt off, resulting in the maximum surface area (Choma et al., 1991). After activation, the remaining chemicals can be removed from the activated carbon through an acid or water wash and later recycled (Yang, 2003). The efficiency of chemical activation is highly dependent upon the following factors: degree of impregnation; initial heating temperature (carbonization phase); activation temperature (activation phase); and, the composition of the atmosphere used during heating (Bansal et al., 1988).

The shapes of the pores produced throughout either physical or chemical activation differ based on the activation temperature. For temperatures around 500°C (preferred for chemical activation), the carbon can be said to be in a plastic state where the gases released through thermal decomposition create hollows-escaping through small passage-ways (Bansal et al., 1988). This process creates bottle-shaped pores, providing a better adsorbate interaction with the surface of the activated carbon. At higher temperatures (typically used for physical activation), a concentration gradient is formed between the entrance to the pores as well as at the center of the pores; creating wider entrances and smaller centers (cone-shape) (Bansal et al., 1988). These pores have the potential to be blocked by larger particles, preventing access by smaller particles during adsorption. Consequently, lower carbonization and activation temperatures are advantageous for the activation of carbonaceous materials. The following flow chart (Figure 2-4) indicates the process of activation leading to either a powder or granular activated product.

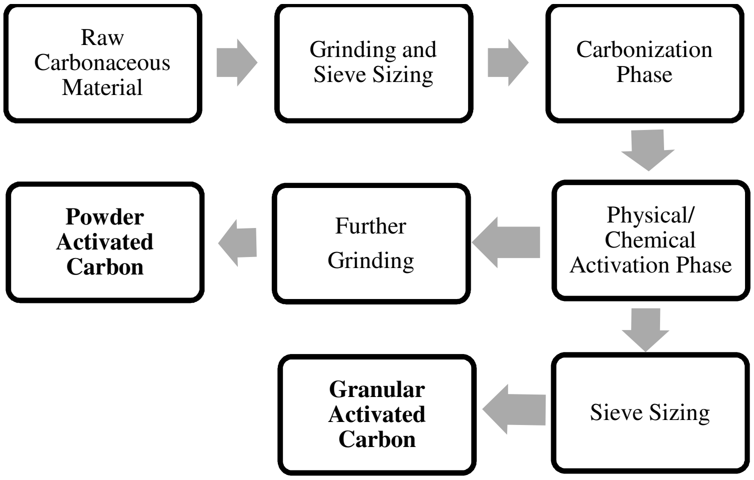

Figure 2-4: The development of powder activated carbon and granular activated carbon.

2.2.6 Application to Petroleum Coke

Throughout the literature, petroleum coke has been observed as a common organic waste product used for the production of activated carbon. When petroleum coke is activated, it has a higher activation yield and surface area than most carbonaceous raw materials (Stavropoulos and Zabaniotou, 2009). However, the costs involved in generating this material through either physical or chemical activation tend to be quite high where, balancing the yield over the total investment cost can be challenging for large-scale industries (Stavropoulos and Zabaniotou, 2009). At the same time, due to the higher associated yield of produced activated coke, there may be lower overall costs associated with the production of activated petroleum coke compared to other common raw materials (such as wood). Petroleum coke is also an abundant waste material, making it a widely available and feasible material for use (Stavropoulos and Zabaniotou, 2009). These low costs may allow for companies to invest in the higher costs associated with activation. Thus, the material may ultimately be an economically viable source to the oil sands industry.

Generally, activated coke is used to treat organic contaminants due to its high organic carbon content (Barczak et al., 2005). Throughout the literature, it has been observed to adsorb both low and high molecular weight compounds. However, the method of activation will control pore and surface area development and ultimately, its adsorption capacity.

The literature indicates that different techniques have been previously used to activate petroleum coke, where tests typically involve chemical activation with KOH. Marsh et al. (1984) chemically activated a variety of petroleum cokes (including green and needle cokes) using solid KOH. When the cokes were added to 80% wt. KOH, they observed a surface area development of 2700 m^2/g. When 10 to 80% wt. KOH was added to the petroleum cokes, they observed a decrease in surface area to 2100 m^2/g. Consequently, increasing the addition of KOH led to an increase in measured surface area. The researchers found that the addition of KOH may cause the separation of constituent lamellae through the process of oxidation of cross-linking carbon atoms, forming functional groups on the edges of lamellae (Marsh et al., 1984). These additional functional groups may cause the edges to pucker out of the once flat carbon formation. Once the KOH salts are removed through washing after activation, the lamellae can no longer return to their flat state- creating an enhanced microporosity (Marsh et al., 1984).

Itoh et al. (1993), chemically activated petroleum coke with varying ratios of KOH. In these experiments, the KOH/carbon ratios ranged from 1 to 10, and the activation temperatures ranged from 600 to 900^oC. Itoh et al. (1993) found that an optimal surface area of 3100 m^2/g resulted from an activated product that used a KOH/carbon ratio equal to 5, and an activation temperature of 700^oC (for 100 minutes). Their research suggested that low KOH/carbon ratios produced relatively small pores, whereas larger pores were developed with higher

KOH/carbon ratios. When activation times exceeding 2 hours were used, it had little effect on the pore size distribution. The study also indicated that through the dehydration of KOH, CO_2 is released from the water-gas reactions and carbonate is formed, leading to the widening of pores (Itoh et al., 1993). The results of this testing indicated the potential commercial use of the activated petroleum coke as an effective adsorbent.

Another study used petroleum fluid coke to conduct chemical and physical activation. More specifically, DiPanfilo and Egiebor (1996) impregnated fluid coke with KOH (at 4% wt.). The mixture was then dried at 110^{o}C in a vacuum before flushing in a tube furnace for 8 hours under a flow of nitrogen gas (18 cm^3/min). An activation temperature of 850^{o}C was achieved through ramping in increments of 5.5 and 6.9^{o}C/min under a flow of steam. The results indicate a maximum surface area of 176 m^2/g. After the tests, only 50% of the KOH was recoverable, indicating that 50% of the KOH may have formed K_2O solids within the coke matrix (DiPanfilo and Egiebor, 1996). The same tests were conducted for raw fluid coke undergoing physical activation with steam, in the same environment as the chemically activated fluid coke. The physically activated fluid coke produced a higher surface area of 318 m^2/g (from an initial surface area of 5.5 m^2/g) than the chemically activated fluid coke. The KOH during chemical activation merely resulted in faster activation with respect to the carbon burn-off rate. According to DiPanfilo and Egiebor (1996), the chemical activation of the fluid coke was counterproductive as it did not promote greater pore structure than the physically activated coke. The produced surface areas within this experiment were within the range of surface areas for commercially available activated carbons (100- 1200 m^2/g) (DiPanfilo and Egiebor, 1996).

In 2000, Lee and Choi activated delayed coke with both KOH and NaOH resulting in surface areas up to 1980 m^2/g and 1350 m^2/g respectively. Results proved that KOH was a more effective activating agent than NaOH. For these experiments the delayed coke was heated at temperatures between 400 and 600^{o}C, in ratios of 1-4 for KOH or NaOH/ coke. Samples were heated in a furnace under the flow of nitrogen for the carbonization stage before activation in a microwave system (Lee and Choi, 2000). The tests suggest a relationship between the production of surface area and the reduction in sulphur content (desulphurization) within the delayed coke. More specifically, the breakage in the C-S bonds on the coke during activation results in a release of sulphur, and the formation of pores and active sites. This allows for the porosity and surface area to develop where the sulphur is removed from the surface of the delayed petroleum coke. Pore development will not occur until the residual sulphur content is decreased to 0.1%, resulting in a total sulphur reduction rate of 98% (Lee and Choi, 2000).

In contrast to the raw petroleum cokes activated with KOH, Buitrón et al. (2000) activated coke using three different chemical agents (H_3PO_4, NaOH, and $ZnCl_2$). For each test, 100g of coke was mixed with each agent before boiling at 110°C for 2 hours under the flow of nitrogen gas (1 L/min). Afterwards, the mixture was washed with distilled water and filtered to remove the activating agents (Buitrón et al., 2000). The researchers found through the use of scanning electron micrographs (SEMs), that not all particles are always affected by the activation procedure. However, the results showed that H_3PO_4 produced the greatest fissuring and cracking within the grains, leading to the production of higher surface areas. The iodine index for H_3PO_4, NaOH, and $ZnCl_2$ were 57 mg/g, 42 mg/g, and 73 mg/g, respectively (Buitrón et al., 2000). At the same time, the surface area produced for all three agents were as follows: 31.6 m^2/g (H_3PO_4), 35.4 $m^2g/$ (NaOH), and 16.3 m^2/g ($ZnCl_2$) (Buitrón et al., 2000). Out of the three activation agents, NaOH produced the greatest surface area and activation with $ZnCl_2$ led to the production of the greatest iodine index. However, during adsorption tests, H_3PO_4 had the greatest adsorption capacity of metals (silver and mercury) and phenol. Overall, the types of fissuring occurring on the surface of the coke due to the chemical activation agents may differ, altering the adsorption capacity.

Shawwa et al. (2001) used a physical activation technique to successfully adsorb colour and chlorinated organics from pulp mill wastewater. For their experiments they utilized dried ground delayed coke between 200 and 300 mesh sizes (Shawwa et al., 2001). The initial drying process allowed for the coke to have a constant weight while removing water particles within the pores. The grinding of the coke allowed for a higher initial surface area preferable for activation. The carbonization stage consisted of heating the coke to 850 ± 2°C at a heating rate of 10°C/min under nitrogen gas. As soon as the temperature of the reactor reached the desired activation temperature, the atmosphere was switched to steam and the activation stage began for periods ranging from 1 to 6 hours (Shawwa et al., 2001). After the physical activation was completed, the surface characteristics of the coke were analyzed using methylene blue adsorption. The adsorption capacity was also determined through the completion of batch tests. Results show that burn-off rates increased with increases in activation time. The application of steam also led to the widening of the pores, ultimately increasing the surface area of the activated delayed coke (Shawwa et al., 2001). A discussion of the results indicated that at low initial surface areas, there are fewer sites for the carbon-steam reaction to occur; with increases in surface area, more active sites for the carbon-steam reaction were exposed (Shawwa et al., 2001). For this experiment, the maximum surface area was achieved at a water efficiency and burn-off of 54.3% and 48.5% respectively; after which point the burning of the carbon walls was suggested to occur (Shawwa et al., 2001). At this point, the development of macropores occurs which is not ideal for the adsorption of chlorinated organics. Maximum adsorption occurred when coke samples were activated for 4 hours leading to a methylene blue value of 100.5 mg/g (Shawwa et al., 2001).

A comparison of the activation techniques was carried out by Guo et al. (2005); more specifically, they investigated chemical activation with KOH, physical activation with H_2O, and a combination of the two activation techniques. Chemical activation consisted of soaking ground coke in KOH for 2 hours, followed by drying at 150°C for 4 hours. Activation occurred at 800°C, and washing was completed with 0.5 M HCl and distilled water in sequence (Guo et al., 2005). Physical and chemical/physical co-activation occurred in a reactor where heating occurred at 800°C under the flow of nitrogen (Guo et al., 2005). In contrast to Lee and Choi (2000) who used a KOH/ coke ratio of 4 to 1; Guo et al. (2005) used a ratio of 2 to 1. The following BET surface areas were found for activation times ranging from 10 to 60 min: less than 3000 m^2/g (KOH+H_2O) > less than 2000 m^2/g (KOH) > less than 100 m^2/g (H_2O). The combination of KOH+H_2O worked effectively due to the formation of cross-linking and aromatization during carbonization which helped to bond the volatile products before pyrolysis. This resulted in a reduction in tar formation and an increase in carbon yield (Guo et al., 2005). The steam produced by the H_2O allowed for the chemical activation agent to access more available pores, further enhancing the pore development and surface area. With respect to the activation times used for the different combinations, Guo et al. (2000) found that increased activation time resulted in a greater pore development within the petroleum cokes. Petroleum cokes tested to contain transitional metals such as manganese, iron, chrome and nickel developed greater surface areas than those containing only iron and manganese. Transitional metals within the cokes tend to act as catalysts speeding up the reaction rates of the activation agents, and leading to the development of highly porous carbons (Guo et al., 2005). As a result, the type of coke material used will alter the rates of the activation agents used in this study.

Changhou et al. (2005) added a pre-carbonization stage to their chemical activation experiments. Pre-carbonization was observed to develop activated carbons with a higher BET surface area (examined through nitrogen adsorption isotherms) and microporosity than those activated without pre-carbonization (Changhou et al., 2005). Petroleum coke (150-180 μm in size) was pre-carbonized under argon flow at various temperatures ranging from 500 to 1200°C for 3 hours. After pre-carbonization, samples underwent chemical activation with 6g of KOH (with a KOH/carbon ratio = 3) under argon flow for 1 hour at temperatures ranging from 400 to 700°C (Changhou et al., 2005). The temperatures chosen for pre-carbonization and chemical activation were higher than those previously used for chemical activation throughout the literature. These temperatures may alter the thermal decomposition of volatiles within the carbon, as well as the development of pores. The highest BET surface area was developed in the activated carbon product produced without pre-carbonization and the lowest surface area was attributed to activated carbons pre-carbonized at 1200°C with values of 1997 m^2/g and 3 m^2/g, respectively. Consequently, an increase in pre-carbonization temperature appears to decrease the amount of surface species (or active sites) before chemical activation with KOH (Changhou et al., 2005). The surface species are important for chemical activation, as they react with the KOH resulting in the development of pores.

The literature also indicates an interest in the activation of bituminous coal, where results may show similarities to activated petroleum coke. This soft coal is also high in carbon content, but contains bitumen. Experiments with bituminous coal typically encompass physical activation which has not been intensely explored with petroleum coke. Linares-Solano et al. (1995) physically activated Spanish bituminous coal in both a fluidized bed and horizontal bed reactor under a N_2/steam mixture and CO_2. It was found that steam activation is not affected by the type of reactor used, but can be completed quicker with the use of a fluidized bed reactor (Linares-Solano et al., 1995). With respect to CO_2 activation, activation within a horizontal bed reactor resulted in a 30% increase in surface area than tests conducted within a fluidized bed reactor. The difference in surface area achieved between CO_2 and steam activation was attributed to the fact that water molecules have a greater accessibility to the inner porosity of a carbon material than CO_2. Activation with steam led to surface areas exceeding 1000 m^2/g (Linares-Solano et al., 1995). As a result, the reactor type and activating agent combination may affect surface area and porosity development within a char.

Asensio et al. (1996) investigated the direct activation (simultaneous carbonization and activation) of bituminous coal in order to create a model to simulate the experimental data. A study of the kinetic reactions during activation indicated that a large presence of hydrogen can inhibit gasification reactions; lowering the reaction rate (Asensio et al., 1996). Consequently, lower quantities of steam may be more appropriate for the development of microporous carbons. Chemical reactions between water molecules and the carbon surface of a char will also lead to the formation of the following gases: CO, CO_2, and CH_4; though, the development of methane is considered to be slow at atmospheric pressures, and can be neglected (Asensio et al., 1996). The developed models also suggested a good correlation between specific surface area and the rate of burn-off (Asensio et al., 1996). Consequently, the rate of burn-off may allow for an approximation of surface area before surface characterization procedures are conducted.

In 1998, Kim and Hong examined the activation of bituminous coal through steam activation processes, where experiments took place within a rotary type furnace. Batch tests were later conducted with benzene and methyl ethyl ketone (MEK) to observe the adsorption capacity of the activated carbons. As they altered the operating conditions they found the following results: optimum activation temperatures with respect to adsorption capacity and activation yield ranged from 850 to 880^{o}C; iodine number and BET surface area tended to increase with heating rate; micropores favoured the temperature range of 850 to 880^{o}C; and, maximum adsorption capacity was associated with a yield of approximately 35 to 40% (Kim and Hong, 1998). This also confirms previous experiments where increased burn-off produced a greater surface area for adsorption.

Porosity development of bituminous coals was investigated in a fluidized bed reactor when activation atmospheres consisted of CO_2 and steam (Cazorla-Amorós et al., 2000). The authors suggest that different oxidant gases may lead to the production of activated products with different pore size distributions

(Cazorla-Amorós et al., 2000). It was clear that CO_2 activation affected the reaction rates during activation, and ultimately the porosity and surface area development leading to larger mesopores (Cazorla-Amorós et al., 2000). In contrast, steam activation in petroleum-based chars led to the development of numerous micropores, more suitable for adsorption.

Consequently, the literature confirms the use of steam and CO_2 for physical activation processes, whereas chemical activation procedures tend to favour the use of KOH as an activating agent. However, it has not been determined which methodology and activation parameters are most optimal for delayed and fluid coke activation. Studies have also yet to thoroughly characterize the individual activated products to describe the structural and behavioural characteristics and properties of activated petroleum coke.

2.3 Chapter 2 References

Allen, E. 2008a. Process water treatment in Canada's oil sands industry: I. Target pollutants and treatment objectives. *Journal of Environmental Engineering and Science*; 7: 123-138.

Allen, E. 2008b. Process water treatment in Canada's oil sands industry: II. A review of emerging technologies. *Journal of Environmental Engineering and Science*; 7: 499-524.

Appelo, C.A.J., and Postma, D. 2007. Geochemistry, groundwater and pollution, Second Edition. A.A. Balkema Publishers, Amsterdam; pp. 78- 343.

Asensio, M., Font, R., Marcilla, A., and Martin-Gullón, I. 1996. Steam activation of a bituminous coal in a multistage fluidized bed pilot plant: operation and simulation model. *Industrial and Engineering Chemistry Research*; 35: 4139-4146.

ASTM. 1999. Standard practice for determination of adsorptive capacity of activated carbon by aqueous phase isotherm technique. *ASTM International*. PA, USA; D3860-98.

ASTM. 2006. Standard test method for determination of iodine number of activated carbon. *ASTM International*. PA, USA; D 4607-94.

ASTM. 2009. Standard test method for methylene blue index of clay. *ASTM International*. PA, USA: C 837- 09.

Bansal, R.C., Donnet, J., and Stoeckli, F. 1988. Active carbon. Marcel Dekker, Inc., New York. 482 pp.

Bansal, R.C., and Goyal, M. 2005. Activated carbon adsorption. Taylor and Francis Group, Florida. 497 pp.

Beier, N., Sego, D., Donahue, R., and Biggar, K. 2007. Trickle-freeze separation of contaminants from saline waste water. *International Journal of Mining, Reclamation and Environment*; 21: 144-155.

Brient, J., Wessnet, P., and Doyler, M. 1995. Naphthenic acids- Kirk-Othmer encyclopedia of chemical technology. John Wiley and Sons, New York: 1017-1029.

Brunauer, S., Emmett, P.H., and Teller, E. 1938. Adsorption of gases in multimolecular layers. *Journal of the American Chemical Society*; 60: 309-319.

Budinova, T., Björnbom, E., Ekinci, E., Goranova, M., Grimm, A., Minkova, V., and Yardim, F. Characterization and application of activated carbon produced by H_3PO_4 and water vapour activation. *Fuel Processing Technology*: 87; 899-905.

Buitrón, G., Duran Moreno, A., Ramirez, Zamora, R.M., and Schouwenaars, R. 2000. Production of activated carbon from petroleum coke and its application in water treatment for the removal of metals and phenol. *Water Science and Technology*; 42: 119-126.

Canadian Association of Petroleum Producers (CAPP). 2009. *Water use in Canada's oil sands*. 2009-0022. CAPP, Calgary, Alberta. Available at http://www.capp.ca/library/publications/crudeOilAndOilSands/pages/pubInfo.aspx?DocId=154986#qizoWOc35CWl (accessed November 29, 2010).

Cazorla-Amorós, D., Linares-Solano, A., Martin-Gullón, I., and Salinas-Martinez de Lecea. 2000. Porosity development during CO_2 and steam activation in a fluidized bed reactor. *Energy and Fuels*; 14: 142-149.

Changhou, L., Chunlan, L., Shaoping, X., Shuqin, L., and Yixiong, G. 2005. Effect of pre-carbonization of petroleum cokes on chemical activation process with KOH. *Carbon*; 43: 2295-2301.

Chen, H. 2010. Microwave heating for adsorbents regeneration and oil sands coke activation. Published PhD thesis. University of Alberta, Edmonton, Canada.

Choma, J., Jankowska, H., and Swiatkowski, A. 1991. Active carbon. Ellis Horward Limited. Chichester, England; 104pp.

Clemente, J.S., and Fedorak, P.M. 2005. A review of the occurrence, analyses, toxicity, and biodegradation of naphthenic acids. *Chemosphere*; 60: 585-600.

Davis, M.L., and Masten, S.J. 2004. Principles of environmental engineering and science. The McGraw Hill Series in Civil and Environmental Engineering, New York; p 472- 475.

DiPanfilo, R., and Egiebor, N.O. 1996. Activated carbon production from synthetic crude coke. *Fuel Processing Technology*; 46: 157-169.

Fedorak, P.M., and Coy, D.L. 2006. Oil sands cokes affect microbial activities. *Fuel*; 85: 1642-1651.

Furimsky, E. 1998. Gasification of oil sands coke: review. *Fuel Processing Technology*; 56: 263-290.

Gao, W., Smith, D.W., and Sego, D.C. 2004. Treatment of pulp mill and oil sands industrial wastewaters by the partial spray freezing process. *Water Research*; 38: 579-584.

Gregg, S.J., and Sing, K.S.W. 1982. Adsorption, surface area and porosity. Academic Press Incorporated, London; pp. 1-39.

Grewer, D.M., Young, R.F., Whittal, R.M., and Fedorak, P.M. 2010. Naphthenic acids and other acid-extractables in water samples from Alberta: What is being measured? *Science of the Total Environment*, doi:10.1016/j.scitotenv.2010.08.013.

Guo, Y., Han, X., Li, Z., Qiu, J., Sun, X., Wu, M., and Zha, Q. 2005. Preparation of porous carbons from petroleum coke by different activation methods. *Fuel*; 84: 1992-1997.

Hall, E.S., and Tollefson, E.L. 1979. *Hydrocarbon removal from and upgrading of aqueous waste water from oil sands recovery operations*. Report prepared for Alberta Environmental Research Trust, Alberta Environment, Edmonton, Alberta.

Hameed, B.H., Ahmad, A.L., and Latiff, K.N.A. 2007. Adsorption of basic dye (methylene blue) onto activated carbon prepared from rattan sawdust. *Dyes and Pigments*; 75: 143-149.

Hassler, J.W. 1941. Active carbon: the modern purifier. Githens-Sohl Corporation. New York: 159 pp.

Hao, C., Headley, J.V., Peru, K.M., Frank, R., Yang, P., and Solomon, K.R. 2005. Characterization and pattern recognition of oil-sand naphthenic acids using comprehensive two-dimensional gas chromatography/ time-of-flight mass spectrometry. *Journal of Chromatography A*; 1067: 277-284.

Holowenko, F.M., MacKinnon, M.D., and Fedorak, P.M. 2002. Characterization of naphthenic acids in oil sands wastewaters by gas chromatography-mass spectrometry. *Water Research*; 36: 2843-2855.

Hong, I.K., and Kim, S.C. Pore development of the activated carbon prepared by steam activation process. *Journal of Industrial and Engineering Chemistry*; 4: 177-184.

Itoh, M., Otowa, T., and Tanibata, R. 1993. Production and adsorption characteristics of MAXSORB: High-surface-area active carbon. *Gas Separation and Purification*; 7: 241-245.

Ityokumbul, M.T. 1994. Experiment evaluation of molten caustic leaching of and oil sand coke residue. *The Canadian Journal of Chemical Engineering*; 72: 370-374.

Janfada, A., Headley, J.V., Peru, K.M., and Barbour, S.L. 2006. A laboratory evaluation of the sorption of oil sands naphthenic acids on organic rich soils. *Journal of Environmental Science and Health Part A*; 41: 985-997.

Jang, H., and Etsell, T.H. 2009. Morphological and mineralogical characterization of oil sands fly ash. *Energy and Fuels*; 19: 2121-2128.

Karanfil, T., and Kilduff, J.E. 1999. Role of granular activated carbon surface chemistry on the adsorption of organic compounds. 1. Priority pollutants. *Environmental Science and Technology*; 33: 3217-3224.

Kelly, E.N., Schindler, D.W., Hodson, P.V., Short, J.W., Radmanovich, R., and Nielsen, C.C. 2010. Oil sands development contributes elements toxic at low concentrations to the Athabasca River and its tributaries. *PNAS*; 107: 16178-16183.

Kim, D., and Sohn, S. 2005. Modification of Langmuir isotherm in solution systems- Definition and utilization of concentration dependent factor. *Chemosphere*: 58; 115-123.

Kumar, B.G.P., Miranda, L.R., Shivakamy, K., and Velan, M. 2006. Preparation of steam activated carbon from rubberwood sawdust (*Hevea brasiliensis*) and its adsorption kinetics. *Journal of Hazardous Materials:* B136; 922-929.

Langmuir, D. 1997. Aqueous environmental geochemistry. Prentice Hall, New Jersey; p 343- 395.

Lee, S.H., and Choi, C.S. 2000. Chemical activation of high sulfur petroleum cokes by alkali metal compounds. *Fuel Processing Technology*; 64: 141-153.

Linares-Solano, A., Munoz-Guillena, M.J., Salinas-Marinez de Lecea, C., and Serrano-Talavera, B. 1995. 'Steam and CO_2 activation of bituminous coal in a fluidized bed reactor' in Carbon Conference: *Proceedings of the 22nd Biennial Conference*, San Diego, CA, 16-21 July 1995, University of California, San Diego, California, pp. 412-413.

Marsh, H., O'Grady, T.M., Wennerberg, A., and Yan, D.S. 1984. Formation of active carbon cokes using potassium hydroxide. *Carbon*; 22: 603-611.

Martin, J.W., Han, X., Peru, K.M., and Headley, J. 2008. Comparison of high- and low-resolution electrospray ionization mass spectrometry for the analysis of naphthenic acid mixtures in oil sands process water. *Rapid Communications in Mass Spectrometry*; 22: 1919-1924.

Martin-Gullón, I., and Menéndez-Diaz, J.A. 2006. Types of carbon adsorbents and their production: Activated carbon surfaces in environmental remediation. Elesvier, Ltd, Spain: pp. 1-45.

Mattson, J.S., and Mark, H.B., Jr. 1971. Activated carbon: surface chemistry and adsorption from solution. Marcel Dekker, Inc. New York: 237pp.

Meredith, W., Kelland, S.-J., and Jones, D.M. 2000. Influence of biodegradation on crude oil acidity and carboxylic acid composition. *Organic Geochemistry*; 31: 1059-1073.

Mohamed, M.H., Wilson, L.D., Headley, J.V., and Peru, K.M. 2008. Screening of oil sands naphthenic acids by UV-VIS absorption and fluorescence emission spectrophotometry. *Journal of Environmental Science and Health Part A*; 43: 1700-1705.

Onder, H., and Bagdoyan, E.A. 1994. Everything you always wanted to know about petroleum coke: a handbook. Svedala Industries, Kennedy Van Saun, Danville, PA: 131pp.

Potgieter, J.H. 1991. Adsorption of methylene blue on activated carbon. *Journal of Chemical Education*; 68: 349- 350.

Quagraine, E.K., Peterson, H.G., and Headley, J.V. 2005. In situ bioremediation of naphthenic acids contaminated tailing pond waters in the Athabasca oil sands region- Demonstrated field studies and plausible options: A review. *Journal of Environmental Science and Health*; 40: 685-722.

Rogers, V.V., Wickstrom, M., Liber, K., and MacKinnon, M.D. 2002. Acute and subchronic mammalian toxicity of naphthenic acids from oil sands tailings. *Toxicological Sciences*; 66: 347- 355.

Rouquerol, J., Avnir, D., Fairbridge, C.W., Everett, D.H., Haynes, J.H., Pernicone, N., Ramsay, J.D.F., Sing, K.S.W., and Unger, K.K. 1994. Recommendations for the characterization of porous solids. *International Union of Pure and Applied Chemistry*; 66: 1739-1758.

Scott, A.C., and Fedorak, P.M. 2004. *Petroleum coking: A review of coking processes and the characteristics, stability, and environmental aspects of coke produced by the oil sands companies*. Report Submitted to Suncor Energy Inc., Syncrude Canada Ltd., and Canadian Natural Resources Ltd.; 66 p.

Scott, A.C., Young, R.F., and Fedorak, P.M. 2008. Comparison of GC-MS and FTIR methods for quantifying naphthenic acids in water samples. *Chemosphere*; 73: 1258-1264.

Shawwa, A., and Smith, D., and Sego, D.C. 1999. *Color and chlorinated organic reduction in Kraft pulp mill wastewater using activated petroleum coke*. Sustainable Forest management Network of Centers of Excellence, Report MIT-6, Edmonton, Canada.

Shawwa, A.R., and Smith D.W., and Sego, D.C. 2001. Color and chlorinated organics removal from pulp mills wastewater using activated petroleum coke. *Water Resources*; 35: 745-749.

Sing, K.S.W., Everett, D.H., Haul, R.A.W., Moscou, L., Pierotti, R.A., Rouquerol, J., and Siemieniewska, T. 1985. Reporting physisorption data for gas/solid systems with special reference to the determination of surface area and porosity. *International Union of Pure and Applied Chemistry*; 57: 603-619.

Sivapullaiah, P.V., Prasad, B.G., and Allam, M.M. 2008. Methylene blue surface area method to correlate with specific soil properties. *Geotechnical Testing Journal*; 31: 1-10.

Stavropoulos, G.G., and Zabaniotou, A.A. 2009. Minimizing activated carbons production cost. *Fuel Processing Technology*; 90: 952-957.

Vlasopoulous, N., Memon, F.A., Butler, D., and Murphy, R. 2006. Life cycle assessment of wastewater treatment technologies treating petroleum process waters. *Science of the Total Environment*; 367: 58-70.

Whitby, C. 2010. Microbial naphthenic acid degradation: Advances in applied microbiology. Elesvier, Ltd, UK: 70: 93- 125.

Yasin, Y., Hussein, M.Z., and Ahmad, F.H. 2007. Adsorption of methylene blue onto treated activated carbon. *The Malaysian Journal of Analytical Sciences*; 11: 400-406.

Yang, R.T. 2003. Adsorbents: fundamentals and applications. John Wiley and Sons, Inc., New Jersey; pp. 70- 130.

Yen, T., Marsh, W.P., MacKinnon, M.D., and Fedorak, P.M. 2004. Measuring naphthenic acids concentrations in aqueous environmental samples by liquid chromatography; *Journal of Chromatogtaphy A*; 1033: 83-90.

Zdravkov, B.D., Cermak, J.J., Sefra, M., and Janku, J. 2007. Pore classification in the characterization of porous materials: A perspective. *Central European Journal of Chemistry*; 5: 385-395.

CHAPTER 3: ACTIVATION AND CHARACTERIZATION OF DELAYED AND FLUID PETROLEUM COKE

3.1 Introduction

The Athabasca oil sands region located in north-eastern Alberta, Canada contains approximately 174 billion barrels of bitumen (Allen, 2008a; CAPP, 2009). Once extracted, the bitumen is upgraded to a synthetic crude oil with either delayed or fluid thermal coking processes (Fedorak and Coy, 2006). Throughout oil production, substantial quantities of wet and dry wastes are produced. The large volumes of water utilized for bitumen extraction are stored on-site within tailings ponds. The major dry waste product produced throughout the upgrading coking processes is delayed and fluid petroleum coke. Though petroleum cokes typically have a high calorific value (approximately 37 MJ kg^{-1}), their high sulphur contents limit their use as a fuel (Lee and Choi, 2000). As a result, petroleum cokes are typically stockpiled on-site. Syncrude Canada Ltd. and Suncor Energy Inc. are producing over 5 million tonnes of coke per year; estimates indicate 1 billion m^3 of total coke production throughout the entire lifetime of the oil sands operations in Alberta (Fedorak and Coy, 2006).

The removal of organic acids from tailings water through the use of adsorbents is considered to be an emerging technology for the oil sands industry (Allen, 2008b). Conventional materials used as adsorbents in the past for organic contaminant removal from industrial wastewaters include: granular activated carbon (GAC), zeolites, synthetic polymers, clays, and organic matter (Allen, 2008b; Dabrowski et al, 2005). However, the costs associated with obtaining and preparing large quantities of these adsorbents for the treatment of tailings ponds (where over $4x10^8$ m^3 of process-affected water is currently stored [Paslawski et al., 2009]) may represent a large investment cost for the oil sands industry. A readily available raw carbon source (of approximately 80-85% by weight) (Karanfil and Kilduff, 1999) to the oil sands companies is their stockpiled petroleum coke. Petroleum coke is a common organic precursor for the development of activated carbon (Lee and Choi, 2000; Chang et al, 2000; Shawwa et al., 2001; and Kawano et al., 2008). When activated, petroleum coke has a higher activation yield and surface area than most precursors (wood, carbon black) (Stavropoulos and Zabaniotou, 2009).

Activation typically consists of two phases: carbonization- causing initial pyrolytic decomposition within the pores of a material; and, activation- turning the carbonized product into one with the greatest number of pores (Bansal and Goyal, 2005). Due to the temperatures used for thermal cracking during bitumen upgrading procedures, the produced coke is considered to be a pre-carbonized material. The activation stage can be completed either physically or chemically.

Physical activation generally consists of conventional heating at high temperatures in the presence of steam, carbon dioxide, air, or any mixture. The active oxygen within the gases reacts with the carbon skeleton, releasing CO_2 and CO; where, external heating drives the reactions on the surface of the carbon-resulting in an etching of pores. In contrast, chemical activation requires the carbon material to be initially impregnated with an activating agent such as KOH, $ZnCl_2$, H_3PO_4, or K_2S before heating (Yang, 2003). These dehydrating reagents allow for lower external heating temperatures as well as shorter activation times to produce a higher yield of active carbon. Depending on the activation conditions, one can expect the production of activated products with different characteristics and adsorbent behaviours. As a result, activation can directly influence the following properties of a material: pore development, adsorbent yield, surface functional groups, surface area, and molecular structure.

Previous studies have activated petroleum coke for various wastewater treatment applications, where tests commonly involved chemical activation with KOH (Itoh et al., 1993; Di Panfilo and Egiebor, 1996; Lee and Choi, 2000; Buitron et al., 2000; Changhou et al., 2005; and Guo et al., 2005). Though this technique is preferred due to the shorter activation time needed to produce higher surface area products, Di Panfilo and Egiebor (1996) found that only 50% of the KOH required for activation was recoverable. Physical activation has the advantage of using readily available activation agents such as steam. However, physical activation has not been well explored on oil sands delayed and fluid coke. Di Panfilo and Egiebor (1996) conducted physical activation of oil sands fluid coke using CO_2 + steam and an activation temperature of 850°C for 6 h. The results indicated a BET surface area of 319 m^2/g and a microporous volume of 0.244 cm^3/g (Di Panfilo and Egiebor, 1996). Shawwa et al. (2001) used CO_2 and steam to activate delayed coke at 850°C for 4 h to produce activated carbon with a methylene blue value of 100 mg/g; however further characterization of the material was not completed. The activated coke was then used to successfully remove >90% chlorinated organics and colour from pulp mill waste water.

Physical activation was also separately conducted on fluid coke by Bratu (2009) using CO_2 and steam to produce activated products with surface areas >500 m^2/g for mercury gas removal. These studies indicate that the physical activation of delayed and fluid petroleum coke may generate high surface area adsorbents that can be useful to the oil sands industry; however, thorough characterization of the adsorbents has yet to be completed, and an investigation of the best physical activation parameters necessary for producing high surface area adsorbents out of delayed and fluid coke has yet to be explored. Studies have also yet to compare characterized activated delayed and fluid coke.

This research investigates the impact of physical activation on raw delayed and fluid oil sands coke. It will also evaluate the activation conditions which would lead to the production of an adsorbent with the greatest surface area and porosity available for potential use in oil sands tailings water treatment. In doing so, a current waste by-product will be converted into a useful product and commodity to the oil sands industry for use in tailings remediation.

3.2 Experimental Methods

3.2.1 Sample Preparation and Activation

Samples of delayed and fluid coke were obtained from Suncor Energy Inc. and Syncrude Canada Ltd., respectively. Due to the grain size distribution of the delayed coke, the material was ground with a grinder and sieved to a 75-150 μm aperture mesh size. The fluid coke was already in a granular form with grain sizes less than 300 μm, and was sieved to achieve the same particle size range of the ground delayed coke. The coke samples were dried in an oven for 24 h at 110°C and stored within a desiccator before activation. All sieved coke samples were stored in labelled plastic containers at room temperature.

Activation of the delayed and fluid coke samples involved conventional heating in a fixed-bed muffle furnace and a two-stage simultaneous carbonization/ activation sequence (Figure 3-2). In each experiment, 20 g of petroleum coke was placed in a 50 mm OD quartz tray inside a 70 mm OD vertical quartz reactor (Figure 3-1). The vertical design allowed for gas flow to circulate throughout the quartz reactor. The quartz reactor was designed to fit within the center of the muffle furnace in order to receive consistent heating from the open coil elements.

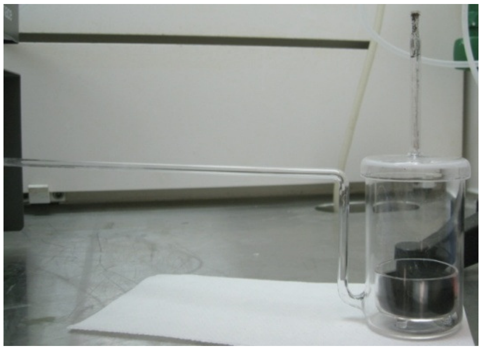

Figure 3-1: Vertical quartz reactor designed to fit into the fixed-bed muffle furnace set-up.

Quartz tubing of ¼” OD was designed to connect the reactor to the ¼” teflon gas tubing to allow for a constant flow through the system. The quartz reactor was manufactured by the University of Alberta Chemistry glass shop.

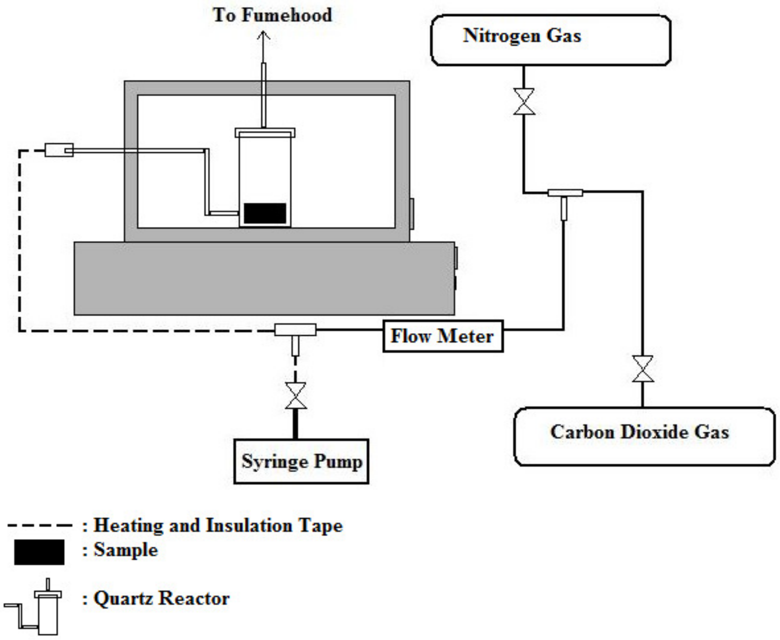

Figure 3-2: Schematic diagram of the physical activation process for delayed and fluid coke in a fixed-bed muffle furnace.

The following parameters were controlled to determine the most effective activation conditions: time (2-6 h); temperature (800-900^{o}C); atmosphere (CO_2, CO_2 + steam, and N_2 + steam); and steam rate (0.3-0.5 mL of $H_2O_{(l)}$/min). Once samples were placed in the furnace, the reactor was purged of oxygen gas with N_2 for 15 minutes. The following compressed gases were obtained from Praxair: CO_2 (bone dry) and N_2 (PP). Experiments conducted in the absence of steam had a gas flow rate of 300 mL/min. When steam was incorporated into the activation procedures, gas flow was switched to 100 mL/min to allow for a greater molar gas composition of steam. At the end of the activation period, the furnace was turned off and left to cool overnight under N_2. Samples were then stored within a desiccator until required for further experimentation. Furnace temperature was monitored through the use of an outside thermocouple (Type K) thermometer placed above the sample at the middle of the furnace. All heat up sequences were monitored and logged. Activation sequences were also monitored hourly in order to ensure consistency throughout the tests. The CO_2 and N_2 flow rates were calibrated a dry flow calibrator (Definer 220, Bios International), where continuous sampling of 10 samples were averaged to achieve the flow rates through a 0.1-1.0 L/min rotameter. The continuous sampling method allowed for any fluctuations in flow to be accounted for. Once passing through the system, the gases were allowed to exit straight to the fume hood. Steam was generated by injecting ultra-pure water into the activation gas stream via a syringe pump (NE-300, New Era Pump Systems, Inc.), a 100 mL glass syringe (Hamilton), and a 18 gage x 4” long stainless steel needle. The water stream was heated to approximately $180^{\circ}C \pm 10^{\circ}C$ using insulated heating tape and a variac (Powerstat 116, Superior Electric Co.).

Samples were weighed before and after activation to determine the yield and burn-off (amount of petroleum coke lost during the activation sequence). Higher yield corresponds to enhanced pore development within the samples. The yield and burn-off were calculated using Equations 3-1 and 3-2.

$$\%\,\text{Yield} = \frac{\text{Final Mass of Activated Petroleum Coke Sample}}{\text{Initial Mass of Petroleum Coke Sample}}\ \text{x}\ 100\% \quad \textbf{(3-1)}$$

$$\%\,\text{Burn} - \text{off} = 100\% - \%\,\text{Yield} \quad \textbf{(3-2)}$$

3.2.2 Characterization of the Raw and Activated Samples

To determine the success of the activation experiments, characterization of the structure and behaviour of the activated delayed and fluid coke samples was necessary. This described the intrinsic properties of the delayed and fluid coke samples.

3.2.2.1 Thermogravimetric Analysis (TGA)

Raw fluid and delayed coke were analyzed on a thermogravimetric analyzer (TA Instruments, Q500) within the National Institute for Nanotechnology (NINT) at the University of Alberta. Samples were heated under N_2 at temperatures ranging from 21 to $800^{\circ}C$ at 60 mL/min, and switched to CO_2 for temperatures ranging from 800 to $950^{\circ}C$ at 60 mL/min. In doing so, the analyses mimicked the temperatures occurring during activation.

3.2.2.2 X-Ray Diffraction (XRD)

An X-ray diffractometer (Bruker D8 Discover) with an area detector and a monochromatic beam operated at 40 kV and 40 mA was used to characterize raw and activated delayed and fluid coke samples. The final spectrum peaks were analyzed with JCPDS PDF2 [International Centre for Diffraction Data (ICDD)]. Analysis was completed at the National Institute for Nanotechnology (NINT) x-ray facilities at the University of Alberta.

3.2.2.3 Scanning Electron Micrographs (SEMs)

Scanning electron microscopy (Hitachi S-2500) was completed on raw and activated delayed and fluid coke samples. Sample preparation included mounting of the coke samples onto a silicon covered stage and a light sputtering of electrically conductive gold film for 13 s due to the conductivity of the coke material. The excitation voltage used was 10 kV, and observations were made with magnifications of 3000 to 4000 x.

3.2.2.4 N_2 Adsorption Isotherms

Adsorption isotherms of N_2 onto activated coke samples were determined at 77.3 K by volumetric measurements using a surface area analyzer (Quantachrome, Autosorb 1-MP). Prior to analyses, approximately 0.1 g of sample was degassed for 3 to 4 h at 250^{o}C under vacuum for approximately 5 h with a backfill gas of helium to remove any moisture or volatiles within the existing pores of the material.

The Brunauer, Emmett, and Teller (BET) model was used to determine the surface area of the activated coke samples from the N_2 isotherms using a relative pressure range of 0.02 to 0.055 (P/P_o). Pore size distribution plots were created using the DFT/ Monte Carlo model for slit pores using a relative pressure range from 10^{-7} to 1. Micropore volume was obtained from t-method micropore analysis using a relative pressure range of 0.2 to 0.5.

3.2.2.5 Iodine Adsorption

Iodine adsorption capacity tests were conducted based on the American Society for Testing and Materials (ASTM) ASTM 4607-94 method (ASTM, 2006). The following amounts of solutions were altered from the ASTM methodology: 25 mL HCl; 50 mL KI/I_2; and, 40 mL filtrate. The resulting values gave the amount of iodine adsorbed per weight of carbon; expressed in mg/g. Iodine adsorption isotherms are used to assess the adsorption capacity of a material to pollutants of a smaller molecular size. As a result, the adsorption of iodine can be related to the microporosity within activated carbon.

3.2.2.6 Methylene Blue Adsorption

Liquid-phase adsorption tests were completed on activated coke samples using methylene blue as the adsorbate. Using a larger sized molecule than iodine provides an indication of the mesoporosity within the activated petroleum coke. Methylene blue adsorption tests are typically used to help characterize adsorbents used in wastewater treatment since the molecule is of intermediate size, and has a high affinity for activated carbon (Hameed et al., 2007).

A methylene blue stock solution of 1200 mg/L was prepared using 5% acetic acid. A standard calibration curve was prepared by diluting the stock solution in 0.25% acetic acid. The following standards were generated: 1/120, 1/150, 1/200, 1/300, and 1/600. Each standard solution was scanned with a UV-VIS spectrometer in order to obtain absorbance values. The stock solution and standards were stored in a refrigerator at 4^oC for up to one month. Activated coke samples were weighed to 0.05 g and mixed with 25 mL of diluted methylene blue stock depending on the expected surface area. For example, samples tested to have a higher iodine number could be expected to have a higher methylene blue number, and thus required a higher methylene blue concentration for the batch test. Samples were mixed for 24 h to allow for the adsorbent and adsorbate to reach equilibrium (ASTM, 2006). Samples were then filtered through filter paper (Whatman No. 2) and the filtrate was scanned with a UV-VIS spectrometer (Shimadzu, UV-2401 PC). The absorbance value was taken at 630 nm (the point of maximum absorbance) and compared with the standard calibration curve to obtain the final concentration of methylene blue at equilibrium. The methylene blue value is described as the amount of methylene blue adsorbed per weight of carbon at equilibrium (mg/g), and was calculated with Equation 3-3 (Hameed et al., 2007):

$$q_e = \frac{(C_{initial} - C_{equilibrium})V}{M} \qquad \textbf{(3-3)}$$

where C is the concentration of methylene blue initially added and measured at equilibrium; V is the volume of the solution; and, M is the mass of the dry adsorbent.

3.3 Results and Discussion

3.3.1 Sample Preparation

Preliminary studies suggested that activating petroleum coke at temperatures ranging from 800 to 900°C under CO_2, N_2, and steam would be sufficient to increase the original surface area of the material. The effect of activation time was tested at 2, 4, and 6 hours to determine the speed of surface area generation under the selected activation conditions.

3.3.2 Sample Characterization

3.3.2.1 Trends in Yield and Burn-off

Burn-off provides an indicator of the microporosity of a char material, since it is common for surface area and porosity to increase with increasing burn-off and activation time. Figures 3-3-a and b show a decrease in yield with increasing temperature, time, and steam rate for both activated delayed and fluid coke. Consequently, a higher activation temperature led to a greater removal of carbon and a higher gasification rate, resulting in a greater internal porosity (Zou et al., 2007).

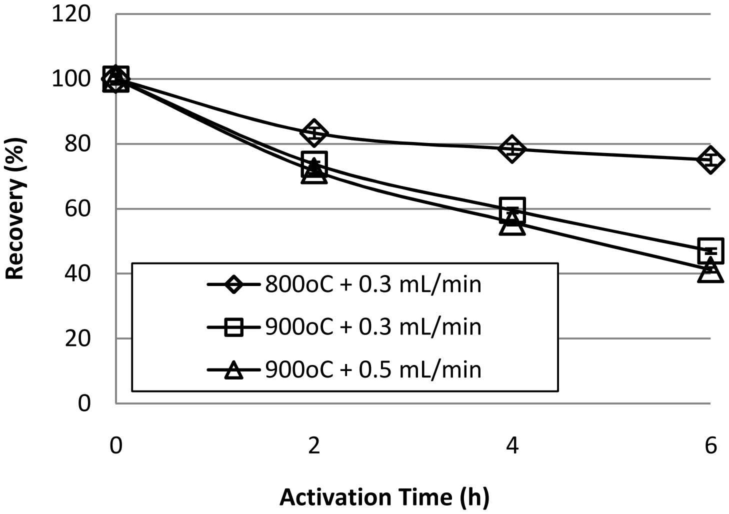

(a) Delayed Coke

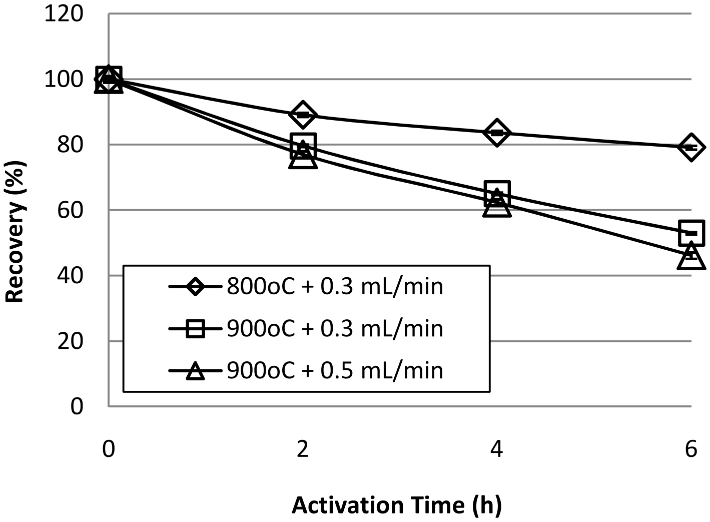

(b) Fluid Coke

Figure 3-3: Impact of activation time, temperature and steam rate on the activation yield for delayed (a) and fluid (b) coke. Tests were completed under an atmosphere of CO_2 + steam. Values are an average of duplicate samples ± one standard deviation.

The yield was greater for the fluid coke samples activated for 2 to 6 hours, indicating fewer gasification reactions. As a result, a lower surface area and porosity can be expected. At the same time, the increased gasification reactions on the delayed coke at 900^{o}C, may have led to the development of mesopores within the material, as discussed in section 3.3.2.5. Past research has indicated that the maximum surface area is achieved during activation when the burn-off is equal to 50% (Choma et al., 1991). Hence, it can be expected that the cokes activated for 6 hours at 900°C will have greater surface areas than those activated at 2 and 4 hours at 800 and 900°C. These results are consistent with previous tests on oil sands fluid coke which depicted burn-off at a constant rate over a 6 hour time period ultimately resulting in 51-60% loss of mass (Di Panfilo and Egiebor, 1996).

3.3.2.2 Thermogravimetric Analysis (TGA)

Petroleum coke typically begins to decompose under oxygen at temperatures exceeding 400°C (Lee and Choi, 2000; Koutcheiko et al., 2007). However, the structural behaviour of raw delayed and fluid coke under select activation temperatures has yet to be explored.

Thermogravimetric analysis was conducted in order to observe the behaviour of petroleum coke to an increase in temperature. Such results aid in understanding pore development and material decomposition during activation. Figure 3-4 shows the response of weight change of raw delayed and fluid coke with increasing temperature under both N_2 and CO_2.

Both delayed and fluid coke samples manifested an initial loss of water. It has been reported that as temperatures increase above 170°C, partial degradation of petroleum coke tends to occur, releasing CO_2, CO, and $C_2H_4O_2$; around 270°C exothermal decomposition begins releasing any tar, methanol, and other substances that may be trapped within the pores of the material (Bansal et al., 1988). A steady decrease in weight at these temperatures is observed for the delayed coke sample, whereas the weight is relatively constant for the fluid coke sample. Such difference is because delayed and fluid cokes contain different concentrations of organic and volatile matter since they undergo different coking processes and coking temperatures during upgrading (Al-Haj-Ibrhim et al., 1992). Due to the lower temperatures during delayed coking, there is a greater amount of volatile matter left in the pores, resulting in a greater weight loss occurring at lower typical carbonization temperatures (Figure 3-4).

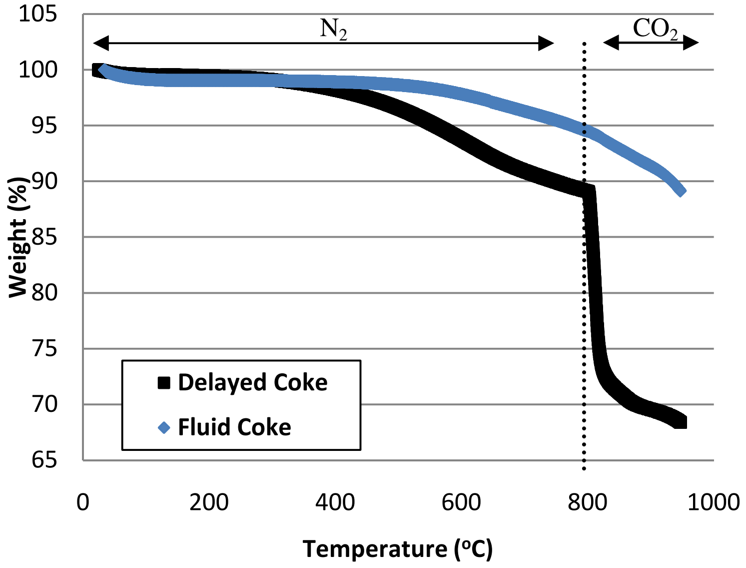

Figure 3-4: Thermogravimetric analysis (TGA) of delayed and fluid petroleum coke. Samples were heated under N_2 up to 800°C, and then heated under CO_2 from 800 to 950°C.

During heating under N_2, (temperatures up to 800°C), the majority of non-carbon elements (such as oxygen, and hydrogen) are driven off as volatile gaseous products which is observed as a gradual and progressive change in weight for the fluid coke sample (Bansal et al., 1988; Yang, 2003). Typically, a raw coke sample contains moisture, excess volatile matter, and hardened residuum from the coker feed (Al-Haj-Ibrahim et al., 1992). The loss of this material will not increase linearly since a range of pores, potential pathways and channels are created within the coke (Zou et al., 2007); as a result, higher temperatures are required to increase the surface area. For this experiment, activation is assumed to occur at temperatures exceeding 800°C in the presence of CO_2. At this point, activation removes any disorganized carbons, exposing the remaining carbon material to the available activation agents; promoting the widening of existing pores (Bansal et al., 1988). As CO_2 is introduced, the delayed coke experiences approximately a 21% decrease in weight. As a result, the surface reaction rate is much greater for delayed coke than for the fluid coke sample, resulting in an abrupt increase in porosity. The tailing off of the delayed coke weight may be due to the ordering of carbon molecules that stabilizes the material resulting in less gasification (Figure 3-4) (Bansal et al., 1988).

3.3.2.3 X-Ray Diffraction (XRD)

The XRD analyses conducted within this experiment, allowed for the identification of structural changes between the raw and activated petroleum coke samples. Figures 3-5 and 3-6 show overlaying XRD scans of activated and raw fluid and delayed coke samples. The activated coke samples chosen [FCS9006(0.5) and DCS9006(0.5)] were those showing the greatest surface area as observed through iodine number, methylene blue, and BET (N_2) adsorption isotherms. The activated samples can be defined through their type and activation conditions: fluid (F) or delayed (D) coke, CO_2 + steam atmosphere (CS); 900°C activation temperature; 6 hour activation time; and a steam rate of 0.5 mL/min. Because the cokes are not initially crystalline (due to the presence of impurities), the observed peaks are not well defined. Depending on the relative proportions of elements available within the raw material, different sized elements can be substituted into the molecular lattices creating a range of d-spacings. This is dependent on the elemental resources required for a particular molecular structure (for example, carbon or graphite) to be thermodynamically stable.

The raw fluid coke samples (Figure 3-5) exhibit a series of peaks which can be correlated to various rhombohedra and hexagonal carbon and graphite phases corresponding to the JCPDS-ICDD PDF2 database (ICDD, 2010). As the coke was produced, the material did not reach equilibrium while cooling; as a result, the sample appears to be partially graphitized as indicated by the presence of graphite peaks (including molybdenum chloride, graphite, and graphite hydrogen nitrate- as identified through the use of the PDF2 database). With activation, these graphite peaks appear to be augmented, and various carbon iron phases begin to appear. The residual carbon atoms within the material has grouped into condensed aromatic ring systems with a degree of planar structure; the overlapping of these sheets is irregular leaving free interstices between themwhich can later produce pores (Bansal et al., 1988). Consequently, the activated fluid coke is observed to be graphitizing (Yang et al., 2003) where the broadness of the peaks and existence of different graphite phases suggests the following: there is no preferential direction of graphite; there is a random distribution of graphite within the material; and, there is no perfect alignment of sheets.

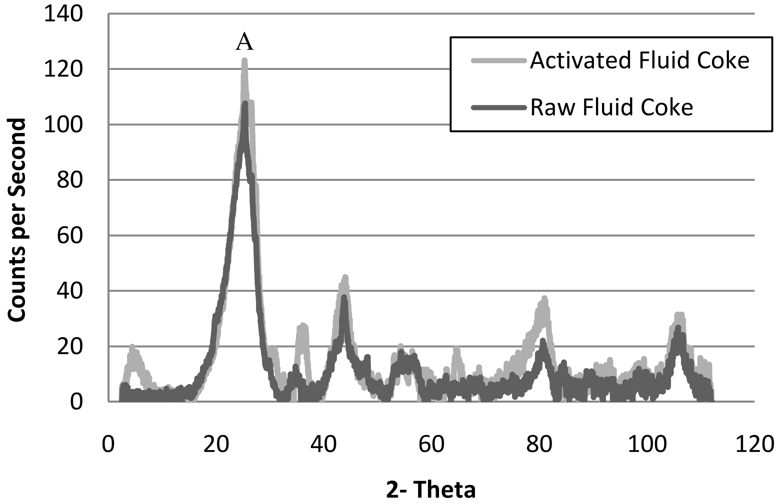

Figure 3-5: XRD scans of activated [FCS9006(0.5)] and raw fluid coke samples. Selected activated conditions are as follows: CO_2 + steam atmosphere, 900^oC, 6 hour activation time, and steam rate = 0.5 mL/min.

For both activated delayed and fluid coke samples there is scattering at 4^o and less which implies the existence of either nanoparticles or pores (Figures 3-5 and 3-6). The main diffraction peaks (A) observed within the delayed and fluid coke samples around $2\theta = 25^o$ (corresponding to a 002 plane) are consistent with activated carbon peaks in the literature (Mantell, 1968; Chunlan et al., 2005; and Jiang et al., 2008). Development of this specific peak area (A) indicates crystallite growth (Jiang et al., 2008).

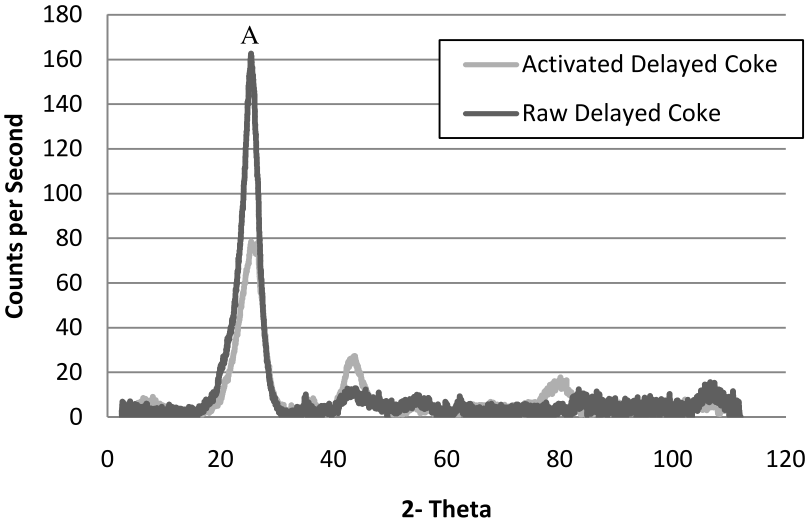

Figure 3-6: XRD scans of activation [DCS9006(0.5)] and raw delayed coke samples. Selected activation conditions are: CO_2 + steam atmosphere, 900^{o}C, 6 hour activation time, and steam rate = 0.5 mL/min.

The raw delayed coke sample displays one major peak, indicating that the material is mainly amorphous (Figure 3-6). This main peak (A) has a d-spacing of 3.506 Å, where the closest carbon phase peak resides around d-spacing 3.346 Å. This miss-match in peaks may be attributed to a lattice substitution within the raw material. Previous research has indicated that delayed coke consists of a more uniform crystalinity than other coke materials since the coking process allows more time for the crystals to re-orient themselves on top of one another (Al-Haj-Ibrahim, 1992). Within the raw delayed coke sample, specific carbon and graphite sequences could not be identified suggesting the absence of crystalinity. With activation, the main peak area (A) is degraded and broadened, where new peaks are produced. These new peaks are correlated with carbon, graphite, and carbon-iron phases; and ultimately, a greater organization of carbon indicating graphitizing potential. This is expected since higher temperatures associated with carbonization and activation sequences promote the growth of graphitic microcrystallites (Chunlan et al., 2005). Within the main peak area (A), there exists 3 separate peaks, one of which is associated with a d-spacing of 3.347 Å. Graphitization is associated with an increase in crystal size and a decrease in interlayer spacing to 3.35 Å (Mantell, 1968). Consequently, the activated delayed coke can said to be graphitizing.

3.3.2.4 Scanning Electron Micrographs (SEMs)

SEMs allow for the observation of physical changes on the surface of materials. Figures 3-7 and 3-8 show SEMs of the raw and activated delayed and fluid coke samples. The raw delayed and fluid coke samples displayed smoother surfaces than their activated counterparts. The raw delayed coke samples exhibited a build up of flakes on the surface, making it difficult to distinguish pores from a change in depth. Conversely, the surface of the raw fluid coke was consistent in displaying pores of varying sizes. Once activated, the surface of the delayed coke developed erratic cracking and enhanced roughness and flaking. Larger cracks within the structures may have also been attributed to a progressive opening of existing cracks within the raw material. The activated fluid coke also developed a rougher surface, but it was easier to distinguish the enrichment of pores across the surface of the material. The roughness of the surfaces can be contributed to the irregular loss of carbon due to gasification reactions, and a re-arrangement of carbon sheets at the molecular level. These figures do not specify the internal micro/ mesoporous surface area and porosity that are responsible for adsorption.

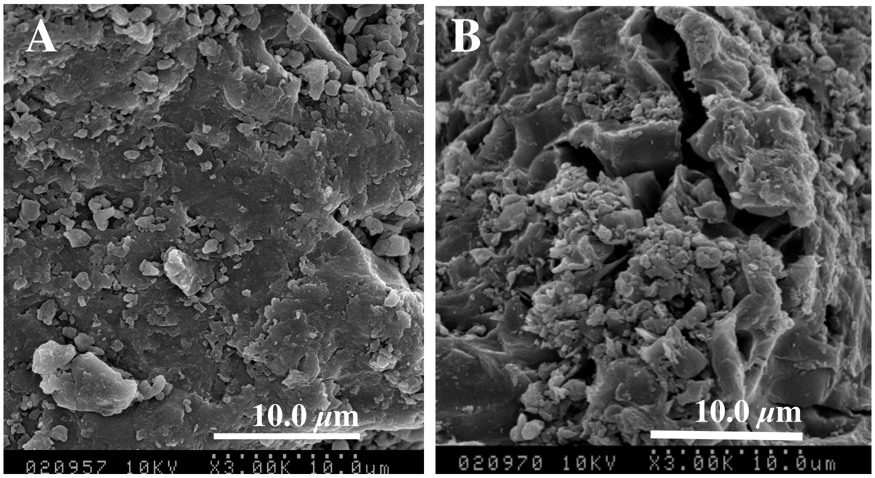

Figure 3-7: SEMs of raw (a) and activated (b) delayed coke. Activation conditions chosen were: 900°C, 6 h, and CO_2 + steam (0.5 mL/min).

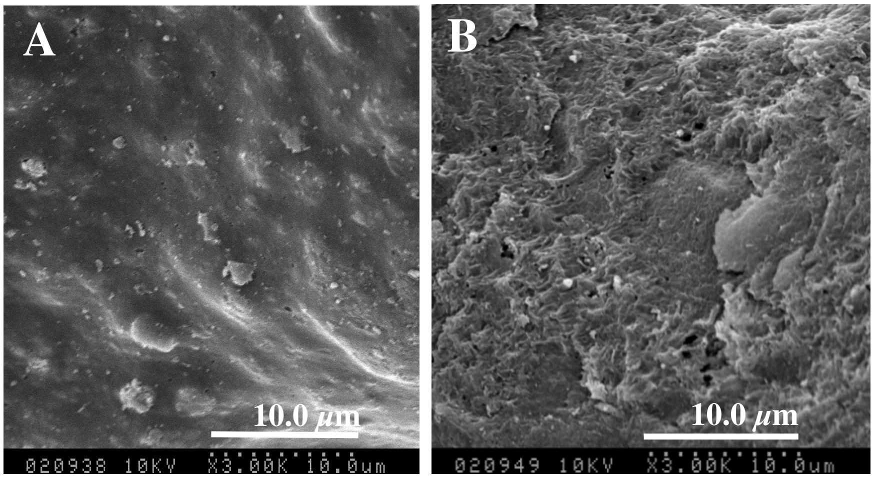

Figure 3-8: SEMs of raw (a) and activated (b) fluid coke. Activation conditions chosen were: 900^{o}C, 6 h, and CO_2 + steam (0.5 mL/min).

3.3.2.5 N_2 Adsorption Isotherms

Activated carbons observed to have the greatest iodine and methylene blue values were characterized by N_2 adsorption at 77.3 K (Table 3-1). The results indicate that increasing activation time leads to the production of a greater surface area for activated delayed coke samples. Delayed coke activated for 6 hours with a steam rate of 0.3 mL/min had a greater surface area and micro-/ mesopore volume than samples activated at 4 hours with 0.5 mL/min. Consequently, longer activation times may lead to the development of a microporous pore structure within the delayed coke. The development of mesopores can be attributed to the burn-out of walls between micropores. Within the fluid coke samples, activation for 6 hours at 0.3 mL/min of steam produced the greatest surface area; however, increasing the steam rate to 0.5 mL/min began to negatively impact the development of microporosity within the material.

Table 3-1: BET surface areas and distribution of pore volume for activated delayed and fluid coke samples observed to have the largest iodine and methylene blue values.

	BET Area (m^2/g)	Pore Volume (cm^3/g)		
		Micro- Pores	Meso-Pores	Total Pores
DCS9006(0.5)	577.5	0.166	0.154	0.320
FCS9006(0.5)	493.5	0.132	0.166	0.298
DCS9004(0.5)	425.6	0.133	0.079	0.212
FCS9004(0.5)	398.9	0.123	0.088	0.211
DCS9006(0.3)	472.0	0.139	0.112	0.251
FCS9006(0.3)	532.9	0.151	0.156	0.307

* Samples are named based on their activation conditions and defined by the following parameters: D: delayed coke, F: fluid coke, CS: CO_2 + steam, 4/ 6: activation time, 0.5/0.3: steam rate of 0.5 or 0.3 mL/min.

It can also be seen from Table 3-1 that higher BET surface areas are associated with larger micropore volumes for both delayed and fluid coke. However, the surface areas found for all activated carbons are low compared to commercially available granular activated carbons. Physical activation is a heterogeneous, solid-gas reaction where higher degrees of activation occur at the periphery of a particle rather than at the core; leading to the development of a wider distribution of pore sizes (Wu et al., 2005). The pore size distributions outlined in Figure 3-9 show that there exists an abundance of both micro- and mesopores within the activated samples. The greatest BET surface areas [DCS9006(0.5) and FCS9006(0.3)] are associated with a mesopore to micropore ratio of approximately 50:50.

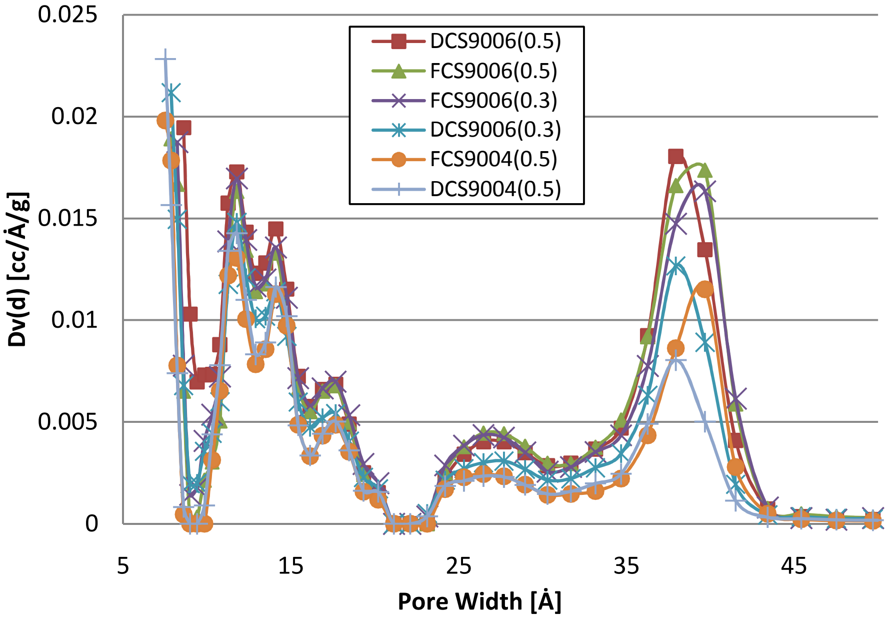

Figure 3-9: Comparison of pore size distribution of micro- and mesopores within activated delayed and fluid coke samples.

3.3.3.6 Iodine Adsorption

Iodine adsorption isotherms are used to assess the adsorption capacity of a material to pollutants of a molecular size ranging from 10 to 28 Å (U.S., 2001). As a result, the adsorption of iodine can be related to the microporosity within activated products. Figures 3-10-a and b show the outcome of iodine tests conducted on samples activated under different atmospheres and temperatures. When the delayed and fluid coke samples were activated under CO_2 only, there were no major observable changes in iodine number suggesting that this method is ineffective in increasing surface area. At low iodine numbers, it also becomes difficult to obtain consistency among tests. Lower rates of gasification may have resulted in less removal of sulphur within the pores of the cokes limiting the effectiveness of the iodine test. When activation was conducted under CO_2 and steam, a greater change in iodine number occurred due to the increased surface area developing within the coke samples. These results were improved when the activation temperature was increased from 800°C to 900°C. The gasification reaction between CO_2, steam, and the carbon material is endothermic, and requires a higher temperature to allow for pore development. Higher temperatures can also be utilized to overcome longer activation times.

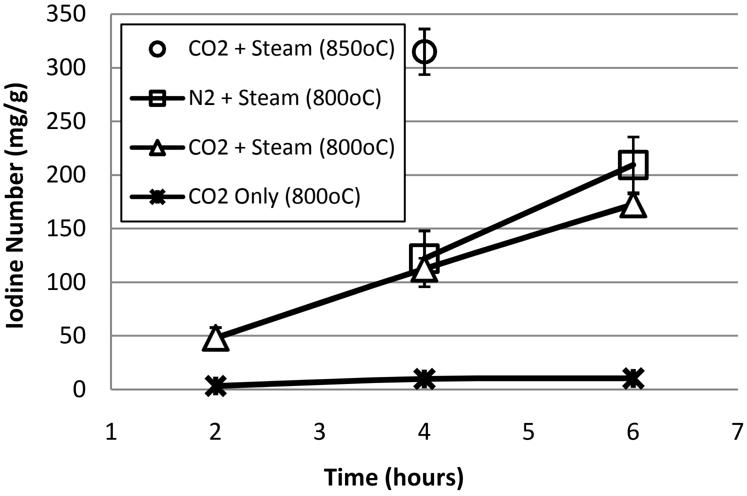

(a) Delayed Coke

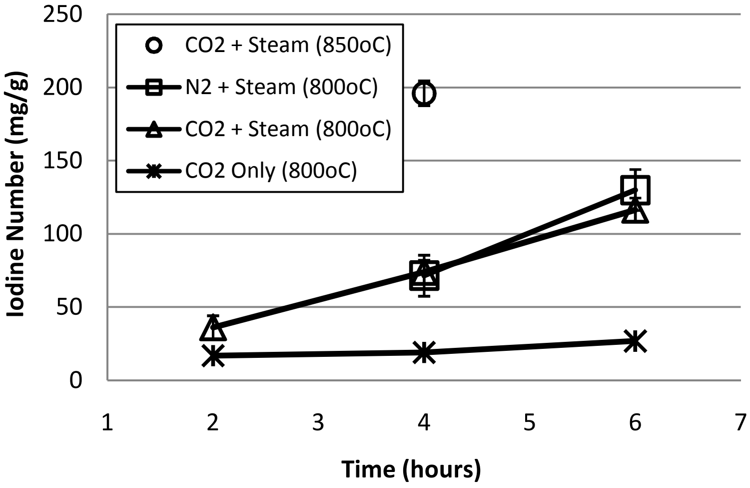

(b) Fluid Coke

Figure 3-10: Impact of activation atmosphere, temperature and time on iodine number for delayed (a) and fluid (b) coke. Values are an average of duplicate samples ± one standard deviation. The steam rate for all tests was 0.3 mL/min. For comparison, non-activated delayed and fluid cokes have iodine numbers of 23 and 16 mg/g, respectively.

The delayed coke samples had higher iodine number for all tests conducted with steam, indicating a greater development of pores than the fluid coke samples. This may be due to the greater surface reaction rate between CO_2 and the delayed coke, as observed through the TGA results.

As an oxidizing gas, CO_2 has an intrinsic surface reaction rate that is slower than the rate of pore diffusion; therefore, there is a uniform reaction between CO_2 and a carbon material resulting in uniform gasification and development of pores (Mattson and Mark, 1971; Yang, 2003). For these reasons, the CO_2 + steam samples were tested further at 900°C to determine whether steam rate had an effect on the pore size (Figure 3-11). Figure 3-11 indicates that a higher steam rate (molar composition of water) will result in higher iodine numbers. The treatment gas composition (in mole %) for H_2O:CO_2 at 0.5 mL/ min and 0.3 mL/ min were 86:14 and 79:21, respectively. The introduction of more molecules of H_2O interacting with the carbon material is expected to increase gasification rates leading to the volatilization of more CO_2, CO, CH_4, and H_2. This would result in an enhancement of carbon removal, where these reactions are favoured at higher temperatures.

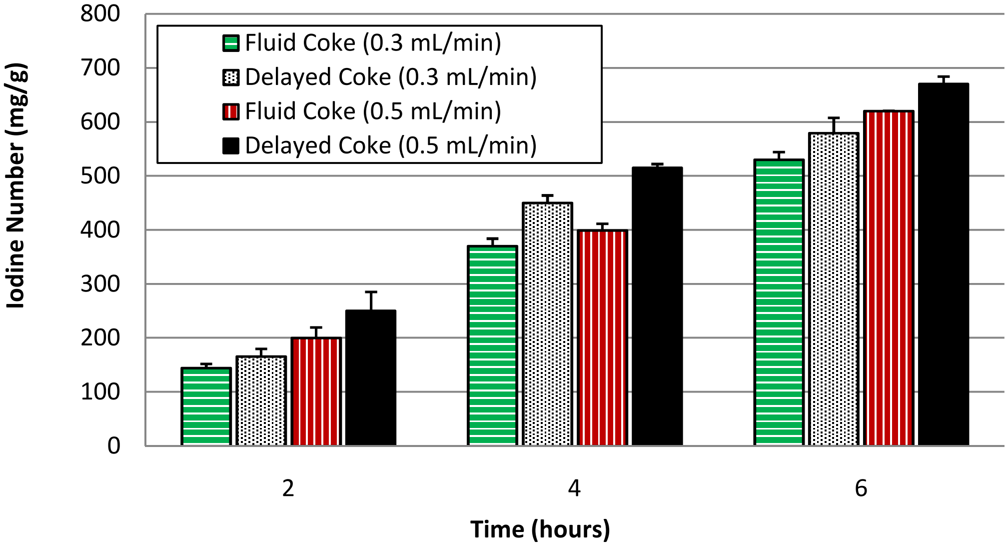

Figure 3-11: Impact of increased steam rate and activation time on iodine number for both delayed and fluid coke at 900°C under CO_2. Values are an average of duplicate samples + one standard deviation. Steam rate is indicated in the legend.

The most effective activation time observed in Figure 3-11 is 6 hours for both delayed and fluid coke, where values are greater for the delayed coke samples. However, these longer activation times lead to a lower overall carbon yield. The structure of the fluid coke particles may inhibit the gasification reactions, as the pores may not be as accessible. Fluid coke has been described as spherical with a layered ‘onion-like’ internal structure; whereas, the internal structure of delayed coke is porous and ‘sponge-like’ (Fedorak and Coy, 2006). Consequently, the development of pores within the fluid coke may be inhibited by the structural pattern pre-determined by the raw state of the material.

3.3.3.7 Methylene Blue Adsorption

Methylene blue adsorption tests are typically used to help characterize adsorbents used in wastewater treatment since the molecule is of intermediate size, and has a high affinity for activated carbon (Sontheimer et al., 1988). Similar trends as found through the iodine tests were observed for delayed and fluid cokes activated under CO_2 at 900^{o}C (Table 3-2). Tests conducted on samples activated at 800^{o}C consistently had low methylene blue values ranging from 2 to 9 mg/g. Consequently, delayed and fluid coke samples activated at 800^{o}C were ineffective in producing surface areas sufficient for methylene blue adsorption. The greatest values were obtained at 6 hours for both steam rates of 0.3 and 0.5 mL/min for activated delayed coke, and only 0.5 mL/min at 6 hours for activated fluid coke.

Table 3-2: Methylene blue values at equilibrium for delayed and fluid coke samples activated at 900^{o}C under CO_2.

Coke Sample	Activation Time (h)	Steam Rate (mL/min)	Average Methylene Blue Value at Equilibrium (mg/g)
Delayed	2	0.3	9.7 ± 1.9
	4		48.3 ± 1.2
	6		122.6 ± 1.0
Delayed	2	0.5	11.8 ± 0.4
	4		68.5 ± 2.6
	6		123.9 ± 0.5
Fluid	2	0.3	10.9 ± 0.4
	4		47.8 ± 0.2
	6		98.4 ± 0.1
Fluid	2	0.5	16.5 ± 0.0
	4		67.7 ± 1.2
	6		122.6 ± 0.5

Values are the average of duplicate samples ± one standard deviation

Figure 3-12 shows the relationship between iodine number and methylene blue for the two best activated delayed and fluid coke products [DCS9006(0.5) and FCS9006(0.5)]; activated at 900^{o}C for 2-6 h under CO_2 + steam (0.5 mL/min). Iodine number is a good indicator of pores with diameter ranging from 10 to 28 Å in which mainly fall in the micropore range (< 20 Å) (U.S, 2001). In contrast, methylene blue adsorption tests are better suited for intermediately sized molecules (Sontheimer et al., 1988). The results demonstrate that these parameters are well correlated, and reflect that the coke samples have an equal volume of micropores to mesopores as indicated in Table 3-1 and section 3.5.

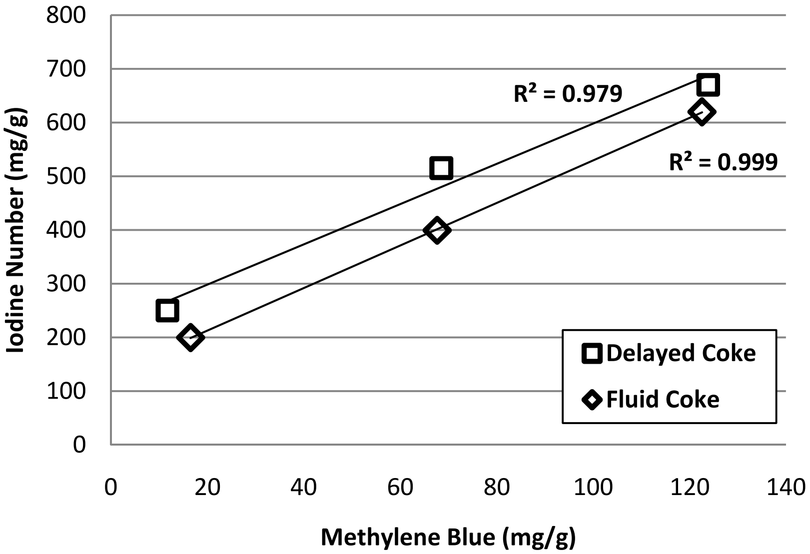

Figure 3-12: Relationship between iodine number and methylene blue for delayed and fluid coke activated at 900°C for 2-6 h under CO_2 + steam (0.5 mL/min). Values are an average of duplicate samples.

3.3.3.8 Comparison of Results

Table 3-3 compares the results of characterization techniques between oil sands delayed and fluid coke samples from this study to those reported in the literature. All tests were conducted using CO_2 and steam as the activating atmosphere.

Table 3-3: Comparison of surface area, methylene blue number, and iodine number for physically activated delayed and fluid coke samples conducted under CO_2 + steam.

Sample	Activation Time	Activation Temperature	BET (m^2/g)	Methylene Blue (mg/g)	Iodine Number (mg/g)
Activated Delayed Coke	6 h	900°C	578	124	670
Activated Fluid Coke	6 h	900°C	494	123	620
Activated Fluid Coke[1]	6 h	850°C	319	80-100	200
Activated Delayed Coke[2]	4 h	850°C	NA*	101	NA*
Activated Fluid Coke[3]	4 h	800°C	539.9	NA*	NA*

*NA: Not available; [1]Di Panfilo and Egiebor, 1996; [2]Shawwa et al., 2001; [3]Bratu, 2009

The best delayed and fluid coke samples in this study were prepared under the following conditions: 6 h activation time, 900°C activation temperature, CO_2 and steam activating atmosphere. These conditions resulted in the largest surface area, methylene blue value, and iodine number. The results indicate that raw delayed and fluid petroleum coke has the potential to be used as an adsorbent once activated.

3.4 Summary and Conclusions

This paper has studied the influence of physical activation on the properties of activated delayed and fluid petroleum coke. Iodine number, methylene blue, N_2 adsorption, SEMs, and X-ray diffraction were used to characterize the surface area and porosity of the activated products. The results support the following conclusions:

- Higher activation temperatures along with longer activation times result in a higher gasification rate of carbon from the surface of petroleum coke, resulting in an enhanced etching of pores.
- Delayed and fluid cokes contain different initial concentrations of volatile matter; the subsequent development of the pores during activation follows

the structural pattern pre-determined by the raw state of the material. The gasification rate of carbon is greater for delayed coke than for fluid coke.

- The most successful activation atmosphere was CO_2 + steam; the reaction requires a higher activation temperature, where 900^{o}C was determined to be the most successful activation temperature as observed through the iodine number results.
- BET surface areas indicated that the best physical activation conditions for delayed coke are as follows: 6 hours, CO_2 + steam activating atmosphere, 0.5 mL/min steam rate, 900^{o}C activating temperature. The same conditions apply for fluid coke, where a 0.3 mL/min steam rate led to highest produced surface area.
- The raw fluid coke samples can be considered to be partially crystallized with graphitizing potential. Raw delayed coke was not observed to contain graphite phases; however, upon activation, graphitization was observed.

These results are important because they show that delayed and fluid oil sands cokes can be converted into activated carbons with a high surface areas and porosity available for adsorption. This may provide a means for the oil sands industry to utilize this readily available waste by-product for the remediation of organic contaminants in the process affected mine tailings waters. Future studies should test the ability of activated coke to remove organic pollutants from oil sands tailings and investigate the impact of activation techniques on the development of microporosity in delayed and fluid petroleum coke.

3.5 Chapter 3 References

Allen, E. 2008a. Process water treatment in Canada's oil sands industry: I. Target pollutants and treatment objectives. *Journal of Environmental Engineering and Science*; 7: 123-138.

Allen, E. 2008b. Process water treatment in Canada's oil sands industry: II. A review of emerging technologies. *Journal of Environmental Engineering and Science*; 7: 499-524.

Al-Haj-Ibrahim, H., and Morsi, B. 1992. Desulfurization of petroleum coke: A review. *Industrial and Engineering Chemistry Research*; 21: 1835-1840.

ASTM. 2006. Standard test method for determination of iodine number of activated carbon. *ASTM International*. PA, USA; D 4607-94.

Bansal, R., Donnet, J., and Stoeckli, F. 1988. Active carbon. Marcel Dekker Inc, New York, USA; 482 p.

Bansal, R.C., and Goyal, M. 2005. Activated carbon adsorption. Taylor and Francis Group, Florida, 497 pp.

Bratu, M. 2009. Activation of fluid coke for mercury removal from gases. Published PhD thesis: AAT MR45780. University of Alberta, Edmonton, Canada.

Buitron, G., Duran Moreno, A., Ramirez, Zamora, R.M., and Schouwenaars, R. 2000. Production of activated carbon from petroleum coke and its application in water treatment for the removal of metals and phenol. *Water Science and Technology*; 42: 119-126.

Canadian Association of Petroleum Producers (CAPP). 2009. *Water use in Canada's oil sands*. 2009-0022. CAPP, Calgary, Alberta. Available at http://www.capp.ca/library/publications/crudeOilAndOilSands/pages/pubInfo.aspx?DocId=154986#qizoWOc35CWl (accessed November 29, 2010).

Chang, C-F., Chang, C-Y., and Tsia, W-T. 2000. Effects of burn-off and activation temperature on preparation of activated carbon from corn cob agrowaste by CO_2 and Steam. *Journal of Colloid and Interface Science*; 232: 45-49.

Changhou, L., Chunlan, L., Shaoping, X., Shuquin, L., and Yixiong, G. 2005. Effect of precarbonization of petroleum cokes on chemical activation process with KOH. *Carbon*; 43: 2295-2301.

Choma, J., Jankowska, H., and Swiatkowski, A. 1991. Active carbon. Ellis Horward Limited. Chichester, England; 104 pp.

Chunlan, L., Shaoping, X., Yixiong, G., Shuqin, L., and Changhou, L. 2005. Effect of pre-carbonization of petroleum cokes on chemical activation process of KOH. *Carbon*; 43: 2295-2301.

Dabrowski, A., Podkościelny, P., Hubicki, Z., and Barczak, M. 2005. Adsorption of phenolic compounds by activated carbon- a critical review. *Chemosphere*; 58: 1049-1070.

DiPanfilo, R., and Egiebor, N.O. 1996. Activated Carbon Production from Synthetic Crude Coke. *Fuel Processing Technology*; 46: 157-169.

Fedorak, P.M., and Coy, D.L. 2006. Oil sands cokes affect microbial activities. *Fuel*; 85: 1642-1651.

Guo, Y., Han, X., Li, Z., Qiu, J., Sun, X., Wu, M., and Zha, Q. 2005. Preparation of porous carbons from petroleum coke by different activation methods. *Fuel*; 84: 1992-1997.

Hameed, B.H., Ahmad, A.L., and Latiff, K.N.A. 2007. Adsorption of basic dye (methylene Blue) onto activated carbon prepared from rattan sawdust. *Dyes and Pigments*; 75: 143-149.

International Centre for Diffraction Data (ICDD). 2010. Powder Diffraction File 2 Database. Available [online]: <http://www.icdd.com/products/pdf2.htm>. Accessed September 13, 2010.

Itoh, M., Otowa, T., and Tanibata, R. 1993. Production and adsorption characteristics of MAXSORB: high-surface-area active carbon. *Gas Separation and Purification*; 7: 241-245.

Jiang, B., Zhang, Y., Zhou, J., Zhang, K., and Chen, S. 2008. Effects of chemical modification of petroleum cokes on the properties of the resulting activated carbon. *Fuel*; 87: 1844-1848.

Karanfil, T., and Kilduff, J.E. 1999. Role of granular activated carbon surface chemistry on the adsorption of organic compounds. 1. Priority Pollutants. *Environmental Science and Technology*; 33: 3217-3224.

Kawano, T., Kubota, M., Onyango, M.S., Watanabe, F., and Matsuda, H. 2008. Preparation of activated carbon from petroleum coke by KOH chemical activation for adsorption heat pump. *Applied Thermal Engineering*; 28: 865-871.

Koutcheiko, S., McCracken, T., Kung, J., Kotlyar, L. 2007. Production of activated carbon from Athabasca oilsands bitumen. *Petroleum Science and Technology*; 25: 1215-1224.

Lee, S.H., and Choi, C.S. 2000. Chemical activation of high sulfur petroleum cokes by alkali metal compounds. *Fuel Processing Technology*; 64: 141-153.

Mantell, C.L. 1968. Carbon and graphite handbook. John Wiley and Sons; New York, USA.

Mattson, J.S., and Mark, H.B. 1971. Activated carbon: surface chemistry and adsorption from solution. Marcel Dekker, Inc., New York, USA.

Paslawski, J.C., Headley, J.V., Hill, G.A., and Nemati, M. 2009. Biodegradation kinetics of trans-4-methyl-1-cyclohexane carboxylic acid. *Biodegradation*; 20: 125-133.

Shawwa, A.R., Smith, D.W., and Sego, D.C. 2001. Color and chlorinated organics removal from pulp mills wastewater using activated petroleum coke. *Water Resources*; 35: 745-749.

Sontheimer, H., Crittenden, J., Summers, R., Fettig, J., Horner, G., Hubele, C., and Zimmer, G. 1988. Activated carbon for water treatment. AWWA Research Foundation, Denver, CO.

Stavropoulos, G.G., and Zabaniotou, A.A. 2009. Minimizing activated carbons production cost. *Fuel Processing Technology*, 90: 952-957.

U.S. Army Corps of Engineers. 2001. *Engineering and Design- Adsorption Design Guide*. Design Guide No. 1110-1-2. Department of the Army: 1-99.

Wu, M., Zha, Q., Qiu, J., Han, X., Guo, Y., Li, Z., Yuan, A., and Sun, X. 2005. Preparation of porous carbons from petroleum coke by different activation methods. *Fuel*; 84: 1992-1997.

Yang, R.T. 2003. Adsorbents: fundamentals and applications. John Wiley and Sons, New Jersey, 410 p.

Zou, J.H., Zhou, Z.J., Wang, F.C., Zhang, W., Dai, Z.H., Liu, H.F., and Yu, Z.H. 2007. Modeling reaction kinetics of petroleum coke gasification with CO_2. *Chemical Engineering and Processing*; 46: 630-636.

CHAPTER 4: THE ADSORPTION OF OIL SANDS NAPHTHENIC ACIDS ONTO RAW AND ACTIVATED DELAYED AND FLUID PETROLEUM COKE

4.1 Introduction

The oil sands industry residing in the northern Athabasca region, Alberta, Canada is rapidly expanding, where oil production has reached approximately 1 million barrels per day (Allen, 2008a). Here, bitumen is extracted from the oil sands and converted to synthetic crude oil through upgrading processes. Extraction requires large volumes of both recycled and imported fresh water. More specifically, in the mining of 1 m^3 of oil sands, 3 m^3 of water is required, producing approximately 4 m^3 of slurry waste (Quagraine, 2005). The slurry waste is a mixture of water, non-recoverable bitumen, sand, fine clays and inorganic and organic contaminants (Lo et al., 2006; Kavanagh et al., 2009; CAPP, 2009). This material is stored on-site in large tailings ponds. Currently, 4×10^8 m^3 of tailings is stored in the Athabasca oil sands region (Headley, 2009). The increased recycling of tailings pond process-affected water has resulted in a long-term decline in water quality that affects not only the oil recovery, but also the refining and extraction infrastructure due to increased scaling and corrosion (Allen, 2008a). As the recycled water becomes increasingly contaminated, it intensifies the demand for imported fresh water resources.

The dissolved organic by-products within the process-affected water contribute to the poor water quality with respect to colour, toxicity, and total organic carbon. Consequently, the accumulation of waste corresponds to various environmental challenges for the oil sands industry. Of the organic acids residing within the tailings ponds, 80% can be attributed to oil sands naphthenic acids (Allen, 2008a). Oil sands naphthenic acids (OSNAs) represent a class of alkyl-substituted acyclic and cycloapliphatic carboxylic acids, where their structure varies depending upon the number of hydrogen atoms lost as linear hydrocarbon chains are gained (Scott et al., 2008). The term 'naphthenic acid' has been recently described as ambiguous due to the range of organic compounds measured as a part of the group of polar organic carboxylic acids (Grewer et al., 2010). The uncertainty surrounding this class of compounds is further extended to the presence of pyrroles, thiophenes, and phenols detected in some OSNAs (Whitby, 2010). Although a large knowledge gap surrounds the unique characterization and measurement of OSNAs they have been referred to as the primary source of toxicity within oil sands tailings pond water (Hao et al., 2005; Lo et al., 2006; Grewer, 2010; Whitby, 2010). OSNAs also contribute to corrosivity within oil sands infrastructure, causing chelation of metal ions in the presence of carboxylic acids groups at typical operating temperatures (Clemente and Fedorak, 2005). As a result, innovative and feasible methods aiming at reducing OSNAs within tailings pond water are necessary to allow for increased recycling of the process-affected water and for remediation of the tailings pond water at mine closure.

The use of adsorbents (including activated carbon) has been used as a treatment technology due to their ability to remove a wide range of organic contaminants within oilfield process-water (Shawwa et al., 2001; Quinlivan et al., 2005; Allen, 2008b). Oil sands petroleum coke may be an excellent candidate for the production of activated carbon used in the remediation of process-affected water due to its high carbon content ranging from 80-85% wt. (Karanfil and Kilduff, 1999; Barczak et al., 2005). Petroleum coke is a waste by-product of the oil sands industry generated during upgrading of bitumen to synthetic crude oil. Major oil sands companies within the Athabasca oil sands region, such as Suncor Energy Inc., and Syncrude Canada Ltd. are cumulatively producing approximately 62.5 kg of delayed and fluid coke per barrel of processed bitumen (Fedorak and Coy, 2006). Due to the minimal use of the material, most of the petroleum coke is stockpiled on-site as an undesirable waste by-product. When activated, petroleum coke has a higher activation yield and surface area than most raw materials, where the higher yield provides a lower overall investment cost for the user (Stavropoulos and Zabaniotou, 2009). As a result, delayed and fluid petroleum coke represents a useful commodity that can be used for wastewater treatment applications.

Though the literature indicates that petroleum coke can be used as an adsorbent in wastewater treatment, the specific application of the removal of

OSNAs from process-affected water through the use of raw and activated delayed and fluid coke has yet to be explored. The main objective of this research is to investigate the adsorption of OSNAs onto raw and physically activated delayed and fluid cokes. A second objective is to understand the extent of uptake and leaching of inorganic compounds in the process-affected water during the adsorption process. Toxicity measurements will provide a bigger picture understanding of the competing inorganic and organic adsorption processes and their affect on water quality. This research will provide a unique remediation strategy for the growing tailings water management concerns residing in the Athabasca oil sands region.

4.2 Experimental

4.2.1 Activated Carbon Preparation

Delayed petroleum coke was obtained from Suncor Energy Inc., and fluid coke samples were provided by Syncrude Canada Ltd. Prior to use, delayed coke samples were ground and sieved to a 75-150 μm mesh size due to the well graded nature of the material. The fluid coke was fine grained and was sieved to achieve the same particle size range as the delayed coke preventing bias between the materials. Physical activation was chosen as a more economically viable option for the oil sands industry than chemical activation techniques where the purchasing, transportation, and waste management of chemical products would have to be considered.

Activation took place in a fixed-bed muffle furnace and consisted of a two-stage simultaneous carbonization/ activation sequence. A vertical quartz reactor was positioned in the center of the furnace and designed to hold 20 g of sample for each experiment. The reactor was initially purged of oxygen and heated to the desired activation temperature of 900^{o}C under $N_{2\ (g)}$. At this point, activation began, and the samples were heated for 6 h under a CO_2 + steam atmosphere. Steam was generated using a syringe pump and heating tape. A detailed outline of the experimental procedures is presented in Chapter 3. The development of surface area within the petroleum coke samples was evaluated through iodine and nitrogen adsorption isotherms. The adsorption procedure was based on the American Society of Testing and Materials (ASTM, 2006) ASTM 4607-94 method. Using iodine as the adsorbate onto the produced activated coke, the resulting values gave the amount of iodine adsorbed per weight of carbon (mg/g). The surface area was determined using a Brunauer, Emmett, and Teller (BET) model with N_2 isotherms measured at 77.3 K by volumetric measurements (Quantachrome, Autosorb 1-MP) using a relative pressure range of 0.02 to 0.055 (P/P_o). Micropore volume was obtained from t-method micropore analysis using a relative pressure range of 0.2 to 0.5 (P/P_o). Additional information on adsorbent structural and physical characteristics can be found within Chapter 3 methodology.

4.2.2 Adsorption of Organics

Batch adsorption tests were conducted on raw and activated delayed and fluid coke mixed with 500 mL of process-affected (PA) tailings pond water. The PA water used came from different batches of the same source water for the raw delayed coke experiments, the raw fluid coke experiments, and for the activated delayed and fluid coke experiments. The PA water was first centrifuged at 4,150 rpm for 30 min and then filtered through 0.45 μm nylon filters in order to remove any clays or colloids that may compete with the coke during adsorption. This step created a baseline for adsorption processes by the petroleum coke samples. Due to the low initial surface areas of the raw delayed and fluid petroleum cokes, the following weight percentages were added to 500 mL of process-affected water: 5%, 10%, 20%, and 30% (50 to 300 g/L). The activated petroleum coke sample weight intervals were as follows: 0.0625%, 0.125%, 0.25%, and 0.5% (0.625 to 5 g/L). The higher surface areas developed after activation, allowed for lower carbon doses to be used. Procedures for batch testing followed the ASTM D 4646 (2008) methodology. Samples were left to agitate for 24 h at 160 rpm to ensure efficient contact between the PA water and the raw and activated coke samples. Subsequently, the samples were filtered through 0.45 μm nylon filters to separate the cokes from the filtrate. Adsorption experiments were also conducted on commercially available coal-based granular activated carbon (GAC) known to have a high adsorption capacity for organics, representing a positive control within the experiment.

To observe whether the samples reached equilibrium within the 24 h time period suggested by ASTM D 4646 (2008), the batch tests were run with 0.5% wt. activated delayed and fluid coke and GAC and 500 mL of PA water. During these tests, samples were taken at the following time intervals and filtered through 0.45 µm nylon filters: 0 min, 10 min, 30 min, 1 h, 2 h, 4 h, 8 h, 12 h, 24 h, and 30 h. Filtered samples were subsequently scanned using a fluorescence spectrometer (Varian Cary Eclipse) to observe the removal of the OSNA signature once treated with activated carbon samples. No sample preparation was necessary.

The adsorption of organics was evaluated on untreated (negative control consisting of PA water with no addition of coke) and treated PA water samples. Method 10173 (HACH-DR/2400) for mid-range organic carbon (15-150 mg/L carbon), was used to obtain the dissolved organic carbon (DOC) results for the PA waters treated with raw delayed and fluid coke. For PA water treated with activated delayed and fluid cokes and granular activated carbon, DOC was measured according to standard methods (Clesceri et al., 1999) using a Shimadzu, TOC-5000A instrument. Three injections were averaged per sample, where the instrumental drift was measured to be within 10%. Proficiency testing by the Canadian Association for Laboratory Accreditation (CALA) ensured quality assurance on the laboratory technique. For both methodologies, it was assumed that the filtration of the samples through 0.45 µm filters allowed for the direct translation of DOC readings, typically obtained as total organic carbon content.

Fourier Transform Infrared (FTIR) spectrometry is currently used as an industry standard for measuring OSNAs (Holowenko et al., 2001; Yen et al., 2004; and Clemente and Fedorak, 2005). This infrared analysis tool involves the quantitative analysis of functional groups through the comparison of an unknown material with a known infrared adsorption spectra of a reference material (ASTM, 2007). For this study, OSNAs were extracted from acidified (pH = 2.5) sample filtrates into methylene chloride, and absorbance peak heights were observed at 1706 and 1743 cm^{-1}. These results were summed and compared to a standard calibration curve generated through known concentrations of commercially prepared naphthenic acids (Sigma Aldrich) and measured peak heights. Chemically, the adsorption of mid-infrared light results in a change of molecular vibrational and rotational status (Beekes et al., 2007). Consequently, the unique vibrational frequency reached will describe the intensity of the absorption.

Treated PA water samples were scanned with a fluorescence spectrometer (Varian Cary Eclipse) at excitation wavelengths ranging from 260 to 600 nm, where emission wavelengths were obtained from 250 to 600 nm in 1 nm increments. Fluorescence spectrometry is a screening tool used to detect and measure typical OSNA signatures within PA water (Mohamed et al, 2008). No sample preparation was necessary. Afterwards, sample absorbance was collected from 250 to 600 nm using a UV-VIS spectrometer (Shimadzu UV 2401-PC) in order to correct for inner and outer filtering effects caused by solute self-absorption (Tucker et al., 1992). Primary inner filtering can be described as the absorbance of excitation wavelengths by other molecules within the sample, where only a fraction of the light reaches the specific molecules of interest. This effect occurs as the excitation radiation enters the sample cell (Asanov et al., 1998). After the molecules are excited by the excitation wavelengths, the emitted wavelengths have the potential to be absorbed by molecules as it leaves the sample cell; termed secondary outer filtering (Asanov et al., 1998). Consequently, the fluorescence signature observed can be skewed or distorted due to the absorbance of energy through the sample. Since the excitation wavelengths are shorter in length than the emission wavelengths, they are more commonly absorbed within organic samples (Asanov et al., 1998). As a result, the primary filtering effect can be considered to be more of a significant issue than that of secondary filtering. Mathematical correction factors have been established in order to adjust the fluorescence signal intensities based on the assumption of monochromatic excitation and emission beams for simplification (Tucker et al., 1992). These factors were used to correct for primary and secondary filtering, and can be described by the following Equations (4-1 to 4-3) adapted from Tucker et al. (1992):

$$F_{primary} = \frac{2.303A(y-x)}{10^{-Ax}-10^{-Ay}} \qquad \textbf{(4-1)}$$

$$F_{secondary} = \frac{(v-u)\left(\frac{1}{b}\right)lnT}{T_{at\,v/b}-T_{at\,u/b}} \qquad \textbf{(4-2)}$$

$$F^{Corrected} = F_{primary}F_{secondary}Intensity \qquad \textbf{(4-3)}$$

Where,

- A = Absorbance per centimetre obtained experimentally (ex. UV-VIS Spectrometer)
- Y,V and U, X = Represent the width of the excitation and emission beams
- B = Path length of the beam through the sample cell
- T = Transmittance related to the absorbance through the cell (10^{-A})
- Intensity = Measured through the fluorescence spectrometer in auxiliary units

The adsorption capacity was estimated for activated delayed and fluid coke from adsorption isotherm data for OSNAs. The adsorption data were fitted using a logarithmic linearization of the Freundlich isotherm equation of the form:

$$q = KC^{1/n} \qquad \textbf{(4-4)}$$

where q represents the amount of OSNAs adsorbed per weight of activated delayed and fluid coke (mg/g), K and n are Freundlich adsorption constants, and C is the aqueous solution-phase concentration (mg/L). The Freundlich isotherm was chosen due to its traditional application to porous activated carbon materials, where the model describes a heterogeneous adsorption system (Smith, 1991; Shawwa et al., 2001; Pavoni et al., 2006; Qi and Schideman, 2008).

4.2.3 Process-Affected Water Characterization

Untreated PA water and the filtrate samples were analyzed for: pH, electrical conductivity (EC), total alkalinity, major cations and anions with ion chromatography (IC) [Dionex IC 2500 and ICS 2000], and trace metals with inductively coupled plasma mass spectrometry (ICPMS) [Perkin Elmer, Elan 9000]. Alkalinity values were determined through potentiometric titrations with 0.02N H_2SO_4 using a Bromocresol Green indicator.

IC anion calibration standards were prepared in 1x, 2x, 5x, 10x, and 20x dilutions using Seven Anions Standard II (Dionex). Cation calibration standards were prepared in 2x, 10x, 20x, 100x, and 200x using Six Cation II standard (Dionex). The IC 2500 instrumentation required an eluent stream of 8.0 mM Na_2CO_3 + 1.0 mM $NaHCO_3$ (1 mL/min), nitrogen pressure of 60 kPa, and separator columns. Whereas the ICS 2000 used an eluent of ultra-pure water (1 mL/min), nitrogen pressure of 60 kPa, and separator columns (IonPac® CG12A). Injections consisted of 25 µL of sample, where quality control check standards and sample blanks were run every 10 samples.

ICPMS sample preparation involved the filtration of 10 mL of sample through 0.45 µm nylon filters; 5 mL of filtered sample were then diluted (10x) into 1% $HNO_{3(aq)}$. The addition of 250 µL of an internal standard solution was then added to each sample. Five multi-element standards were prepared using additional elemental additions: 0.2 µg/L (1 µL B, Mo, P), 2 µg/L (10 µL B, Mo, P, Si), 10 µg/L (50 µL B, Mo, P, Si), 50 µg/L (250 µL B, Mo, P, Si), 100 µg/L (500 µL B, Mo, P, Si). Standard six contained 200 µg/L Al, 500 µg/L Si, and 500 µg/L Fe, K, Ca, Na, and Mg. All standards were measured into 50 mL vials and diluted with 1% $HNO_{3(aq)}$. Instrument optimization was performed before each test allowing for the following optimal instrumental operating conditions: vacuum ($9.8\text{x}10^{-6}$ torr), nebulizer flow rate (0.97 L/min), RF power (1200 W), lens voltage

(7.75 V), pulse stage voltage (1400 V), and analog stage voltage (-1850 V). Daily performance checks obtained CeO/Ce and Ba^{2+}/Ba ratios less than 0.03% for each analytical run, where the background was less than 30 cps at mass 200.

4.2.4 Leaching Tests with Ultra-Pure (DI) Water

Batch adsorption tests were similarly conducted on raw delayed and fluid cokes mixed with 500 mL of ultra-pure (DI) water. These experiments provided a negative control with respect to species capable of leaching from the raw materials. Similar weight percentages used for the PA water batch tests were used in order to maintain consistency between the tests: 5%, 10%, 20%, and 30% (50 to 300 g/L). Procedures also followed the ASTM D 4646 (2008) methodology, where samples were left to agitate for 24 h at 160 rpm to allow for sufficient contact time for the cokes and DI water to reach equilibrium. Samples were then filtered through 0.45 μm nylon filters to separate the spent coke from the filtrate. The following analyses were conducted (outlined in section 4.2.3): pH, EC, total alkalinity, IC, and DOC content (HACH-DR/ 2400).

4.2.5 Toxicity Assays

Microtox™ toxicity assays were conducted on untreated PA water and PA water samples treated with activated delayed and fluid coke. Since the bacterial reagent (*Vibrio fischeri*) is sensitive to pH, all samples were adjusted to pH=8 with HCl to attribute toxicity results to the toxic compounds within the filtrates. Samples were analyzed with a Model 500 Analyzer (AZUR Environmental Corp.). The Microtox™ methodologies used include the 81.9% basic test and the 81.9% screening test at 5 and 15 min to obtain the effective concentration and toxicity effect. The percent effective concentration to decrease 20% (EC_{20}) of the *Vibrio fischeri* luminescence was calculated using the Microtox™ Onmi Software (AZUR Environmental Corp.). Procedures followed ASTM D5660-96 (2009). The freeze-dried luminescent bacteria were used for testing within 3 hours after hydration. All samples were tested in duplicate concentrations.

4.3 Results and Discussion

4.3.1 Untreated PA Water Characterization

Tables 4-1 to 4-3 characterize the untreated PA water before interaction with the raw and activated delayed and fluid coke samples. Initially, the PA water is alkaline with a high conductivity indicating the presence of a saline environment (increased salt content). The DOC content ranges from 39 to 54 mg/L and the OSNAs concentration ranges from 55 to 61 mg/L. The literature indicates that OSNAs have been confirmed to be toxic to a variety of aquatic life at concentrations exceeding 2.5 to 5 mg/L (Clemente and Fedorak, 2005). The high measurable ammonium levels ranging from 6.4 to 6.8 mg/L present within the untreated PA waters may also contribute to the toxicity (Randall and Tsui, 2002). Due to the absence of specific guidelines based on discharge criteria for the Athabasca oil sands region, the Canadian aquatic water quality guidelines are often used for remediation purposes. Tables 4-1 through 4-3 also illustrate that the initial Mo and Cu concentrations are high with respect to the Canadian aquatic water quality guidelines of 73 μg/L and 4 μg/L, respectively (CCME, 2006). The untreated PA waters are also saline with electrical conductivities ranging from 3.1 to 3.6 mS. The high salt content can be attributed to the high measurable concentrations of major cations and anions, including Na^+, Cl^-, and SO_4^{2-}. Consequently, the PA water is initially very toxic to aquatic life requiring the remediation of organic and inorganic compounds and ions.

Table 4-1: Characterization of untreated PA water obtained for the tests conducted with raw delayed coke.

Variable				MAC
pH	8.5 ± 0.1	**NH_4^+ (mg/L)**	6.8 ± 0.1	0.019
Conductivity (mS)	3.1 ± 0.0	**Al (µg/L)**	26.0 ± 4.5	100
Alkalinity (mg $CaCO_3$/ L)	550.8 ± 1.5	**Ni (µg/L)**	11.0 ± 0.1	200
DOC (mg/L)	53*	**Mo (µg/L)**	291.9 ± 1.1	73
OSNAs (mg/L)	56 ± 0.3	**Mn (µg/L)**	12.0 ± 0.1	200
Na^+ (mg/L)	651.5 ± 1.9	**Cu (µg/L)**	190.5 ± 3.8	4
Cl^- (mg/L)	559.5 ± 4.6	**Pb (µg/L)**	9.4 ± 0.7	200
SO_4^{2+} (mg/L)	265.4 ± 3.6	**V (µg/L)**	22.5 ± 0.2	-

Values are an average of duplicates ± one standard deviation
DOC obtained through HACH-DR/2400 method 10173
*****, one value obtained from testing
-, not specified
MAC, Maximum Acceptable Concentration according to Canadian aquatic water quality guidelines (CCME, 2006)

Table 4-2: Characterization of untreated PA water obtained for the tests conducted with raw fluid coke.

Variable				MAC
pH	8.6 ± 0.0	**NH_4^+ (mg/L)**	6.8 ± 0.0	0.019
Conductivity (mS)	3.2 ± 0.0	**Al (µg/L)**	25.4 ± 8.28	100
Alkalinity (mg $CaCO_3$/ L)	587.0 ± 4.2	**Ni (µg/L)**	11.2 ± 1.9	200
DOC (mg/L)	54.0 ± 1.4	**Mo (µg/L)**	276.5 ± 6.9	73
OSNAs (mg/L)	55.1 ± 0.0	**Mn (µg/L)**	25.7 ± 0.1	200
Na^+ (mg/L)	654.8 ± 1.3	**Cu (µg/L)**	190.1 ± 3.4	4
Cl^- (mg/L)	580.7 ± 4.4	**Pb (µg/L)**	9.3 ± 0.1	200
SO_4^{2+} (mg/L)	245.2 ± 1.8	**V (µg/L)**	11.3 ± 0.2	-

Values are an average of duplicates ± one standard deviation
DOC obtained through HACH-DR/2400 method 10173
-, not specified
MAC, Maximum Acceptable Concentration according to Canadian aquatic water quality guidelines (CCME, 2006)

Table 4-3: Characterization of untreated PA water obtained for the tests conducted with activated delayed and fluid cokes and granular activated carbon (GAC).

Variable				MAC
pH	8.7 ± 0.0	**NH_4^+ (mg/L)**	6.4 ± 0.1	0.019
Conductivity (mS)	3.6 ± 0.0	**Al (µg/L)**	47.3 ± 3.6	100
Alkalinity (mg $CaCO_3$/ L)	584.5 ± 7.8	**Ni (µg/L)**	6.9 ± 0.1	200
DOC (mg/L)	39.1 ± 0.7	**Mo (µg/L)**	264.4 ± 1.6	73
OSNAs (mg/L)	60.8 ± 0.4	**Mn (µg/L)**	29.0 ± 1.6	200
Na^+ (mg/L)	707.5 ± 8.7	**Cu (µg/L)**	152.8 ± 3.8	4
Cl^- (mg/L)	501.3 ± 8.1	**Pb (µg/L)**	6.8 ± 0.7	200
SO_4^{2+} (mg/L)	185.2 ± 2.5	**V (µg/L)**	5.3 ± 2.6	-

Values are an average of duplicates ± one standard deviation
DOC obtained by Shimadzu TOC-5000A
-, not specified
MAC, Maximum Acceptable Concentration according to Canadian aquatic water quality guidelines (CCME, 2006)

4.3.2 Activation of Delayed and Fluid Petroleum Coke

Table 4-4 shows the results for the characterization of the raw and activated delayed and fluid coke samples. A range of activation parameters were previously tested including: temperature (800 to 900^{o}C), activation time (2 to 6 h), activation atmosphere (CO_2 only, CO_2 + steam, and N_2 + steam), and steam rate (0.3 to 0.5 mL/min) as found in Chapter 3. The most optimal activation scenario providing the highest surface area and porosity for the delayed and fluid coke samples was chosen for this study. The structural characterization of these activated products is outlined in Table 4-4. The raw delayed and fluid cokes proved to have lower iodine numbers and surface areas than their activated counterparts indicating poor micro- and mesopore development within the materials. The raw delayed coke samples also had a lower initial surface area than the raw fluid coke samples. This can be attributed to less volatilization of organic material within the pores of the delayed coke caused by lower operating coking temperatures of 415 to 450^{o}C in comparison to 480 to 565^{o}C for fluid coking techniques (Fedorak and Coy, 2006). With activation, the iodine numbers increased to 670 and 620 mg/g for activated delayed and fluid coke, respectively. These values are comparable to some commercially available activated carbons.

The iodine number provides a measure of the pores ranging from 10 to 28 Å, indicating the microporosity within a material (U.S. Army Corps of Engineers, 2001). Table 4-4 shows an associated increase in microporosity within the delayed and fluid cokes after activation. The related surface areas were higher for the activated delayed coke sample than for the activated fluid coke sample- these results likely differ due to their raw structures before activation. Raw delayed coke has been described as having a porous or 'sponge-like' structure, whereas raw fluid coke has been described as 'onion-like' or layered in nature (Fedorak and Coy, 2006). The accessibility of the activation agents as well as the development of the pores may be inhibited by the layered structural pattern pre-determined by the raw state of the material within the fluid coke material. The coal-based granular activated carbon (GAC) proved to have a higher associated iodine number and surface area, as expected, indicating an overall higher microporosity throughout the material. As a positive control, it can be expected that the GAC will have a greater adsorption capacity than the activated petroleum cokes. In addition, GAC's wide use in water treatment will be used as a benchmark for comparison to the oil sands coke samples.

Table 4-4: Characterization of the raw and activated delayed and fluid coke samples and granular activated carbon (GAC) through iodine number, Brunauer, Emmett, and Teller (BET) surface area, and micro-/mesoporous volumes.

	Iodine Number (mg/g)	**BET Surface Area (m^2/g)**	**Micropore Volume (cm^3/g)**	**Mesopore Volume (cm^3/g)**
Raw Delayed Coke [A]	21.8	2.7	0	0.0049
Raw Fluid Coke [A]	28.4	27.3	0.0069	0.0095
Activated Delayed Coke	670	577.5	0.1542	0.1660
Activated Fluid Coke	620	493.5	0.1658	0.1322
GAC	1000	1030	0.3313	0.2760

[A] same delayed and fluid raw coke samples measured and reported by Chen, 2010

4.3.3 Adsorption of Organics

To observe whether the activated delayed and fluid coke samples reached equilibrium during the batch tests, samples were incrementally obtained and scanned with fluorescence spectrometry. Fluorescence spectrometry has been recently used as a screening forensics tool to observe characteristic signatures correlated to OSNAs referring to levels of unsaturation and aromaticity (Mohamed et al., 2008). The results indicated that the rate of adsorption was initially fast; however, the system required further time to reach equilibrium. The rate of adsorption depends on the adsorbates ability to reach the boundary layer, diffuse into the adsorbent surface, and diffuse into the porous structure of the adsorbent (Hameed et al., 2007). Samples appeared to have sufficient contact time to reach equilibrium within the first 13 hours, where further mixing proved the stability of the system. Consequently, 24 h mixing time was more than sufficient to ensure equilibrium had been reached.

Figure 4-1-a and b shows the amount of DOC and OSNAs remaining after treatment with raw and activated delayed and fluid coke, as well as GAC. The DOC represents the dissolved fraction of organic carbon found in the oil sands PA water. The OSNAs usually make up 40 to 70 mg/L of the DOC content (typically measured as 50 to 100 mg/L) in oil sands PA waters throughout the Athabasca oil sands region (Allen, 2008a). FTIR spectrometry allows for the analysis of organic compounds within the infrared spectrum through the analysis of absorption signals of a concentrated analyte at a range of frequencies ranging from 400 to 4000 cm^{-1} (ASTM, 2007). The results produce a unique infrared spectral scan based on the frequency in which a material absorbs infrared light, and the intensity of the absorption. Consequently, different analytes will have varying spectral scans; however, there will be unique similarities between materials that contain similar functional groups- allowing for comparisons among samples. The characteristic peaks observed within the spectral scans can be considered to be spectral “fingerprints” (Herres, 1989). This technique can be used for OSNA identification and analysis. Although FTIR spectrometry is the current industry standard used to directly measure OSNA concentrations, it has recently been found that this method overestimates OSNA concentrations by 2-fold (personal communication with Jon Martin, October 15, 2010). Work is currently in progress to better quantify this factor and therefore, the OSNA concentrations obtained through FTIR spectrometry have not been adjusted, but presented as is.

Figure 4-1(a) indicates that with increasing carbon dose of raw delayed and fluid coke, the percent remaining of DOC and OSNAs decreases. The removal efficiency of both DOC and OSNAs is greater for the raw fluid coke than for the raw delayed coke with increasing carbon dose, representing a larger overall adsorption capacity for the raw fluid coke [Figure 4-1(a)]. This is attributed to greater pyrolytic decomposition within the pores of the fluid coke, due to higher upgrading temperatures at the time of production. Consequently, there are initially more mico-/ mesopores within the raw fluid coke structure (total pore volume of 0.0164 cm^3/g) resulting in a higher initial surface area of 27.3 m^2/g (Table 4-4). Adsorption onto the raw delayed coke is affected by the lower initial surface area (2.7 m^2/g) which limits the quantity of exposed adsorption sites. Figure 4-1(a) also shows that overall; the percentage of OSNAs remaining in solution after treatment with raw delayed and fluid coke is less than the amount of DOC remaining in solution. More specifically, the amount of OSNAs remaining for the raw delayed and fluid coke samples is 43% and less than 24%, respectively with the greatest carbon dosage applied. Consequently, raw delayed and fluid coke used at 300 g/L within the PA water, has the potential to remove substantial quantities of OSNAs, depending on the removal objectives for the tailings pond. However, in order to treat the current 4x10^8 m^3 of tailings stored in the Athabasca oil sands region, approximately 1.2x10^8 tonnes of either raw delayed and fluid coke is required; when considering the 300 g/L carbon dose.

Figure 4-1(b) shows that once activated, orders-of-magnitude lower carbon dosages are required to adsorb DOC and OSNAs from the PA water. Here, both activated delayed and fluid cokes are capable of removing similar quantities of DOC (91%) and OSNAs (92%) at the maximum carbon dose of 5 g/L. At lower carbon dosages (ranging from 0.0625 to 0.25 g/L), GAC has a greater removal efficiency of DOC (41 to 12%) and OSNAs (84 to 94%) than the activated delayed and fluid cokes. This is due to the higher surface area within the material (as outlined in Table 4-4).

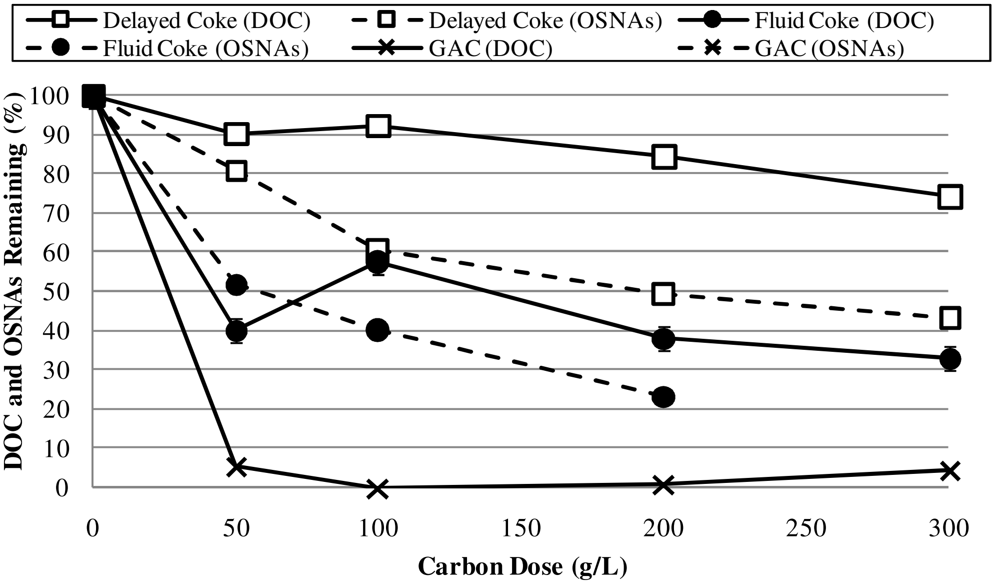

(a) Raw Delayed and Fluid Coke

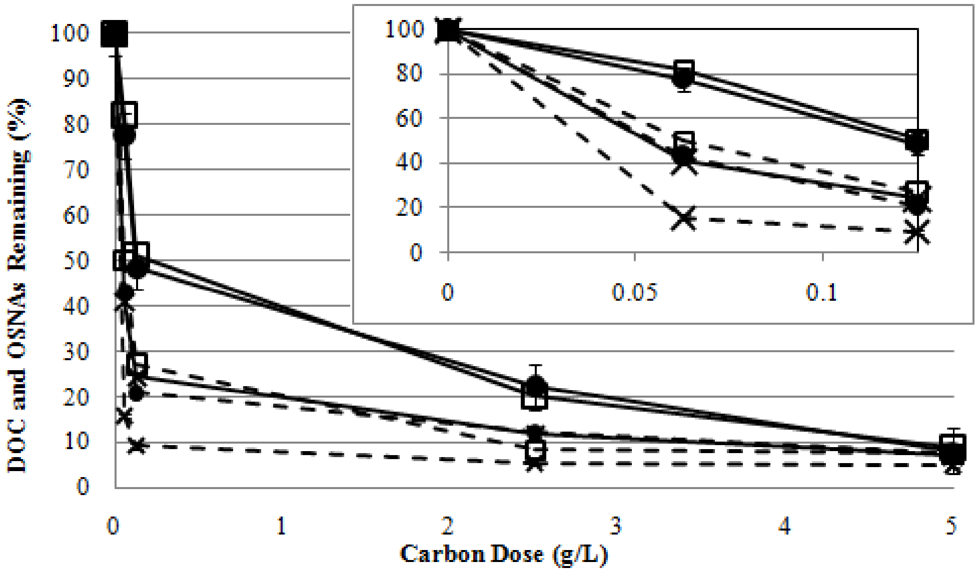

(b) Activated Delayed and Fluid Coke and Granular Activated Carbon (GAC)

Figure 4-1: Effect of carbon dose on dissolved organic carbon (DOC) content and OSNAs within PA water treated with raw (a) and activated (b) delayed and fluid cokes as well as granular activated carbon (GAC). Values are an average of duplicate samples. OSNA results for PA water mixed with GAC at carbon doses ranging from 50 to 300 g/L were not conducted.

At the applied carbon dose of 5 g/L, all activated materials behave similarly, where the amount of DOC and OSNAs remaining in solution differs by approximately 3% between the activated petroleum cokes and the GAC. This suggests that 5 g/L is the optimal dosage for activated delayed and fluid coke use for the removal of organics from the PA water, where results are comparable to commercially available activated carbon products with higher surface areas. The results also indicate that there may be a maximum optimal dosage (around 5 g/L) for most activated carbon materials, or a 'breakthrough' concentration, in which all potential sorption sites for the DOC and OSNAs are occupied. However, reducing the carbon dose by 50% to 2.5 g/L will still allow for the removal of high concentrations of DOC (78%) and OSNAs (90%) for PA waters treated with both activated delayed and fluid coke samples. This should be considered when evaluating remediation targets and goals.

Table 4-5 shows the mass of DOC and OSNAs removed with increasing carbon dose of raw and activated delayed and fluid coke, as well as granular activated carbon. The results in Table 4-5 also indicate that by activating delayed coke, increased masses of DOC and OSNAs can be removed from solution. However, increased doses (ranging from 100 to 300 g/L) of raw fluid coke are capable of removing comparable masses of DOC as the activated fluid coke doses ranging from 0.125 to 5 g/L. The removal of more OSNAs is possible once the fluid coke is activated. This is attributed to the development of an enhanced microporosity within the activated fluid coke sample, increasing the existing surface area. The etching of pores through activation allows for more high-energy adsorption interactions to occur within the activated fluid coke; ultimately increasing the materials adsorption capacity. The activation of the delayed and fluid coke also allows for the application of lower carbon dosages to achieve higher removal rates of OSNAs, increasing the efficiency of the removal technology.

Table 4-5: Mass of dissolved organic carbon (DOC) content and OSNA concentrations removed with the addition of raw and activated delayed and fluid cokes as well as granular activated carbon (GAC).

Sample	Carbon Dose (g/L)	Mass of DOC Removed (mg/L)	Mass of OSNAs Removed (mg/L)
Untreated PA Water ^{A}	0	53.5 ± 1.4	55.5 ± 0.3
Raw Delayed Coke	50	4*	10.7 ± 0.9
	100	3*	22.2 ± 0.0
	200	7*	28.5 ± 1.9
	300	12*	31.9 ± 1.2
Raw Fluid Coke	50	29.0 ± 12.7	27.3 ± 0.0
	100	20.5 ± 3.5	34.0 ± 1.9
	200	30.0 ± 2.8	43.1 ± 0.0
	300	32.5 ± 2.1	-
Untreated PA Water ^{B}	0	39.1 ± 0.7	64.8 ± 0.5
Activated Delayed Coke	0.0625	7.1 ± 0.2	32.2 ± 1.9
	0.125	19.2 ± 2.8	47.4 ± 2.5
	2.5	31.2 ± 0.3	59.4 ± 0.7
	5	35.6 ± 0.3	59.9 ± 0.5
Activated Fluid Coke	0.0625	8.8 ± 0.3	36.8 ± 1.5
	0.125	20.1 ±0.6	51.1 ± 1.5
	2.5	30.4 ± 0.9	56.9 ± 2.5
	5	35.9 ± 0.1	59.9 ± 0.0
GAC	0.0625	22.9 ± 0.4	54.5 ± 0.7
	0.125	29.5 ± 0.6	58.9 ± 0.1
	2.5	34.4 ± 0.4	61.2 ± 1.7
	5	36.3 ± 0.2	61.6 ± 0.5

Values are an average of duplicate samples ± one standard deviation.

A/B, value represents initial measured concentration for the set of samples

-, not available

*****, one value obtained from testing

The adsorption capacity can be estimated from adsorption isotherm data for OSNAs (Figure 4-2). The Freundlich isotherm was used to fit the data due to its ability to model heterogeneous adsorption systems (Shawwa et al., 2001). Figure 4-2 shows the OSNA adsorption isotherms for activated delayed and fluid coke, and GAC. All of the isotherms show a steep initial increase in the curves indicating that the greatest amount of OSNAs adsorbed occurred at the lowest OSNA concentrations. Here, the easily adsorbable compounds are initially removed from solution (Shawwa et al., 2001). As the concentration of OSNAs increases within solution, fewer fractions of OSNAs are adsorbed. The levelling out of the isotherms suggests that increasing carbon dosages may lead to the occupation of all potential sorption sites within the activated carbon materials. This indicates that the highest activated carbon dose (5 g/L) is approaching the optimal equilibrium concentration. The logarithmic adsorption isotherm for OSNAs indicating the linear regression parameters can be found in Appendix E (Figure E-1).

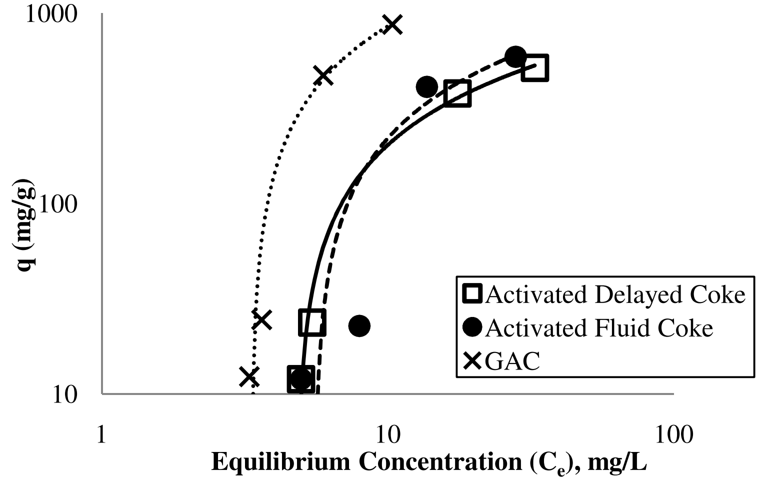

Figure 4-2: Adsorption isotherm for activated delayed and fluid cokes and granular activated carbon (GAC); q represents the amount of OSNAs adsorbed per weight of activated carbon (mg/g) and C_e corresponds to the equilibrium solution-phase concentration (mg/L).

Table 4-6 summarizes the Freundlich parameters obtained from the adsorption isotherms for activated delayed and fluid coke and GAC. The parameter K represents the adsorption capacity (Shawwa et al., 1999) of the activated material for the OSNAs measured within this experiment; K ultimately describes the distribution of the OSNAs between the PA water and the activated carbon materials.

Table 4-6: Freundlich parameters for OSNA adsorption.

Sample	K (mg/g activated carbon)	1/n	n
Activated Delayed Coke	0.7	2.0	0.5
Activated Fluid Coke	0.2	2.5	0.4
GAC	0.2	3.8	0.3

Table 4-6 indicates that a better adsorption of OSNAs was achieved through the application of activated delayed coke. Alternatively, the adsorption of

OSNAs was similar between activated fluid coke and GAC. The parameter 1/n represents the effect of concentration on the adsorptive capacity (Shawwa et al., 1999). Overall, the effect of concentration was greatest for the GAC. Though the adsorption dose and equilibrium concentrations are related, the adsorption capacity of the organic fraction within the PA water is complicated by the competitive adsorption of inorganic compounds, other organic compounds and the individual compounds that make up the larger class of OSNAs (Pavoni et al., 2006; Qi and Schideman, 2008). In this case, it becomes difficult to effectively model the multi-component equilibria with competitive and poorly understood interactions, based on single solute isotherm data (Smith, 1991). The presence of dissolved organic background matter can also further enhance the non-ideality represented within models (Smith, 1991). Consequently, the adsorption capacity may not have been accurately represented through the traditional modelling approach.

Fluorescence spectrometry is a screening tool used to observe characteristic OSNA signatures in PA water. Figure 4-3 shows emission spectra indicative to OSNAs found within untreated PA water. The maximum intensity can typically be found at excitation wavelength of 280 nm around an emission wavelength of 350 nm. After correction for inner and outer-filtering effects, the peak intensity is observed to be exceeding 1200 a.u.

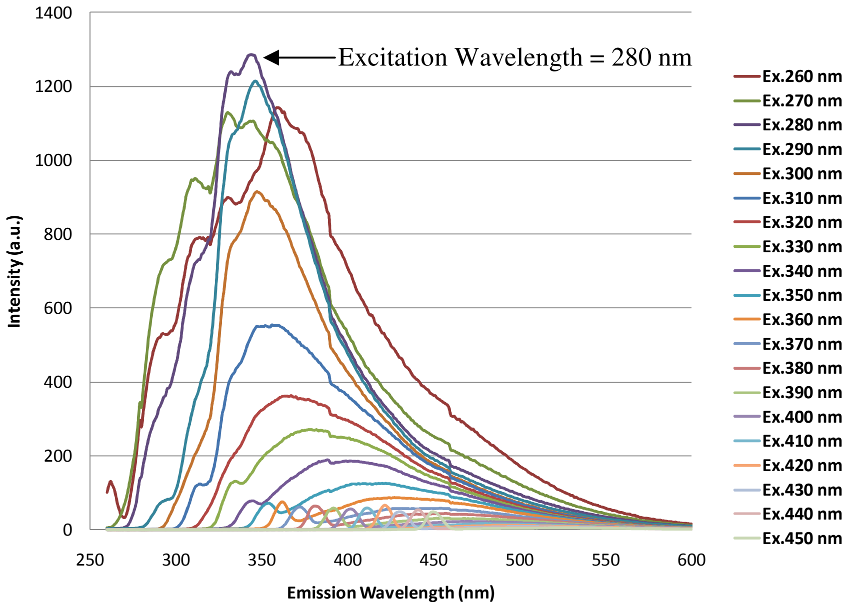

Figure 4-3: Emission spectra of untreated PA water including excitation wavelengths from 260 to 450 nm

The peak intensity at 280 nm excitation wavelength was tracked within PA water samples treated with raw and activated delayed and fluid cokes, as well as GAC (Figures 4-4-a and b). Figure 4-4(a) showed that samples treated with 300 g/L of raw delayed coke removed the maximum peak intensity by 76%. In contrast, when 300 g/L of raw fluid coke was used to treat PA water, 95% of the maximum peak intensity was removed. Consequently, raw fluid coke has the capacity to remove greater percentages of the OSNA peak intensity than raw delayed coke as measured through fluorescence spectrometry.

When 0.0625 to 5 g/L of activated delayed and fluid cokes were mixed with PA water, a similar peak intensity removal efficiency of 83 to 99% was observed [Figure 4-4(b)]. In comparison, GAC showed an overall 97 to 99% removal efficiency. The greater removal efficiency of the GAC at lower carbon doses can be attributed to the greater surface area. However, 5 g/L of all activated carbon materials tested within this experiment were capable of removing the same quantity of the 280 nm peak intensity. This indicates a similar removal efficiency of OSNA concentrations between the adsorbents.

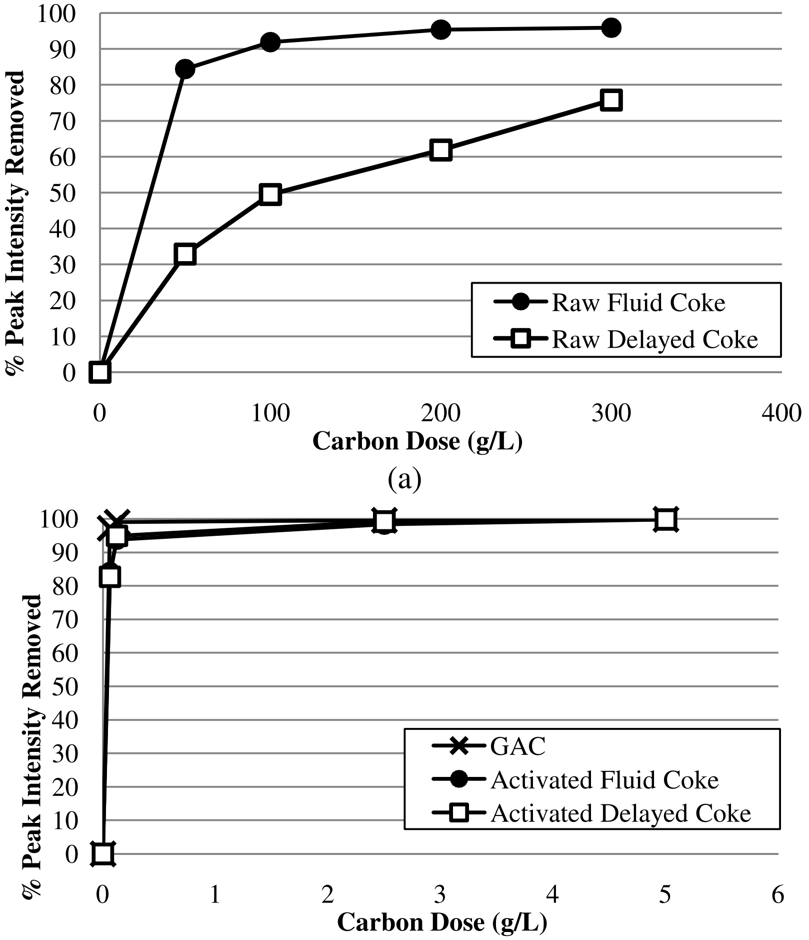

(a)

(b)

Figure 4-4: Removal efficiency of the OSNA peak intensity (280 nm excitation wavelength) for PA water treated with raw (a) and activated delayed and fluid cokes and GAC (b), as obtained through fluorescence spectrometry.

Across the different laboratory techniques, similar decreasing trends in DOC and OSNAs were observed with increasing weight additions of both raw and activated delayed and fluid cokes. However, the results for the fluorescence spectrometry showed greater removal rates of the OSNA signature. Due to the complicated nature of classifying OSNAs, fluorescence spectrometry may overestimate the components involved within the complex mixture of OSNAs.

4.3.4 Treated Process-Affected Water Characterization

Samples treated with raw delayed and fluid coke were analyzed in order to observe major trends in trace metals within solution (Figures 4-5-a and b). With the application of raw delayed coke, the electrical conductivity remained constant, while the pH and total alkalinity ranged from 8.74-9.09 and 521-573 mg $CaCO_3$/L, respectively. For PA water treated with raw fluid coke, the electrical conductivity also remained consistent, where the pH and total alkalinity fluctuated between 8.65-9.05 and 505-569 mg $CaCO_3$/L, respectively. These fluctuations may be due to competitive interactions between the organic and inorganic components within the PA water. Within the PA water treated with raw delayed coke, Li (0.18 mg/L), Cl (559.46 mg/L), and PO_4^{2-} (0 mg/L) remained consistent before and after application. Consequently, the previous cation and anion concentrations originated from the untreated PA water and were not affected by the adsorption processes during the batch tests. All of the other associated major anions and cations fluctuated within the PA water treated with both raw delayed and fluid coke. The increasing trends observed for PA samples treated with raw delayed coke were Ca, Mg, and F; decreasing trends were observed for NH_4, Na, and SO_4 (see Appendix E, Table E-3). Increasing trends observed for PA samples treated with raw fluid coke included Cl, F, SO_4, and PO_4; decreasing trends involved Ca, Mg, NH_4, K, Na, Li, and Br (see Appendix E, Table E-3). The greater influence on cations in the PA water treated with raw fluid coke may be due to the greater initial porosity. The structure of the raw fluid coke differs from the raw delayed coke due to the different upgrading techniques at the time of production. This may have led to the development of different initial functional groups, which may have ultimately impacted the exchange of positively charged atoms on the surface of the material. Previous study has indicated that raw fluid coke contains a larger percentage of oxygen which can influence the chemical properties on the surface of the material (Chen, 2010). The reduction of NH_4 for PA water samples treated with both raw delayed and fluid cokes is beneficial due to its known aquatic toxicity. Figure 4-5-a and b show the major trends in trace metals within PA water samples treated with both raw delayed and fluid cokes.

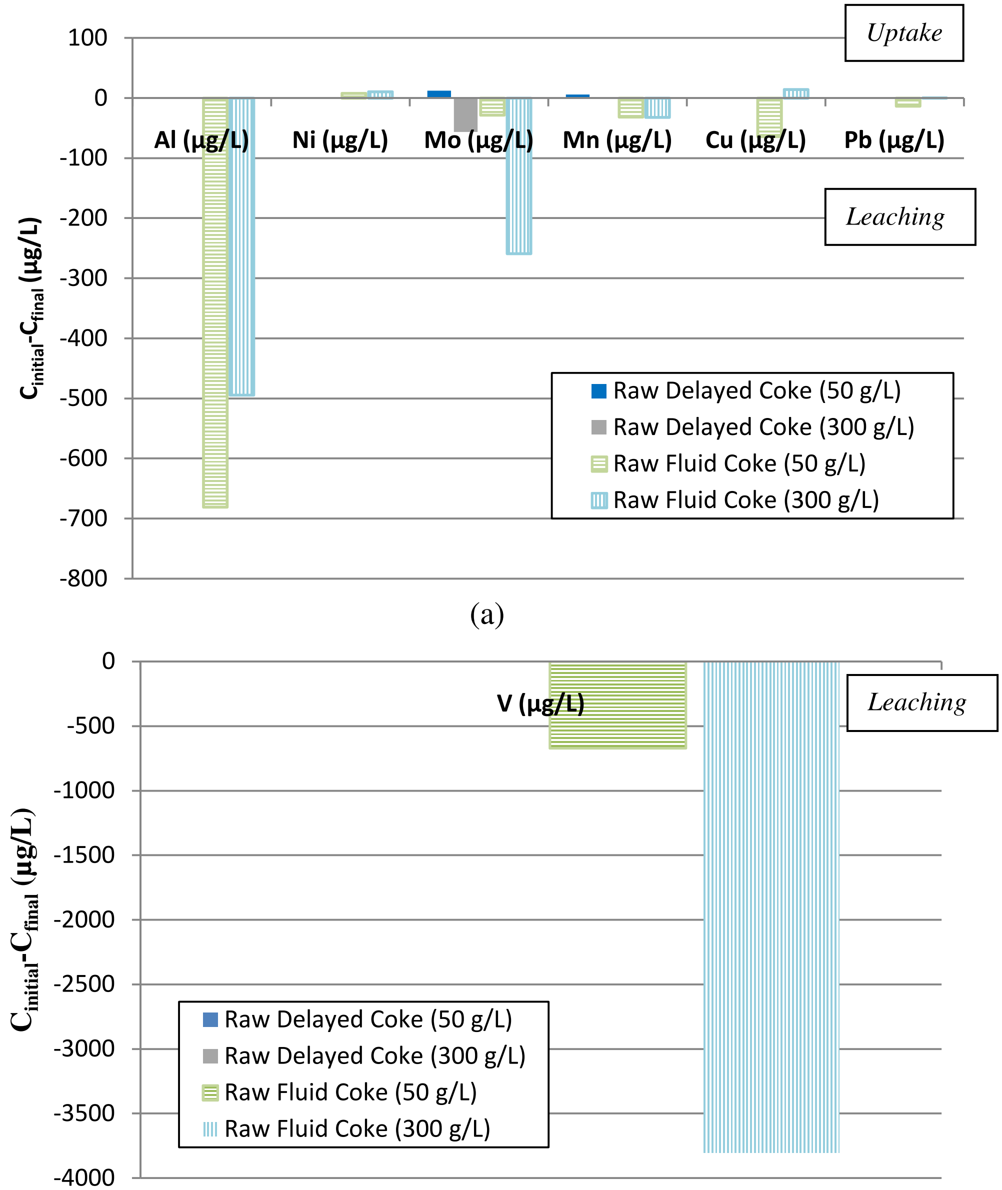

(a)

(b)

Figure 4-5: Characterization of PA water treated with raw delayed and fluid cokes indicating major trends in uptake and leaching of heavy metals (a) and vanadium (b).

Figure 4-5(a) shows that the raw fluid coke has a greater influence on trace metals within the treated PA water where increased leaching of Al (935 to 748 µg/L), Mo (305 to 536 µg/L), Mn (57 to 58 µg/L), Cu (254 to 176 µg/L), and V (682 to 3814 µg/L) was observed with increasing carbon doses from 50 to 300 g/L. The measured levels of Al, Mo, Cu, Pb, and V in PA water samples treated with raw fluid coke all exceed Canadian aquatic water quality guidelines (CCME, 2006). In contrast, PA water treated with 300 g/L of raw delayed coke only showed leaching of Mo (289-358 µg/L) at levels greater than CCME guidelines (2006). Above aquatic water quality guidelines, the trace metals in Figures 4-5-a and b are known to be toxic to aquatic life. Consequently, remediation with raw delayed and fluid coke will require additional inorganic treatment options.

PA water treated with activated delayed and fluid coke samples was characterized in order to further evaluate the efficiency of the technology. When treated with the activated delayed and fluid coke, the PA water maintains a comparable alkalinity and conductivity, where the pH becomes steady around 9.3. The adsorption of organic acids onto the activated material may have resulted in a more alkaline filtrate. The unchanged conductivity indicates that the activated delayed and fluid coke did not contribute to the salt content of the treated PA water. The following cation concentrations obtained through ion chromatography testing were also found to be consistent before and after treatment with activated coke: Ca (8.0 mg/L); Mg (5.6 mg/L); K (10.2 mg/L); Na (707.5 mg/L); Li (0.18 mg/L). The major anions observed as consistent throughout the tests were: Br (0.39 mg/L); Cl (501.3 mg/L); F (1.65 mg/L); and SO_4 (183.4 mg/L). Consequently, the previous cation and anion concentrations originated from the untreated PA water and were not affected by the adsorption processes during the batch tests. Overall, these concentrations of cations and anions within the PA water treated with activated delayed and fluid cokes were more consistent than PA water treated with raw delayed and fluid cokes.

Ammonium (NH_4^+) concentrations within the PA water increased from 6.4 mg/L within the untreated PA water to 7.7 mg/L with the addition of 5 g/L of both activated delayed and fluid cokes. An increase in ammonium negatively impacts the water quality of the treated PA water due to its toxicity within the environment, especially at levels over 0.019 mg/L (CCME, 2006). Ammonium is toxic to all vertebrates through aquatic exposure, where most species of fish cannot tolerate high levels (Randall and Tsui, 2002).

Figure 4-6(a) shows the major increasing and decreasing trends in heavy metals within the treated PA water samples. The following increasing trends in trace metal concentrations were observed with increasing carbon dose of both activated delayed and fluid cokes: Al, Ni, and Mo. Overall, the trends in Al and Mo were greater for the activated fluid coke samples, where concentrations increased ranging from 118 to 217 μg/L and 296 to 437 μg/L, respectively for carbon doses of 0.0625 g/L and 5 g/L. Increasing trends in Ni were greater for the activated delayed coke samples where measureable concentrations ranged from 48 to 96 μg/L for carbon doses of 0.0625 g/L and 5 g/L. The leaching of Ni concentrations may not be a significant issue for the oil sands industry since the levels are below the Canadian aquatic water quality guidelines of 150 μg/L (CCME, 2006). As a result, these increasing trends will not affect the remediation goals of the tailings pond water. Though the Al concentrations measured within the treated PA water increased, the conditions within the PA water are not favourable for acute Al toxicity. Between pH 5 and 6, Al polymerization occurs causing aquatic toxicity for fish species (Poleo, 1995). The treated PA water has a pH of 9.3 creating an environment of reduced Al reactivity towards biological structures, ultimately reducing the acute toxicity (Poleo, 1995). However, at the pH levels measured within the treated PA water (>5), Mo is known to stay in solution (LeGrande and Runnells, 1975). This may cause chronic toxicity issues for aquatic species, such as rainbow trout (CCME, 1999). Consequently, the future removal of Mo will have to be considered for remediation purposes.

Decreasing trends in Mn, Cu and Pb corresponding to a removal of 14-27 μg/L, 113-128 μg/L, and 5-6 μg/L, respectively were observed with the addition of activated delayed and fluid coke doses ranging from 0.0625 to 5 g/L [Figure 4-6(a)]. The removal of these elements can be considered a benefit of the application of the adsorption technology.

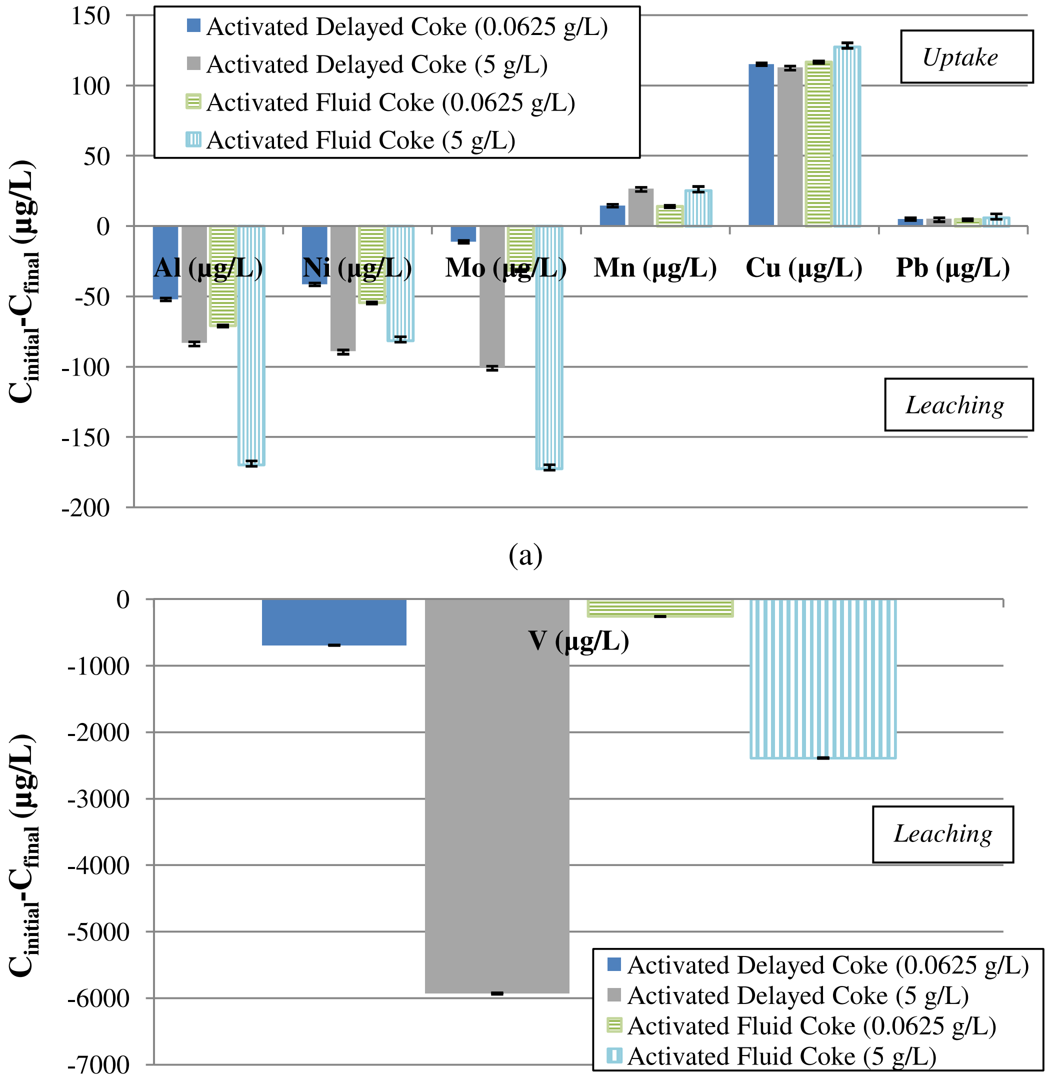

(a)

(b)

Figure 4-6: Characterization of PA water treated with activated delayed and fluid cokes indicating major trends in uptake and leaching of heavy metals (a) and vanadium (b). Values are an average of duplicate samples ± one standard deviation.

Vanadium (V) measured within the untreated PA water was 5 µg/L (Table 4-3). Within the PA samples treated with 5 g/L of activated delayed and fluid coke, V was measured as 5933 µg/L and 2394 µg/L, respectively [Figure 4-6(b)]. The leaching of V is considered to be a negative impact of the application of activated delayed and fluid coke. Both raw delayed and fluid petroleum cokes from the Athabasca oil sands region are known to contain high levels of uniformly distributed vanadium (Ityokumbul, 1994). Increased temperatures during activation allows for V to become available for leaching. Though Ni is also present within the raw petroleum cokes, it is more resistant to leaching than V due to the difference in reactivity between the two metals; V is capable of forming soluble complexes, whereas Ni has the capacity to form precipitates within alkaline media (Ityokumbul, 1994). The presence of V within the tailings pond waters has the ability to negatively impact the water quality, where remediation of the trace metal would need to be considered. If phytoavailable, V is toxic to plant life (Chen et al, 2010) which will impact current reclamation strategies within the Athabasca oil sands region. Consequently, the use of the activated delayed and fluid petroleum coke will have to be combined with an inorganic remediation technique. The remediation of V from wastewater has been considered throughout the literature, where strategies include the following: sorption onto Fe oxides (such as goethite under oxic atmospheric conditions) [Peacock and Sherman, 2004; Tokunaga et al, 2009]; and, the reduction of V by *Geobacter metallireducens* into an insoluble form that readily precipitates in solution (Ortiz-Bernad et al., 2004). Pre-treatment of the raw and delayed petroleum cokes before application through leaching with acids (for example, HCl) have also been shown to increase the solubility and removal of V (Ityokumbul, 1994). The application of these remediation strategies will help to regulate the amount of V measured within the tailings pond water.

Overall, the samples treated with activated fluid coke was observed to have lower concentrations of trace metals (including Al, Mo, Mn, Cu, Pb, and V) than the samples treated with raw fluid coke. As a result, activated fluid coke can be considered to be a more effective remediation option.

4.3.5 Leaching Tests with Ultra-Pure (DI) Water

Raw delayed and fluid cokes were mixed with ultra-pure (DI) water in order to observe further leaching behaviour of the coke materials. Table 4-7 shows the outcome of the DI water mixed with raw delayed and fluid cokes. In comparison to the blank DI water sample, the raw delayed and fluid cokes were observed to alter the pH, alkalinity, and electrical conductivity (EC). More specifically, with the addition of the cokes, the pH dropped from an initial value of 8.2 to values ranging from 7.2 to 7.6 and 7.2 to 8.2 for DI water mixed with delayed and fluid cokes, respectively. With increasing carbon dose of both raw delayed and fluid cokes, the EC was observed to increase as well, indicating an increase in salt content within the treated DI water. Moreover, the change in EC was greater for the DI water samples mixed with the raw delayed coke where the values are orders of magnitude greater than that of the untreated DI water sample. Alkalinity within the DI water treated with raw fluid coke increased slightly, where higher values were observed for lower carbon doses ranging from 50 to 100 g/L. For DI water samples mixed with raw delayed coke, the alkalinity increased with increasing carbon dose. The DOC values measured were all under range (<15 mg/L), indicating the absence of organic compounds.

Table 4-7: Characterization of untreated ultra-pure (DI) water and DI water treated with raw delayed and fluid cokes.

Sample	Carbon Dose (g/L)	pH	EC (µS)	Alkalinity (mg CaCO3/L)	DOC (mg/L)
DI Water	0	8.2 ± 0.4	1.7 ± 0.4	3.3 ± 0.4	3.0 ± 4.9
Delayed Coke	50	7.2 ± 0.0	41.1 ± 3.3	20.3 ± 0.4	1.0 ± 1.4
	100	7.3 ± 0.0	55.9 ± 6.4	18.0 ± 3.5	0.5 ± 0.7
	200	7.3 ± 0.0	96.5 ± 11.0	17.8 ± 3.9	6.5 ± 3.5
	300	7.6 ± 0.0	155.1 ± 4.2	35.4 ± 0.2	1.0 ± 1.4
Fluid Coke	50	8.2 ± 0.1	15.8 ± 1.0	6.5 ± 0.0	8.0 ± 2.8
	100	7.7 ± 0.0	27.3 ± 0.4	6.3 ± 1.1	5.5 ± 4.9
	200	7.4 ± 0.0	50.5 ±1.1	5.3 ± 3.3	1.5 ± 0.7
	300	7.2 ± 0.0	69.7 ± 0.4	4.0 ± 1.4	1.0 ± 1.4

Values are the average of duplicate samples ± one standard deviation
DOC obtained through HACH-DR/2400 method 10173

Figure 4-7 shows major trends in cations and anions measured within the DI water mixed with raw delayed and fluid cokes. These measurable increases in Ca, Na, and SO_4 are associated with the increasing trends in EC. The raw delayed coke was observed to leach higher measureable concentrations of Ca, Na, and SO_4 than the raw fluid coke with increasing carbon dose. The higher concentrations of Ca leached may have contributed to the increase in alkalinity, measured as $CaCO_3$. Though leaching was present with increasing carbon doses, the concentrations of Ca, Na, and SO_4 were all less than the Canadian drinking water quality guidelines (the most stringent guidelines available) (CCME, 2006). Consequently, the leaching from raw delayed and fluid cokes when mixed with DI water will not negatively impact human health with respect to pH, EC, alkalinity, and DOC content.

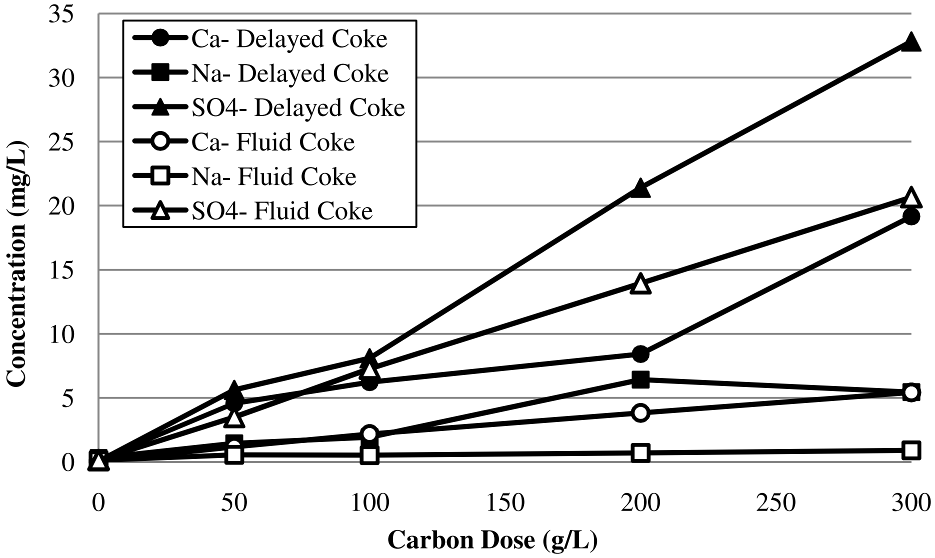

Figure 4-7: Trends in major cations and anions within ultra-pure (DI) water treated with raw delayed and fluid cokes. Values are the average of duplicates ± one standard deviation.

4.3.6 Toxicity Assays

Toxicity assays of the untreated and treated samples were conducted to observe whether the toxic components associated with OSNAs were removed during adsorption (Table 4-8). The 81.9% basic test on untreated PA water indicated that the sample was toxic towards the bacteria, where exposure at 5 min proved to be less toxic than exposure to the sample at 15 min. The light response is dependent upon the different chemicals within a solution, as they can affect the organisms in different ways. Organic compounds typically have an immediate response, where the light response levels off with time (ASTM, 2009). This biological response can, on average, be accurately represented by the 5 min time data. An increasing decay rate of light for an extended time period is characteristic of a heavy metal response, where 15 min data will show an increase in bioreactivity responses towards metal compounds (Petala et al., 2005).

Consequently, the 5 min EC_{20} data indicates toxicity which may be attributed to organic compounds as well as heavy metals within solution. The increased toxicity at 15 min may be attributed to an increased biological response specifically towards the metals within solution.

The 81.9% basic test could not calculate EC_{20} percentages for the PA water treated with activated delayed and fluid cokes due to the detection of hormesis (the biological response was positive towards the sample filtrates). As a result, the treated samples were not toxic enough to kill detectable quantities of the *Vibrio fischeri* species; and ultimately, toxic components were no longer bioavailable.

The 81.9% screening test was preformed to observe the toxicity effect for the PA water treated with 0.0625 g/L and 5 g/L carbon dosages of activated delayed and fluid cokes. Data was normalized to the control within each test in order to compare the toxic effects between samples. The results in Table 4-8 indicate that with increasing carbon dose of activated delayed and fluid coke, the toxicity effect decreases. This suggests that higher carbon dosages are more effective in reducing a toxic biological response within the treated PA water. However, with increasing time from 5 to 15 min, the toxicity effect increases. Consequently, longer exposure time to the treated PA water affected the biological response. Since the FTIR results indicated that a 92% removal of OSNAs with 5 g/L of activated delayed and fluid coke was possible, the potency of the toxicity effect may be due to inorganic compounds (such as metals) within the sample filtrates. Increased exposure to high levels of V, Al, Ni, Mo, and NH_4^+ measurable within the treated water samples may have also led to the increased effect of toxicity with time. The biological response towards the different metals may differ. Though vanadium concentrations are higher for activated carbon doses of 5 g/L, it may take a longer time for the metal to impact the bioreactivity of the *Vibrio fischeri* bacteria. Thus, the higher toxic effect at 5 min for activated carbon doses of 0.0625 g/L may be attributed to increased levels of organics within the treated PA water. High levels of salinity (due to chlorine, sodium and sulphate ions) can also contribute to toxicity as measured through Microtox™ assays (Del Rio et al., 2006). These different components within the treated PA water may have an additive effect on the biological response of the bacteria. These factors outline that inorganic treatment options should be used after organic contaminant removal by activated delayed and fluid cokes in order to reduce heavy metal toxic effects that may harm aquatic organisms from a variety of trophic levels.

Table 4-8: EC$_{20}$ values for untreated pH-adjusted PA water and toxicity effect of pH-adjusted PA water treated with activated delayed and fluid cokes.

81.9% Basic Test			
Sample	**Carbon Dose (g/L)**	**EC$_{20}$- 5 min (%)**	**EC$_{20}$- 15 min (%)**
Untreated PA Water	0	26.5 ± 1.8	14.5 ± 0.2
81.9% Screening Test			
Sample	**Carbon Dose (g/L)**	**Effect- 5 min (%)**	**Effect- 15 min (%)**
Treated PA Water with Activated Delayed Coke	0.0625	13.8 ± 0.9	20.8 ± 2.1
	5	4.8 ± 0.6	7.7 ± 2.0
Treated PA Water with Activated Fluid Coke	0.0625	12.0 ± 1.0	18.7 ± 0.9
	5	2.1 ± 1.5	5.5 ± 0.5

Values are an average of duplicate samples ± one standard deviation

4.4 Conclusions

Activation experiments demonstrated that high iodine numbers of 670 mg/g and 620 mg/g and surface areas of 578 m^2/g and 494 m^2/g were possible with the activation of raw delayed and fluid coke samples. Due to the differing structures of the raw materials, the activated fluid coke samples produced a greater microporosity than the activated delayed coke samples.

The adsorption test results led to the development of different remedial options dependent upon the remediation goals/ or strategies of the user. If 50 to 80% removal of OSNAs is desired, then 300 g/L of raw delayed and fluid coke can be used as a treatment option. However, large quantities of petroleum coke will be required, which may lead to another solid waste management issue.

Complete removal of OSNAs may not be possible due to the adsorptive capacity of activated carbon (either GAC or activated petroleum coke) as observed through the adsorption isotherms; 92% removal of OSNAs and 91% of the associated DOC content is achievable with using either technique at 5 g/L. This material will not affect the alkalinity or conductivity of the tailings pond, but leaching of ions and trace metals (specifically NH_4^+, Al, Mo, and V) will be observed. Inorganic treatment technologies will have to be set in place for the high initial salt content of the PA water, and such treatments can be extended to solve the potential trace metal toxicity issues. In order to reduce the quantity of leaching, 2.5 g/L of activated delayed and fluid coke should be considered due to their ability to remove 90% of the total OSNAs. No measureable toxicity was found with the application of petroleum coke concentrations ranging from 0.0625 to 5 g/L.

Overall, the application of activated petroleum coke has the potential to remove large proportions of organics solving water quality issues surrounding toxicity, total organic carbon, and colour within the Athabasca oil sands region. This technique would provide a means for the oil sands industry to turn their large stockpiles of petroleum coke into a feasible tailings pond remediation technology.

4.5 Chapter 4 References

Allen, E.W. 2008a. Process water treatment in Canada's oil sands industry: I. Target pollutants and treatment objectives. *Journal of Environmental Engineering and Science*; 7: 123-138.

Allen, E.W. 2008b. Process water treatment in Canada's oil sands industry: II. A review of emerging technologies. *Journal of Environmental Engineering and Science*; 7: 499-524.

Asanov, A.N., Kao, S., and Oldham, P.B. 1998. A comparison of fluorescence inner-filter effects for difference cell configurations. *Instrumentation Science and Technology*; 26: 375-387.

ASTM. 2006. Standard test method for determination of iodine number of activated carbon. *ASTM International*. PA, USA; D 4607-94.

ASTM. 2007. Standard Practice for General Techniques for Obtaining Infrared Spectra for Qualitative Analysis. *ASTM International*. PA, USA; E1252-98.

ASTM. 2008. Standard test method for 24-h batch-type measurement of contaminated sorption by soils and sediments. *ASTM International*. PA, USA; D 4646-03.

ASTM. 2009. Standard test method for assessing the microbial detoxification of chemically contaminated water and soil using a toxicity test with a luminescent marine bacterium. *ASTM International*. PA, USA; D5660-96.

Barczak, M., Dabrowski, A., Hubicki, Z., and Podkoscielny, P. 2005. Adsorption of phenolic compounds by activated carbon- A critical review. *Chemosphere*; 58: 1049-1070.

Beekes, M., Lasch, P., Naumann, D. 2007. Analytical applications of Fourier Transform-Infrared (FT-IR) Spectrometry in microbiology and prion research. *Veterinary Microbiology*; 123: 305-319.

Canadian Association of Petroleum Producers (CAPP). 2009. *Water use in Canada's oil sands*. 2009-0022. CAPP, Calgary, Alberta. Available at http://www.capp.ca/library/publications/crudeOilAndOilSands/pages/pubInfo.aspx?DocId=154986#qizoWOc35CWl (accessed November 29, 2010).

Canadian Council of Ministers of the Environment. 1999. *Canadian water quality guidelines for the protection of aquatic life- Molybdenum*. Canadian Council of Ministers of the Environment, Winnipeg, Canada.

Canadian Council of Ministers of the Environment. 2006. *Canadian Environmental Quality Guidelines*. Canadian Council of Ministers of the Environment, Winnipeg, Canada.

Chen, H. 2010. Microwave heating for adsorbents regeneration and oil sands coke activation. Published PhD thesis. University of Alberta, Edmonton, Canada.

Chen, L., Kost, D., and Dick, W.A. 2010. Petroleum coke circulating fluidized bed combustion product effects on soil and water quality. *Soil Science*; 175: 270-277.

Clemente, J.S., and Fedorak, P.M. 2005. A review of the occurrence, analyses, toxicity, and biodegradation of naphthenic acids. *Chemosphere*; 60: 585-600.

Clesceri, L.S., Greenberg, A.E., and Eaton, A.D. 1999. Standard methods for the examination of water and wastewater, 20th edition. American Public heath Association; Washington, DC: 1325 pp.

Del Rio, L.F., Hadwin, A.K.M., Pinto, L.J., MacKinnon, M.D., and Moore, M.M. 2006. Degradation of naphthenic acids by sediment micro-organisms. *Journal of Applied Microbiology*; 101: 1049-1061.

Fedorak, P.M., and Coy, D.L. 2006. Oil sands cokes affect microbial activities. *Fuel*; 85: 1642-1651.

Grewer, D.M., Young, R.F., Whittal, R.M., and Fedorak, P.M. 2010. Naphthenic acids and other acid-extractables in water samples from Alberta: What is being measured? *Science of the Total Environment*, doi:10.1016/j.scitotenv.2010.08.013.

Hameed, B.H., Ahmad, A.L., and Latiff, K.N.A. 2007. Adsorption of basic dye (methylene blue) onto activated carbon prepared from rattan sawdust. *Dyes and Pigments*; 75: 143-149.

Hao, C., Headley, J.V., Peru, K.M., Frank, R., Yang, P., and Solomon, K.R. 2005. Characterization and pattern recognition of oil-sand naphthenic acids using comphrehensive two-dimensional gas chromatography/ time-of-flight mass spectrometry. *Journal of Chromatography A*; 1067: 277-284.

Headley, J.V., Hill, G.A., Nemati, M., and Paslawski, J.C. 2009. Biodegradation Kinetics of Trans-4-methyl-1-cyclohexane Carboxylic Acid. *Biodegradation*; 20: 125-133.

Heres, W. 1989. Capillary gas chromatography- Fourier transform infrared spectroscopy: theory and applications. *Fresenius' Journal of Analytical Chemistry*; 33: 754.

Ityokumbul, M.T. 1994. Experimental evaluation of molten caustic leaching of an oil sand coke residue. *The Canadian Journal of Chemical Engineering*; 72: 370-374.

Karanfil, T., and Kilduff, J.E. 1999. Role of granular activated carbon surface chemistry on the adsorption of organic compounds. 1. Priority pollutants. *Environmental Science and Technology*; 33: 3217-3224.

Kavanagh, R.J., Burnison, B.K., Frank, R.A., Solomon, K.R., and Van Der Fraak, G. 2009. Detecting oil sands process-affected waters in the Alberta oil sands region using synchronous fluorescence spectroscopy. *Chemosphere*; 76: 120-126.

LeGrande, G.R., and Runnells, D.D. 1975. Removal of dissolved molybdenum by precipitation of ferric iron. *Environmental Science and Technology*; 9: 744-749.

Lo, C.C., Brownlee, B.G., and Bunce, N.J. 2006. Mass spectrometric and toxicological assays of Athabasca oil sands naphthenic acids. *Water Research*; 40: 655-664.

Mohamed, M.H., Wilson, L.D., Headley, J.V., and Peru, K.M. 2008. Screening of oil sands naphthenic acids by UV-Vis absorption and fluorescence emission spectrophotometry. *Journal of Environmental Science and Health Part A*; 43: 1700-1705.

Ortiz-Bernad, I., Anderson, R.T., Vrionis, H.A., and Lovley, D.R. 2004. Vanadium respiration by Geobacter metallireducens: Novel strategy for in situ removal of vanadium from groundwater. *Applied and Environmental Microbiology*; 70: 3091-3095.

Peacock, C.L., and Sherman, D.M. 2004. Vanadium (V) adsorption onto goethite (α-FEOOH) at pH 1.5 to 12: A surface complexation model based on ab initio molecular geometries and EXAFS spectroscopy. *Geochimica et Cosmochimica Acta*; 68: 1723- 1733.

Pavoni, B., Drusian, D., Giacometti, A., and Zanette, M. 2006. Assessment of organic chlorinated compound removal from aqueous matrices by adsorption on activated carbon. *Water Research*; 40: 3571-3579.

Petala, M., Tsiridis, V., Kyriazis, S., Samaras, P., Kungolos, A., and Sakellaropoulos, G.P. 2005. Evaluation of toxic response of heavy metals and organic pollutants using microtox acute toxicity test. In Proceedings, *9th International Conference on Environmental Science and Technology*; Rhodes Island, Greece. 1-3 Spetember, 2005. 1-6 pp.

Poleo, A.B.S. 1995. Aluminum polymerization- a mechanism of acute toxicity of aqueous aluminum to fish. *Aquatic Toxicology*; 31: 347-356.

Qi, S., and Schideman, L.C. 2008. An overall isotherm for activated carbon adsorption of dissolved natural organic matter in water. *Water Research*; 42: 3353-3360.

Quagraine, E.K., Peterson, H.G., and Headley, J.V. 2005. In situ bioremediation of naphthenic acids contaminated tailing pond waters in the Athabasca oil sands region- Demonstrated field studies and plausible options: A review. *Journal of Environmental Science and Health*; 40: 685-722.

Quinlivan, P.A., Li, L., and Knappe, R.U. 2005. Effects of activated carbon characteristics on the simultaneous adsorption of aqueous organic micropollutants and natural organic matter. *Water Research*; 39: 1663-1673.

Randall, D.J., and Tsui, T.K.N. 2002. Ammonia toxicity in fish. *Marine Pollution Bulletin*; 45: 17-23.

Scott, A.C., Young, R.F., and Fedorak, P.M. 2008. Comparison of GC-MS and FTIR methods for quantifying naphthenic acids in water samples. *Chemisphere*; 73: 1258-1264.

Shawwa, A., Smith, D..W., and Sego, D.C. 1999. *Color and chlorinated organic reduction in Kraft pulp mill wastewater using activated petroleum coke*. Sustainable Forest Management Network Centers of Excellence, Report MIT-6, Edmonton, Canada.

Shawwa, A.R., Smith, D.W., and Sego, D.C. 2001. Color and chlorinated organics removal from pulp mills wastewater using activated petroleum coke. *Water Research*; 35: 745-749.

Smith, E.H. 1991. Evaluation of multicomponent adsorption equilibria for organic mixtures onto activated carbon. *Water Research*; 25:125-134.

Stavropoulos, G.G., and Zabaniotou, A.A. 2009. Minimizing activated carbons production cost. *Fuel Processing Technology*; 90: 952-957.

Tokunaga, T.K., Kim, Y., and Wan, J. 2009. Potential remediation approach for uranium-contaminated groundwaters through potassium uranyl vanadate precipitation. *Environmental Science and Technology*; 43: 5467-5471.

Tucker, S.A., Amszi, V.L., and Acree Jr., W.E. 1992. The modern student laboratory: fluorescence spectroscopy. *Journal of Chemical Education*; 69: A8-A12.

U.S. Army Corps of Engineers. 2001. Engineering *and Design- Adsorption Design Guide*. Design Guide No. 1110-1-2. Department of the Army; 1-99.

Whitby, C. 2010. Microbial naphthenic acid degradation. Advances in applied microbiology. Elsvier, Ltd., UK: 70L 93-125.

CHAPTER 5: SUMMARY, CONCLUSIONS AND RECOMMENDATIONS

This research has added to the understanding of how petroleum delayed and fluid coke can be used as a remediation tool for the oil sands industry. Through the characterization of the structural properties, adsorption capacity, and leaching potential, it was found that raw and activated delayed and fluid cokes have the ability to remove toxic and corrosive organic by-products from contaminated tailings pond water. This is significant because it provides a means for the oil sands industry to utilize an abundant waste by-product for the remediation of another; promoting sustainable development in the Athabasca region.

This study has demonstrated that raw delayed and fluid petroleum coke can be turned into high surface area activated carbons through the use of physical activation, where surface areas ranging from 399 to 578 m^2/g are possible. Optimal physical activation treatment conditions were as follows: 900^oC, 0.5 mL/min steam rate, 6 hour duration, under a CO_2 + steam atmosphere. These conditions led to the highest iodine numbers and methylene blue values of 620 to 670 mg/g, and 123 to 124 mg/g for activated fluid and delayed coke, respectively. The high surface areas and porosities measured, indicated that the activated products would be excellent candidates for use as adsorbents. Table 5-1 provides a summary of the range of physical activation conditions tested throughout the study.

Table 5-1: Summary of tested physical activation conditions.

Condition/ Parameter	**Value**
Sample Size	20 g
Petroleum Coke	Delayed, Fluid
Petroleum Coke Grain Size	75 to 150 μm
Activation Temperature	800 to 900^oC
Activation Time	2 to 6 hours
Activation Atmosphere	CO_2 only, CO_2 + steam, N_2 + steam
Activation/ Carrier Gas Feed Rate	100 mL/min
Steam Rate	0.3 to 0.5 mL/min
Heating Tape Temperature	180^oC
Heat Up/ Cool Down Atmosphere	N_2
Heat Up/ Cool Down Gas Feed Rate	300 mL/min
Cool Down Time	Overnight (12 hours)

5.1 Characterization of Activated Delayed and Fluid Coke

The physically activated delayed and fluid cokes were characterized to assess their structural and behavioural properties. Characterization allowed for altering of parameters to find the most efficient conditions leading to the development of the greatest achievable surface area and porosity within the activated samples. The following tests were completed: thermogravimetric analysis (TA Instruments, Q500), X-ray diffraction (Bruker D8 Discover), iodine and methylene blue adsorption tests, N_2 adsorption isotherms (Quantachrome, Autosorb 1-MP), and scanning electron micrographs (Hitachi S-2500). The subsequent conclusions based on characterization experiments summarize the results of the activation trials:

1. A decrease in yield is experienced for both delayed and fluid cokes with increasing activation temperature, activation time and steam rate. The overall yield was less for the fluid coke samples (ranging from 53 to 80%) activated for 2 to 6 hours at 900^{o}C than the delayed coke samples (ranging from 47 to 74%), indicating fewer gasification reactions. Activation at 900^{o}C for 6 hours with 0.5 mL/min of steam led to approximately a 47% yield for activated delayed coke, where the greatest surface area and porosity was expected.
2. Thermogravimetric analysis showed a greater initial weight loss for delayed coke at temperatures less than 500^{o}C under N_2. Lower associated upgrading temperatures led to a loss of a greater amount of volatile matter within the pores of the delayed coke. When the CO_2 atmosphere was introduced, the delayed coke experienced a 20.8% decrease in weight, whereas the fluid coke experienced a 5.4% decrease in weight.
3. Activation led to the development of graphite peaks and carbon phases in both delayed and fluid coke samples as observed through X-ray diffraction. The development of graphite showed no preferential direction, was randomly distributed, and showed no perfect alignment of sheets. The activated fluid coke was determined to be graphitizing, whereas the

activated delayed coke had graphitizing potential primarily due to the amorphous nature of the raw material.

4. Scanning electron micrographs showed that activation led to increased surface roughness, widening of surface pores, and erratic cracking. The roughness of the surface was attributed to the irregular loss of carbon on the activated delayed and fluid cokes.
5. For the activated delayed coke samples, longer activation times led to the development of a microporous pore structure; activation in a CO_2 + steam (0.5 mL/min) atmosphere at 900°C for a activation time of 6 hours led to a BET surface area of 578 m^2/g. A lower steam rate was necessary for obtaining the maximum surface area for activated fluid coke, where activation in a CO_2 + steam (0.3 mL/min) atmosphere at 900°C for an activation time of 6 hours led to a BET surface area of 533 m^2/g. These surface areas are associated with a mesopore to micropore ratio of approximately 50:50.
6. Iodine adsorption tests indicated that activation under CO_2 only was not effective in increasing the surface area of both the activated delayed and fluid coke samples. Higher activation time, temperature and steam rate led to the development of the most optimal iodine numbers for both activated delayed and fluid cokes. The most successful activation atmosphere was CO_2 + steam, resulting in iodine numbers of 620 and 670 mg/g for fluid and delayed coke, respectively. Increased steam rate allowed for more molecules of water to interact with the surface of the carbon allowing for increased gasification reactions.
7. Methylene blue values were insignificant (< 10 mg/g) for delayed and fluid coke samples activated at 800°C. Activation under CO_2 + steam (0.5 mL/min) for 6 hours at 900°C demonstrated the greatest methylene blue values of 122.6 and 123.9 mg/g for both fluid and delayed coke, respectively.

8. Activation under CO_2 + steam was preferred over N_2 + steam due to the uniform gasification and development of pores. For this reason, most of the tests were conducted under CO_2 + steam.

The surface areas, methylene blue values and iodine numbers established within this research were the greatest in comparison to those found in the literature for oil sands delayed and fluid petroleum cokes activated under similar conditions. These results indicated that delayed and fluid petroleum coke can be converted into activated carbon with a high surface area and porosity available for adsorption.

5.2 Application of the Activated Delayed and Fluid Cokes

5.2.1 Characterization of the Adsorption Capacity

The adsorption capacity of dissolved organic carbon (DOC) and oil sands naphthenic acids (OSNAs) onto raw and prepared activated delayed and fluid coke was assessed in order to determine the effectiveness of the adsorbents. The optimal carbon dose required for maximum adsorption of organics was determined for activated delayed and fluid coke, and compared to that of a high surface area commercially available granular activated carbon (GAC). Characterization of the treated process-affected (PA) water was completed through the following tests: DOC content (Shimadzu, TOC-5000A), Fourier Transform Infrared (FTIR) spectrometry (Perkin Elmer, Spectrum 100), and fluorescence spectrometry (Varian Cary Eclipse). The following conclusions summarize the results of the testing:

1. With increasing carbon dose of raw delayed and fluid coke (ranging from 50 to 300 g/L), the removal efficiency of DOC and OSNAs increased. The maximum removal of DOC and OSNAs for 300 g/L of raw delayed coke was 12 mg/L and 32 mg/L, corresponding to a removal efficiency of 26% and 57%, respectively. In contrast, the maximum removal of DOC and OSNAs for raw fluid coke was 33 mg/L and 43 mg/L, corresponding to a

removal efficiency of 67% and 77%, respectively. Differences can be attributed to the initial pore structure of the raw materials.

2. Once activated, lower carbon doses of delayed and fluid coke were required to remove similar quantities of DOC (91%) and OSNAs (92%), where the maximum removal was achieved at 5 g/L. These values were comparable to results achieved using commercially available GAC.
3. Adsorption isotherms indicated that easily adsorbable compounds were initially removed from the PA water; whereas fewer fractions of OSNAs were adsorbed as the adsorption continued. The adsorption isotherm for activated delayed and fluid coke began to level out at a carbon dose of 5 g/L, suggesting the occupation of all potential adsorption sites.
4. OSNA signatures within treated PA water were removed to 99.8% with the application of activated delayed and fluid coke and GAC, as measured through the reduction of the maximum fluorescence peak intensity (residing at excitation wavelength 280 nm). Raw fluid coke had the capacity to remove upwards of 95% of the peak intensity with the application of 300 g/L. At similar carbon doses, raw delayed coke had the ability to remove 76%.

Similar trends in removal efficiencies of both DOC and OSNAs were observed across the laboratory techniques. The results indicate that the adsorption rates for the activated delayed and fluid coke are comparable to commercially activated GAC. Though raw fluid coke had the potential to remove high concentrations of both DOC and OSNAs, large carbon doses are required which would create large waste management issues for the oil sands industry.

5.2.2 Characterization of the Leaching Potential

Characterization of the untreated and treated PA water after interaction with raw and activated delayed and fluid cokes was conducted to understand the competition between organic and inorganic ions and molecules, representing both adsorption and leaching reactions. The following tests measured the key parameters necessary for the PA water characterization: pH, electrical conductivity, total alkalinity, ion chromatography (for major cation and anion concentrations) [Dionex IC2500/ ICS 2000], inductively couple plasma mass spectrometry (for trace metal concentrations) [Perkin Elmer, Elan 9000], and Microtox^{TM} toxicity assays (Model 500 Analyzer). The characterization led to the follow conclusions:

1. The initial PA water was alkaline with a conductivity and alkalinity around 3.56 mS and 545 mg $CaCO_3$/L, respectively. The high levels of organics (measured as DOC and OSNAs) were previously explained as the major contributors to acute toxicity of the PA water. High levels of measurable ammonium (6.42 mg/L), molybdenum (264 µg/L), and copper (152.75 µg/L) may have contributed to the chronic toxicity of the PA water.
2. PA water treated with 50 to 300 g/L of raw fluid coke resulted in increased leaching of aluminum (935-748 µg/L), molybdenum (305-536 µg/L), manganese (57-58 µg/L), copper (254-176 µg/L), and vanadium (682-3814 µg/L). In contrast, only Mo (289-358 µg/L) was measured to leach from the application of raw delayed fluid coke at levels greater than Canadian aquatic water quality guidelines. Consequently, though raw fluid coke has the potential to remove large proportions of DOC and OSNAs, the leaching of heavy metals reduced the efficiency of the treatment technology.
3. PA water treated with 0.0625 to 5 g/L of activated delayed and fluid coke samples became more alkaline (pH = 9.3) which may have resulted from the increased adsorption of organic acids from solution. The activated cokes did not alter the alkalinity (585 mg $CaCO_3$/L) and electrical conductivity (3.56 mS) of the PA water, indicating that the major cations and anions remained consistent within solution. However, their addition resulted in similar trends in the leaching of ammonium, aluminum, nickel, molybedum, and vanadium; uptake of manganese, copper, and lead was also observed. For activated fluid coke, the leaching of vanadium (265-2394 µg/L), molybdenum (296-437 µg/L), and aluminum (118-217 µg/L)

were lower than those concentrations observed from PA water treated with raw fluid coke.

4. The leaching of vanadium from 5 g/L of activated delayed and fluid coke samples at the high measureable concentrations of 5933 µg/L and 2394 µg/L, respectively represent a negative impact of the proposed remediation technology. Consequently, the application of activated delayed and fluid coke will have to be combined with an inorganic treatment technology in order to fully remediate the tailings ponds. Another option includes the pre-treatment of the raw delayed and fluid coke with HCl before activation in order to increase the solubility and initial removal of vanadium within the materials.
5. Microtox™ toxicity assays indicated a positive bacterial response for PA water treated with activated delayed and fluid cokes at carbon doses ranging from 0.0625 to 5 g/L. The toxicity decreased by 9% and 10% at 5 min with increasing carbon doses of 0.0625 and 5 g/L for activated delayed and fluid cokes. With an increased exposure time of 15 min, the toxicity effect decreased by 13% with increasing carbon doses from 0.0625 to 5 g/L for activated delayed and fluid cokes. The calculated toxicity effect proved that the initial reduction of toxicity at 5 min was attributed to the adsorption of organics; however, the toxicity effect increased with time due to the toxic effects associated with trace metals.

PA water characterization indicated that the application of activated delayed and fluid cokes was a more optimal treatment option over the use of raw delayed and fluid coke, due to the levels of leached trace metals and quantities of organics adsorbed. These experiments proved that physically activated delayed and fluid coke can be used to remove organics (including naphthenic acids) from oil sands PA water. The application of this treatment technology would greatly improve tailings pond water quality issues surrounding toxicity, total organic carbon, and colour allowing for increased recycling of the available water supply.

5.3 Recommendations

Future work should focus on increasing the effectiveness of the activation delayed and fluid coke products. Such experiments may include the following:

1. Improvement of the physical activation technique. This can be tested using either fluidized bed reactors or microwave heating to observe whether enhanced surface area of the activated coke is possible. Grinding of the fluid coke before physical activation should also be tested to observe whether this has a positive effect on surface area development. The effect of an oxygen gas activation atmosphere should be considered, as the exothermic reaction may allow for much lower activation times.
2. Chemical activation of raw delayed and fluid coke, where increased recycling and use of less environmentally harmful chemical dehydration reagents (such as KOH) is considered. These experiments should also be conducted within a fixed bed muffle furnace in order to compare the efficiency of the technique to the results from this study.
3. Experiments focussed on the regeneration of activated petroleum coke are also needed to prove feasibility, and recycling potential of the activated delayed and fluid coke. If regeneration is successful, batch tests should be completed again to observe the effect on adsorptive capacity.
4. Removal of vanadium from activated delayed and fluid cokes before interaction with the tailings pond water should also be investigated. This can be completed through leaching experiments using acids (such as HCl) to increase the initial solubility and removal of vanadium.
5. Future experiments should also examine whether changes in pH, alkalinity, ion and metal concentrations alter petroleum coke adsorption, as this may increase the removal efficiency of the organic contaminants. Control experiments should be conducted using artificially mixed PA water to better model adsorptive behaviour, as well as to resolve the competitive organic and inorganic behaviours with the PA water. Modelling of these experiments should be completed using better

developed models than Freundlich or Langmuir in order to describe the relationships on the non-ideal adsorbent surfaces.

6. Lastly, an investigation of the contaminants released during activations (such as CO_2, CO, CH_4, etc.) should be completed to observe the concentrations of emissions. If high levels of emissions are detected, then an emission control strategy should be designed and implemented into the overall process.

This future work will add to the viable implementation of the activated delayed and fluid coke to the oil sands industry to remove toxic and corrosive organic by-products from the process-affected tailings pond water. This will ultimately turn an undesirable waste by-product of the bitumen upgrading process into a valuable commodity for oil sands companies across the Athabasca region. Additional significance of the implementation of this technology includes the increased recycling of process water, limiting the amount of imported fresh water taken from the nearby Athabasca River. The removal of toxicity from the tailings ponds will also aid in the reclamation of these ponds allowing for the potential stocking of aquatic life. This research is a preliminary step towards creating sustainable development within the Athabasca oil sands region.

CHAPTER 6: APPENDICES

Appendix A: Summary of Activation Experiments

Table A-1: Summary of activation experiments

Coke Material	Activation Temp. (^{o}C)	Activation Time (h)	Soaking/ Carrier Gas	Carrier Gas Rate (mL/min)	Particle Size (µm)	Yield (%)	Burn-off (%)	Iodine Number (mg/g)	Methylene Blue (mg/g)	BET (N_2) (m^2/g)
Delayed	-	-	n/a	n/a	75-150	n/a	n/a	23.0 ± 1.4	1.6 ± 0.2	n/a
Fluid	-	-	n/a	n/a	75-150	n/a	n/a	16.0 ± 0.0	1.7 ± 0.2	n/a
Jacobi GAC	-	-	n/a	n/a	75-150	n/a	n/a	1000.0 ± 0.0	95.9 ± 3.7	n/a
Delayed	800	2	CO_2 only	300	75-150	87.9	12.1	3.5*	n/a	n/a
Delayed	800	4	CO_2 only	300	75-150	87.3	12.7	10.0*	n/a	n/a
Delayed	800	6	CO_2 only	300	75-150	95.7	4.3	10.5*	n/a	n/a
Fluid	800	2	CO_2 only	300	75-150	92.7	7.3	16.9*	n/a	n/a
Fluid	800	4	CO_2 only	300	75-150	92.2	7.8	19.2*	n/a	n/a
Fluid	800	6	CO_2 only	300	75-150	90.7	9.3	27.0*	n/a	n/a
Delayed	800	4	Humidified CO_2	300	75-150	86.7	13.3	14.0*	n/a	n/a
Delayed	800	2	Steam/CO_2	0.3/ 300	75-150	83.3	16.7	48.0*	n/a	n/a
Delayed	800	4	Steam/CO_2	0.3/ 300	75-150	78.4	21.6	112.5 ± 5.3	n/a	n/a
Delayed	800	6	Steam/CO_2	0.3/ 300	75-150	75.1	24.9	172.5 ± 31.8	4.0 ± 0.0	
Delayed	850	4	Steam/CO_2	0.3/ 300	75-150	69.7	30.3	315.0 ± 21.2	9.1 ± 1.1	n/a
Delayed	900	2	Steam/CO_2	0.3/ 300	75-150	73.7	26.3	166.0 ± 19.8	9.7 ± 1.9	n/a
Delayed	900	4	Steam/CO_2	0.3/ 300	75-150	59.5	40.5	450.5 ± 12.0	48.3 ± 1.2	n/a
Delayed	900	6	Steam/CO_2	0.3/ 300	75-150	47.0	53.0	579.5 ± 0.7	122.6 ± 1.0	472.0
Delayed	900	2	Steam/CO_2	0.5/ 300	75-150	71.6	28.4	250.0 ± 35.4	11.7 ± 0.3	n/a
Delayed	900	4	Steam/CO_2	0.5/ 300	75-150	55.8	44.2	515.0 ± 7.1	68.5 ± 2.6	425.6
Delayed	900	6	Steam/CO_2	0.5/ 300	75-150	41.2	58.8	670.0 ± 14.1	123.9 ± 0.5	577.5

Coke Material	Activation Temperature (°C)	Activation Time (h)	Soaking/ Carrier Gas	Carrier Gas Rate (mL/min)	Particle Size (µm)	Yield (%)	Burn-off (%)	Iodine Number (mg/g)	Methylene Blue (mg/g)	BET (N_2) (m^2/g)
Fluid	800	2	Steam/CO_2	0.3/ 300	75-150	89.2	10.8	n/a	n/a	n/a
Fluid	800	4	Steam/CO_2	0.3/ 300	75-150	83.7	16.3	74.0 ± 1.4	2.5 ± 0.0	n/a
Fluid	800	6	Steam/CO_2	0.3/ 300	75-150	79.1	20.9	116.5 ± 16.3	4.8 ± 0.3	n/a
Fluid	850	4	Steam/CO_2	0.3/ 300	75-150	76.4	23.6	196.0 ± 8.5	8.3 ± 0.0	n/a
Fluid	900	2	Steam/CO_2	0.3/ 300	75-150	79.7	20.3	144.5 ± 7.8	10.9 ± 0.4	n/a
Fluid	900	4	Steam/CO_2	0.3/ 300	75-150	65.0	35.0	370.0 ± 14.1	47.8 ± 0.2	n/a
Fluid	900	6	Steam/CO_2	0.3/ 300	75-150	53.0	47.0	530.0 ± 14.1	98.4 ± 0.1	539.9
Fluid	900	2	Steam/CO_2	0.5/ 300	75-150	77.0	23.0	200.0 ± 14.1	16.5 ± 0.0	n/a
Fluid	900	4	Steam/CO_2	0.5/ 300	75-150	62.3	37.7	399.5 ± 13.4	67.7 ± 2.6	398.9
Fluid	900	6	Steam/CO_2	0.5/ 300	75-150	46.2	53.8	620.0 ± 28.3	122.6 ± 0.5	493.5
Delayed	800	4	Steam/N_2	0.3/ 300	75-150	78.6	21.4	122.0 ± 26.9	2.1 ± 0.1	n/a
Delayed	800	6	Steam/N_2	0.3/ 300	75-150	73.6	26.4	209.5 ± 6.7	5.6 ± 0.4	n/a
Fluid	800	4	Steam/N_2	0.3/ 300	75-150	84.4	15.6	71.5 ± 5.3	2.5 ± 0.0	n/a
Fluid	800	6	Steam/N_2	0.3/ 300	75-150	79.2	20.8	130.0 ± 7.1	4.7 ± 0.0	n/a

Values are an average of duplicate samples
-, not applicable
*, one value obtained from testing
n/a, not available

.

Appendix B: BET Isotherms and DFT/ Monte Carlo Pore Volume

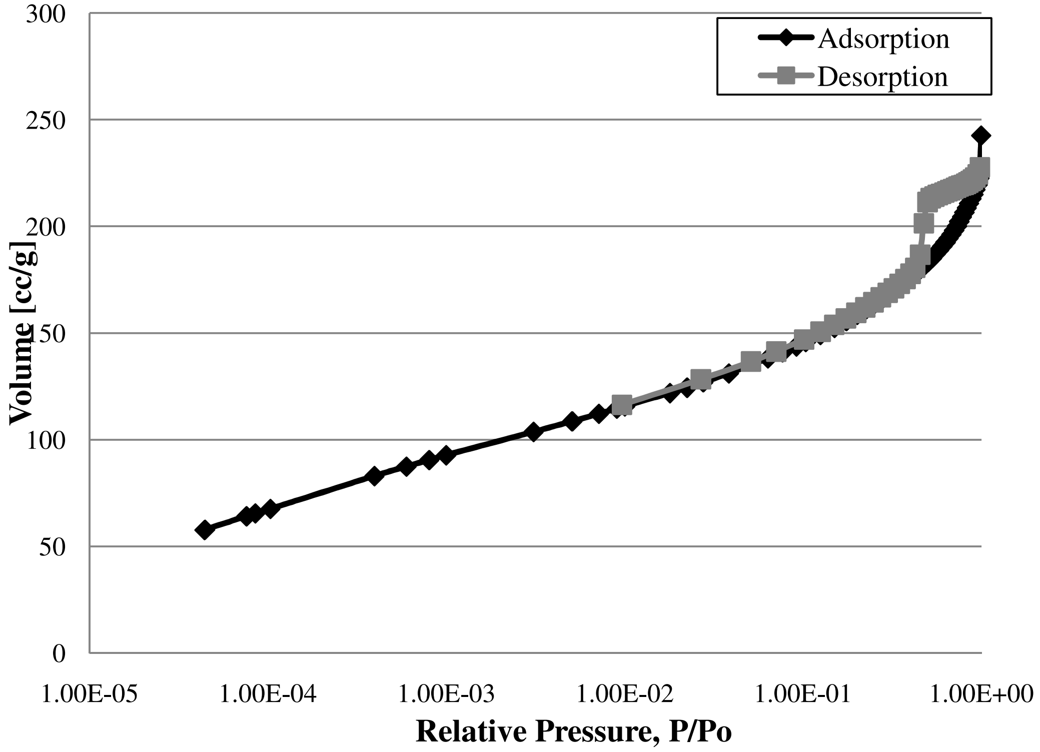

Figure B-1: P/P_o isotherm for activated delayed coke (900^{o}C, CO_2 + steam [0.5 mL/min], 6 h)

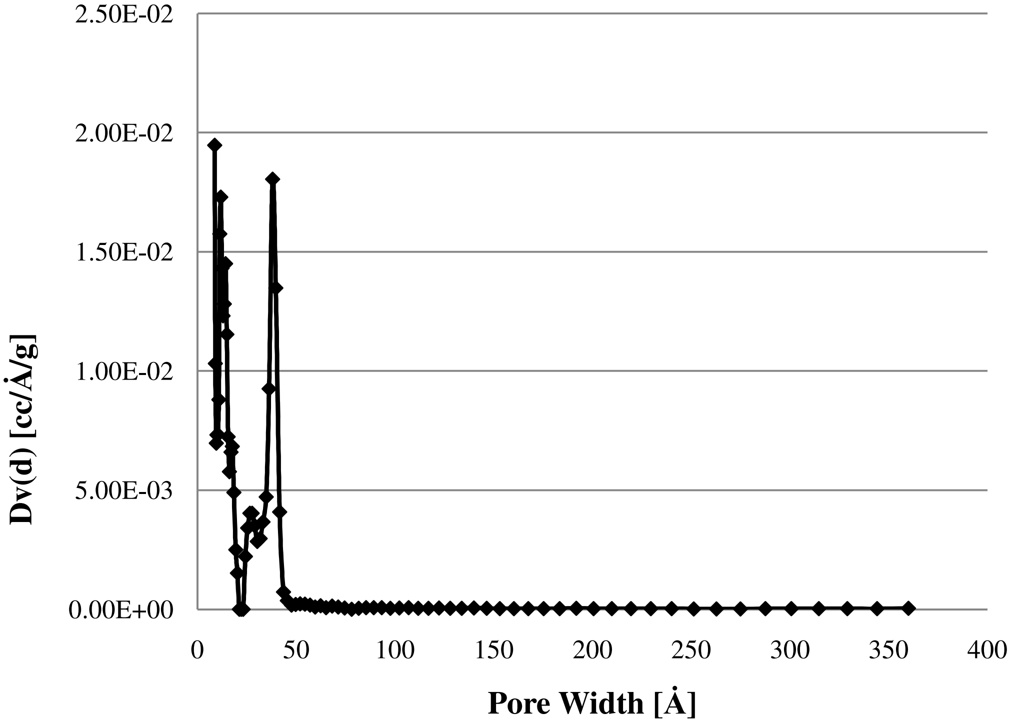

Figure B-2: DFT/ Monte-Carlo differential pore volume distribution for activated delayed coke (900^{o}C, CO_2 + steam [0.5 mL/min], 6 h)

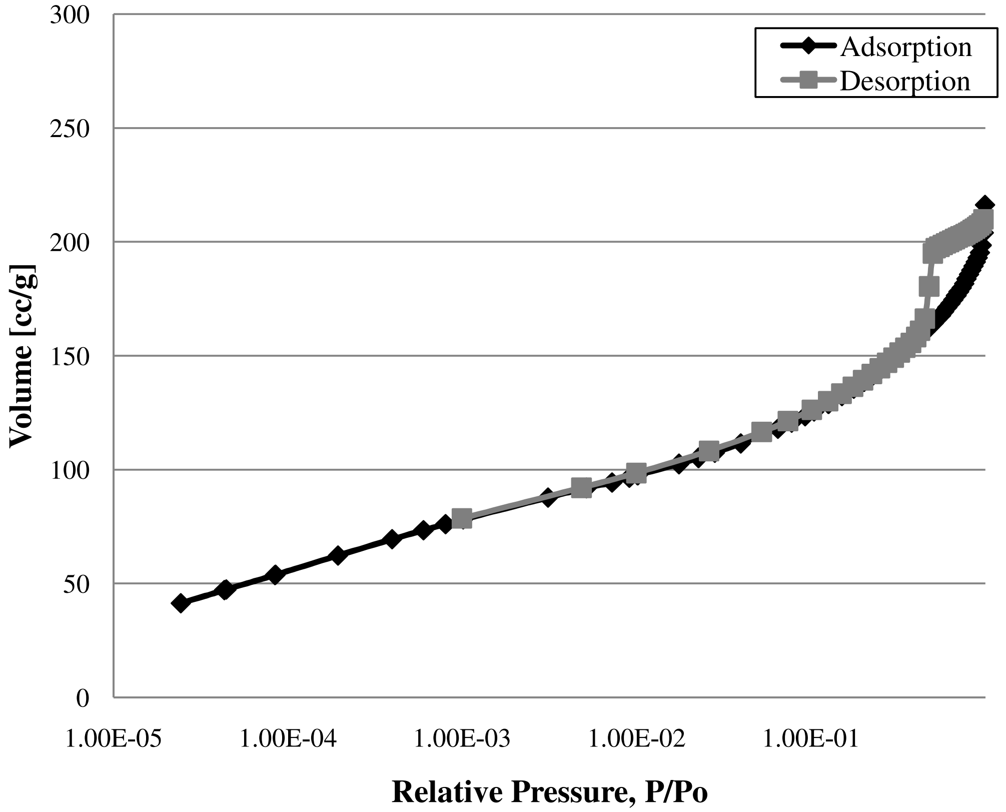

Figure B-3: P/P_o isotherm for activated fluid coke (900^{o}C, CO_2 + steam [0.5 mL/min], 6 h)

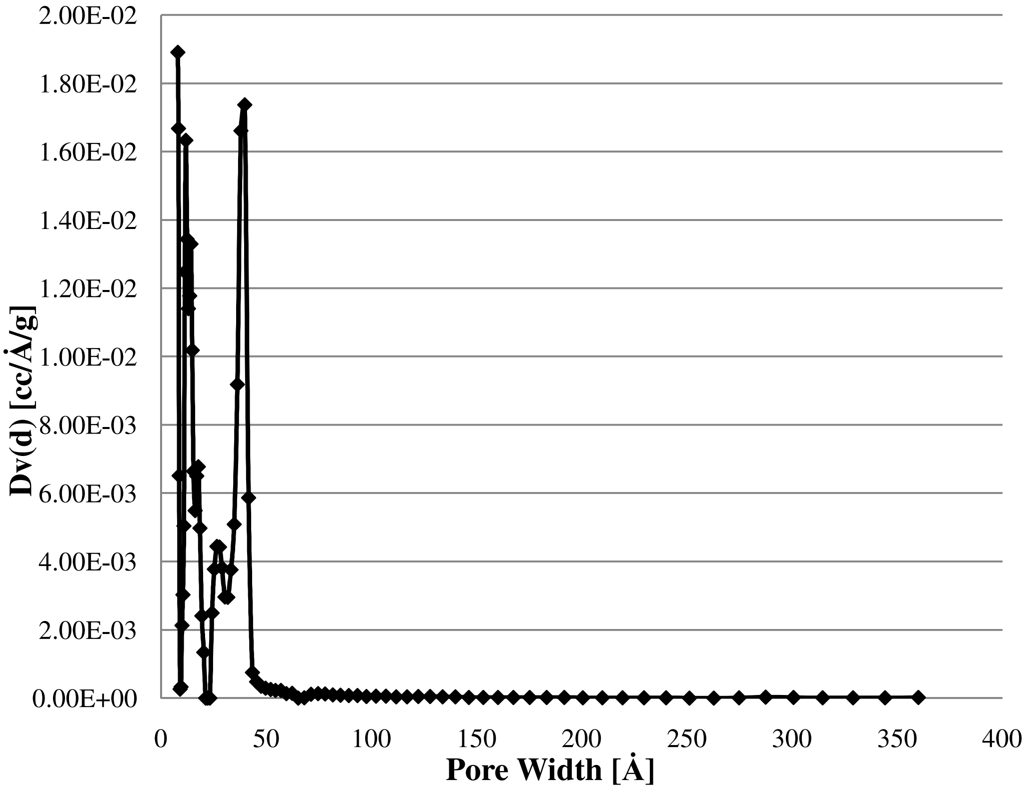

Figure B-4: DFT/ Monte-Carlo differential pore volume distribution for activated fluid coke (900^{o}C, CO_2 + steam [0.5 mL/min], 6 h)

Appendix C: SEM Images of the Activated Delayed and Fluid Coke

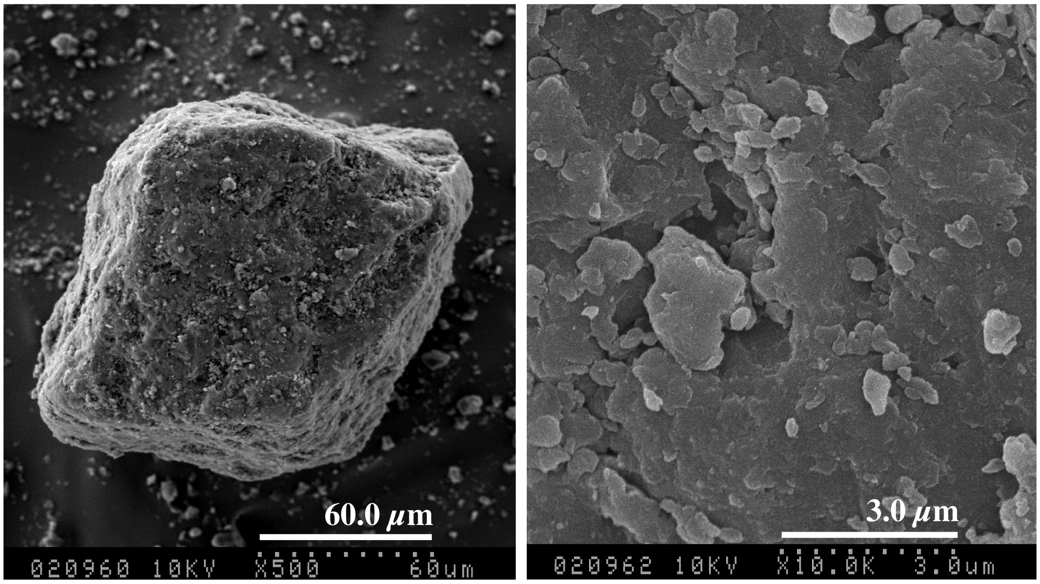

Figures C-1: SEM images of raw delayed coke before activation

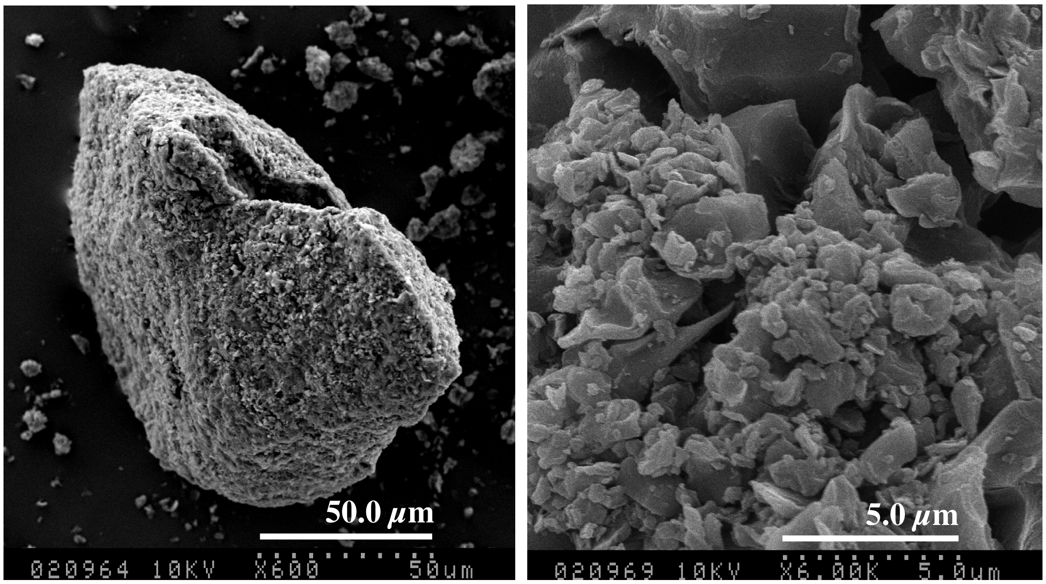

Figures C-2: SEM images of activated delayed coke (900^{o}C, CO_2 + steam [0.5 mL/min], 6 h)

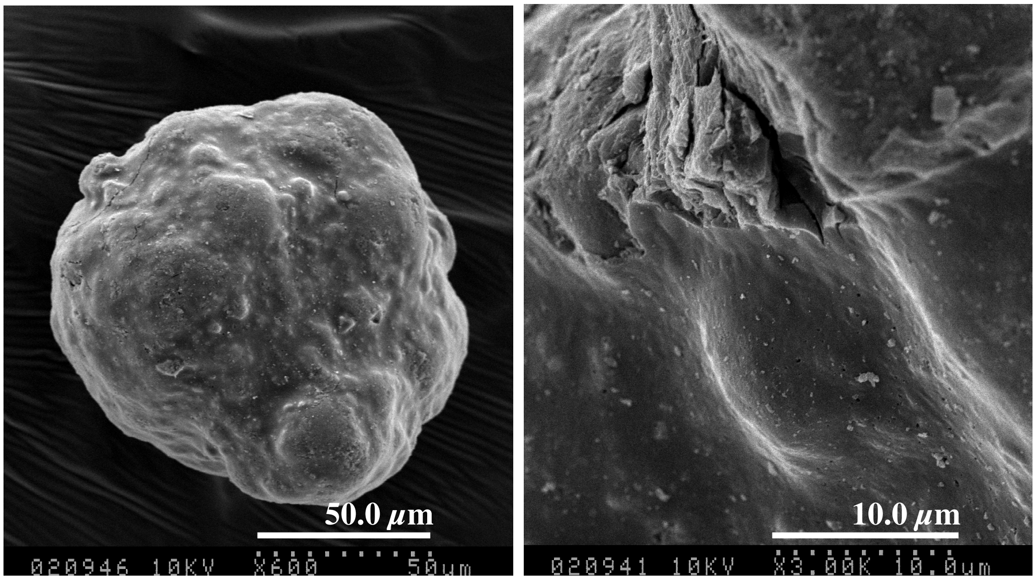

Figures C-3: SEM images of raw fluid coke before activation

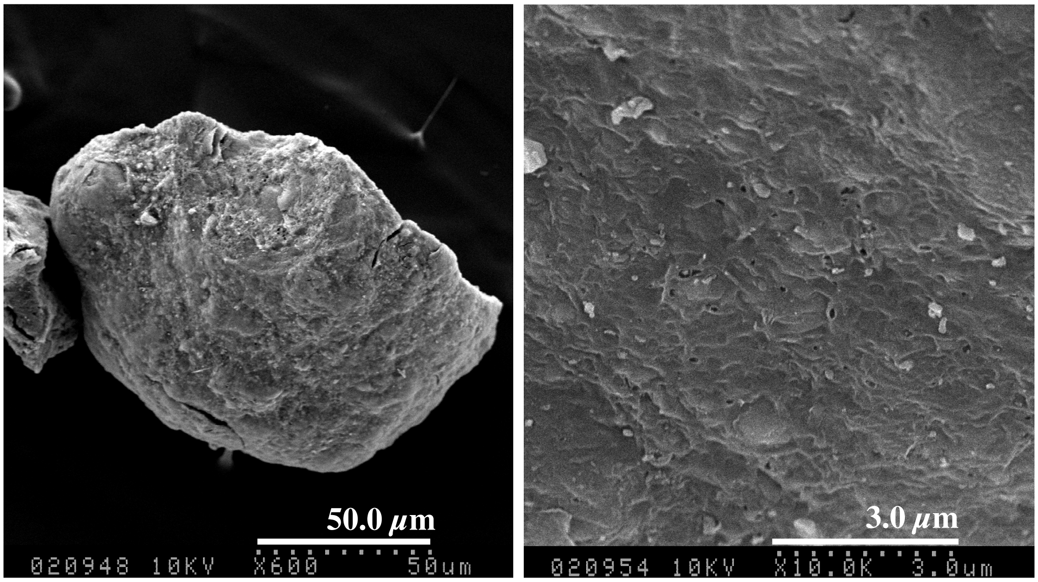

Figures C-4: SEM images of activated fluid coke (900°C, CO_2 + steam [0.5 mL/min], 6 h)

Appendix D: Adsorption Equilibrium Curves

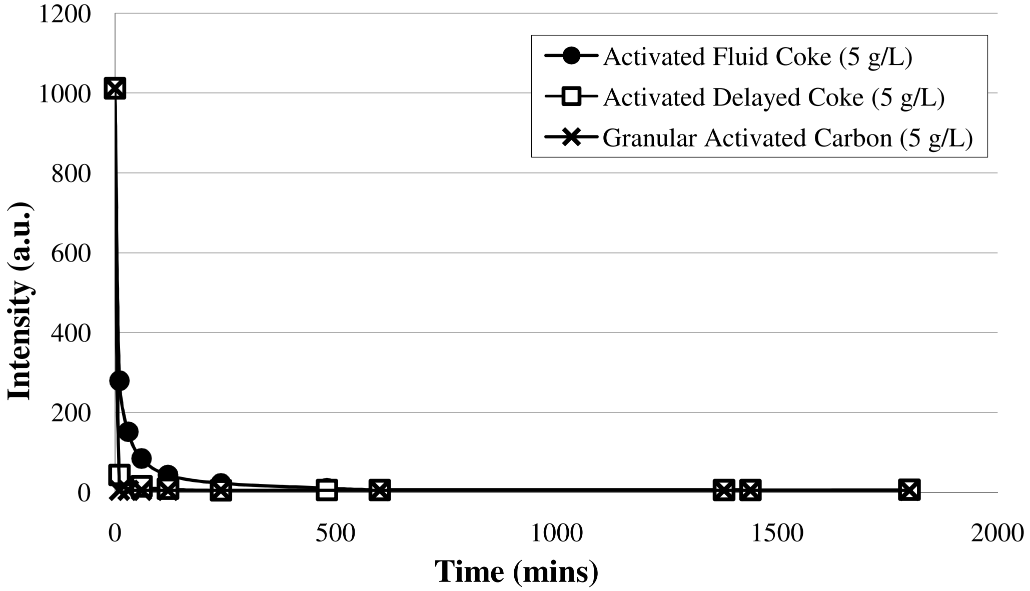

Figure D-1: Adsorption of the OSNA signature with increasing time onto activated delayed and fluid coke (900°C, CO_2 + steam [0.5 mL/min], 6 h) and granular activated carbon (Jacobi) as measured through fluorescence spectrometry (corrected with UV-Vis spectrometry)

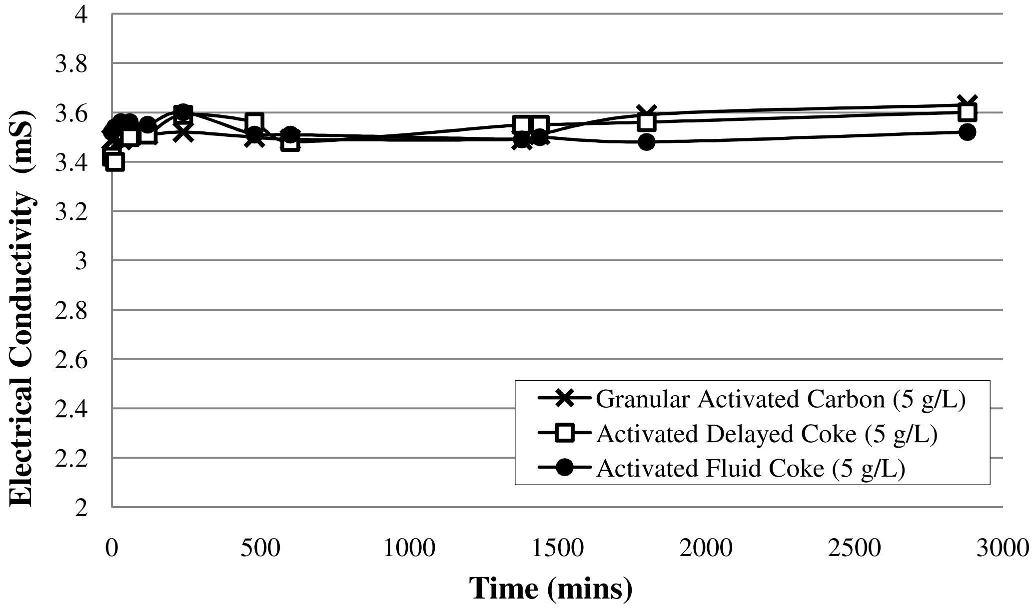

Figure D-2: Change in electrical conductivity with increasing time during 24-h batch adsorption tests with activated delayed and fluid coke (900°C, CO_2 + steam [0.5 mL/min], 6 h) and granular activated carbon (Jacobi Carbons, Aquasorb 1500).

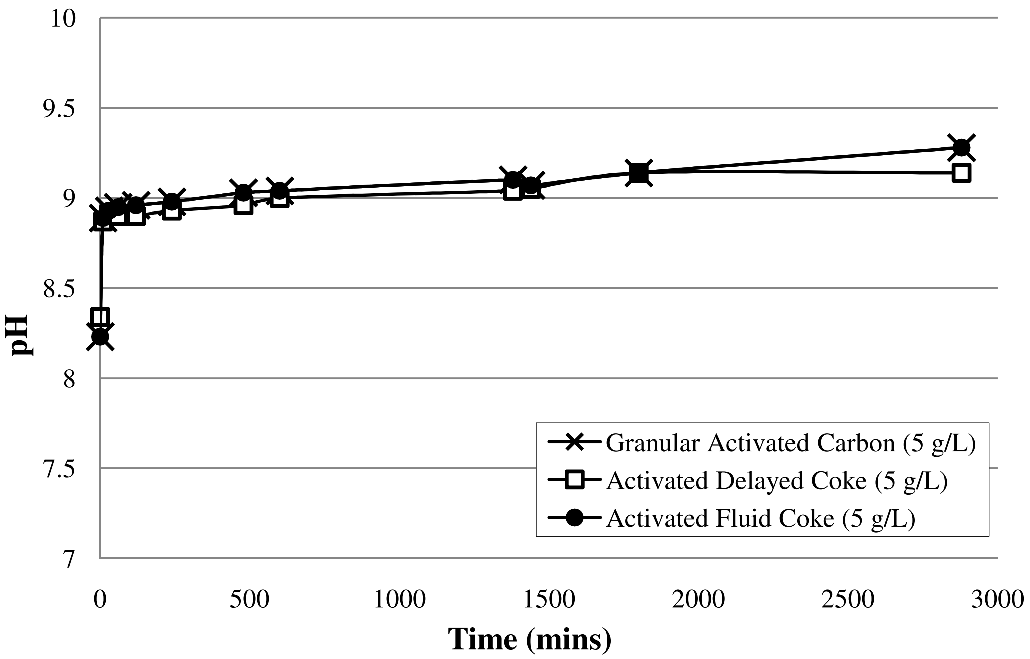

Figure D-3: Change in pH with increasing time during 24-h batch adsorption tests with activated delayed and fluid coke (900°C, CO_2 + steam [0.5 mL/min], 6 h) and granular activated carbon (Jacobi Carbons, Aquasorb 1500).

Appendix E: Summary of the Adsorption Experiments

Table E-1: Summary of the pH, electrical conductivity (EC), and alkalinity for untreated PA water and PA water treated with raw and activated delayed and fluid cokes, and granular activated carbon (GAC). Values are an average of duplicate samples ± one standard deviation.

Sample	Carbon Dose (g/L)	pH	EC (mS)	Alkalinity (mg CaCO3/ L)
Untreated PA Water	0	8.5 ± 0.1	3.1 ± 0.0	550.8 ± 1.5
Raw Delayed Coke	50	9.1 ± 0.1	3.1 ± 0.0	571.3 ± 12.4
	100	9.1 ± 0.0	3.1 ± 0.0	547.5 ± 17.7
	200	8.7 ± 0.0	3.1 ± 0.0	572.5 ± 14.1
	300	9.1 ± 0.0	3.1 ± 0.0	520.5 ± 13.4
Untreated PA Water	0	8.6 ± 0.0	3.2 ± 0.0	587.0 ± 4.2
Raw Fluid Coke	50	8.7 ± 0.2	3.1 ± 0.0	568.5 ± 19.1
	100	8.7 ± 0.1	3.1 ± 0.0	557.4 ± 4.1
	200	8.8 ± 0.1	3.1 ± 0.0	541.3 ± 3.9
	300	9.1 ± 0.0	3.2 ± 0.0	505.0 ± 21.2
Untreated PA Water	0	8.7 ± 0.0	3.6 ± 0.0	584.5 ± 7.8
Activated Delayed Coke	0.0625	9.3 ± 0.0	3.5 ± 0.0	591.5 ± 0.0
	0.125	9.3 ± 0.0	3.5 ± 0.0	582.5 ± 3.5
	2.5	9.3 ± 0.0	3.5 ± 0.0	580.0 ± 0.0
	5	9.3 ± 0.1	3.5 ± 0.0	575.8 ± 0.4
Activated Fluid Coke	0.0625	9.3 ± 0.0	3.5 ± 0.0	590.8 ± 1.1
	0.125	9.3 ± 0.0	3.5 ± 0.0	583.0 ± 1.4
	2.5	9.2 ± 0.0	3.5 ± 0.0	584.0 ± 4.9
	5	9.3 ± 0.1	3.5 ± 0.0	575.0 ± 0.0
GAC	0.0625	9.3 ± 0.0	3.5 ± 0.0	595.1 ± 0.2
	0.125	9.4 ± 0.0	3.6 ± 0.0	594.5 ± 0.7
	2.5	9.3 ± 0.0	3.5 ± 0.0	583.0 ± 2.8
	5	9.3 ± 0.0	3.5 ± 0.0	579.6 ± 0.9

Table E-2: Summary of organic and OSNA adsorption onto raw and activated delayed and fluid cokes and granular activated carbon (GAC) showing dissolved organic carbon (DOC), Fourier transform infrared spectrometry (FTIR), and fluorescence spectrometry results. Values are an average of duplicate samples ± one standard deviation.

Sample	Carbon Dose (g/L)	**DOC** Organics Concentration (mg/L)	**FTIR** OSNA Concentration (mg/L)	**Fluorescence** OSNA Signature Intensity (a.u.)[A]
Untreated PA Water	0	53*	56.0 ± 0.3	1286.7
Raw Delayed Coke	50	45*	45.3 ± 0.2	863.4
	100	46*	33.8 ± 0.0	649.7
	200	42*	27.5 ± 1.9	490.0
	300	37*	24.1 ± 1.2	311.1
Untreated PA Water		54.0 ± 1.4	55.1 ± 0.0	1286.1
Raw Fluid Coke	50	20 ± 12.7	28.7 ± 0.0	199.7
	100	28.5 ± 3.5	21.9 ± 1.9	103.3
	200	19.0 ± 2.8	12.9 ± 0.0	58.9
	300	16.5 ± 2.1	-	51.7
Untreated PA Water	0	39.1 ± 0.7	64.8 ± 0.5	1213.7
Activated Delayed Coke	0.0625	32.1 ± 0.2	32.6 ± 1.9	209.7
	0.125	19.9 ± 2.8	17.5 ± 2.5	61.7
	2.5	7.9 ± 0.3	5.4 ± 0.7	10.1
	5	3.5 ± 0.3	4.9 ± 0.5	2.3
Activated Fluid Coke	0.0625	30.3 ± 0.3	28.0 ± 1.5	192.8
	0.125	19.0 ± 0.6	13.7 ± 1.5	75.2
	2.5	8.7 ± 0.9	7.9 ± 2.5	20.4
	5	3.2 ± 0.1	4.9 ± 0.0	3.2
Jacobi GAC	0.0625	16.2 ± 0.4	10.4 ± 0.7	33.8
	0.125	9.7 ± 0.6	5.9 ± 0.1	12.2
	2.5	4.7 ± 0.4	3.6 ± 1.7	5.2
	5	2.9 ± 0.2	3.3 ± 0.5	1.7

[A], *inner/ outer filtering correction accounts for duplicate emission-excitation spectra*

**, one sample available*

-, not available

Table E-3: Summary of major cations and anions within sample filtrates mixed with raw delayed and fluid cokes and granular activated carbon (GAC) as measured through ion chromatography (IC). Values are an average of duplicate samples ± one standard deviation.

Sample	Carbon Dose (g/L)	Calcium (mg/L)	Magnesium (mg/L)	Potassium (mg/L)	Ammonium (mg/L)	Sodium (mg/L)	Lithium (mg/L)
Untreated PA Water	0	8.5 ± 0.0	5.5 ± 0.0	10.1 ± 0.0	6.8 ± 0.1	651.5 ± 1.9	0.2 ± 0.0
Raw Delayed Coke	50	9.1 ± 0.6	5.5 ± 0.1	10.3 ± 0.0	6.1 ± 0.0	661.2 ± 9.7	0.2 ± 0.0
	300	9.2 ± 0.7	6.2 ± 0.2	9.3 ± 0.7	0.0 ± 0.0	670.3 ± 6.3	0.2 ± 0.0
GAC	50	4.9 ± 0.0	5.2 ± 0.2	10.7 ± 0.2	5.3 ± 0.2	768.4 ± 1.9	0.2 ± 0.0
	300	6.8 ± 0.4	1.7 ± 0.1	7.8 ± 0.7	0.6 ± 0.3	747.8 ± 0.3	0.2 ± 0.0
Untreated PA Water	0	5.9 ± 0.7	4.4 ± 0.1	9.4 ± 0.2	6.8 ± 0.0	654.8 ± 1.3	0.1 ± 0.0
Raw Fluid Coke	50	4.3 ± 0.1	3.3 ± 0.1	8.4 ± 0.7	0.0 ± 0.0	656.3 ± 3.1	0.1 ± 0.1
	300	3.8 ± 0.3	3.6 ± 0.1	8.9 ± 0.1	0.0 ± 0.0	647.2 ± 3.2	0.1 ± 0.1
Sample	**Carbon Dose (g/L)**	**Nitrate (mg/L)**	**Bromide (mg/L)**	**Chloride (mg/L)**	**Fluoride (mg/L)**	**Sulphate (mg/L)**	**Phosphate (mg/L)**
Untreated PA Water	0	0.0 ± 0.0	0.4 ± 0.0	559.5 ± 4.6	1.9 ± 0.0	265.4 ± 3.6	0.0 ± 0.0
Raw Delayed Coke	50	0.0 ± 0.0	0.4 ± 0.0	559.5 ± 1.3	1.9 ± 0.1	250.1 ± 1.8	0.0 ± 0.0
	300	0.0 ± 0.0	0.4 ± 0.0	560.6 ± 1.1	2.0 ± 0.0	267.4 ± 3.6	0.0 ± 0.0
GAC	50	0.0 ± 0.0	0.2 ± 0.0	521.5 ± 4.7	1.9 ± 0.1	233.6 ± 6.5	1.6 ± 0.1
	300	0.0 ± 0.0	0.1 ± 0.0	357.7 ± 8.9	1.9 ± 0.0	212.2 ± 3.0	4.9 ± 0.0
Untreated PA Water	0	0.2 ± 0.0	0.1 ± 0.1	580.7 ± 4.4	1.9 ± 0.0	245.2 ± 1.8	0.0 ± 0.0
Raw Fluid Coke	50	0.0 ± 0.0	0.1 ± 0.1	591.1 ± 6.5	2.0 ± 0.1	252.3 ± 2.3	0.0 ± 0.0
	300	0.0 ± 0.0	0.4 ± 0.0	594.5 ± 1.7	2.2 ± 0.0	279.0 ± 0.2	0.7 ± 0.1

Table E-4: Summary of major cations and anions within sample filtrates mixed with activated delayed and fluid cokes and granular activated carbon (GAC) as measured through ion chromatography (IC). Values are an average of duplicate samples ± one standard deviation.

Sample	Carbon Dose (g/L)	Calcium (mg/L)	Magnesium (mg/L)	Potassium (mg/L)	Ammonium (mg/L)	Sodium (mg/L)	Lithium (mg/L)
Untreated PA Water	0	8.0 ± 0.2	5.6 ± 0.0	10.2 ± 0.3	6.4 ± 0.13	707.5 ± 8.7	0.2 ± 0.0
Activated Delayed Coke	5	8.0 ± 0.1	5.6 ± 0.0	10.6 ± 0.4	7.7 ± 2.09	716.8 ± 11.2	0.2 ± 0.0
Activated Fluid Coke	5	8.7 ± 0.5	5.9 ± 0.1	11.0 ± 0.4	7.8 ± 1.41	707.8 ± 0.2	0.2 ± 0.0
GAC	5	7.9 ± 0.4	5.5 ± 0.4	10.6 ± 0.0	3.6 ± 3.06	690.6 ± 0.1	0.2 ± 0.1

Sample	Carbon Dose (g/L)	Nitrate (mg/L)	Bromide (mg/L)	Chloride (mg/L)	Fluoride (mg/L)	Sulphate (mg/L)	Phosphate (mg/L)
Untreated PA Water	0	0.0 ± 0.0	0.4 ± 0.0	501.3 ± 8.1	1.7 ± 0.0	183.4 ± 2.5	0.0 ± 0.0
Activated Delayed Coke	5	0.0 ± 0.0	0.3 ± 0.0	500.0 ± 9.4	1.7 ± 0.1	186.1 ± 4.6	0.0 ± 0.0
Activated Fluid Coke	5	0.0 ± 0.0	0.4 ± 0.0	498.7 ± 2.4	1.9 ± 0.1	186.6 ± 2.2	0.0 ± 0.0
Jacobi GAC	5	0.0 ± 0.0	0.2 ± 0.1	493.5 ± 3.6	1.6 ± 0.0	188.4 ± 0.7	0.0 ± 0.0

Table E-5: Summary of trace metals within sample filtrates mixed with raw and activated delayed and fluid cokes as measured through inductively coupled plasma mass spectrometry (ICPMS). Values are an average of duplicate samples.

Sample	Carbon Dose (g/L)	B (μg/ L)	Si (μg/ L)	P (μg/ L)	Cr (μg/ L)	Co (μg/ L)	Ga (μg/ L)	As (μg/ L)	Rb (μg/ L)	Sr (μg/ L)	Cd (μg/ L)	Cs (μg/ L)	Ba (μg/ L)	U (μg/ L)
Untreated PA Water	0	1872.0	1720.0	0.0	5.9	2.8	0.1	7.8	9.6	237.9	0.0	0.1	42.2	5.4
Raw Delayed Coke	50	1749.4	1749.4	29.2	2.2	2.0	0.2	7.0	10.6	244.4	0.0	0.2	38.7	5.5
	300	1998.1	1896.0	167.9	7.8	3.5	0.4	8.6	10.1	245.4	0.0	0.1	40.7	5.7
Untreated PA Water	0	2711.8	4322.6	68.8	12.9	2.8	0.1	9.0	11.7	277.1	0.4	0.2	69.9	5.6
Raw Fluid Coke	50	2688.1	5009.9	167.8	13.7	1.2	0.9	10.1	11.5	261.1	0.5	0.3	47.7	5.8
	300	2554.7	3963.1	348.7	10.3	0.9	3.9	16.9	16.6	185.3	0.5	0.4	17.2	6.9
Untreated PA Water	0	1910.9	3237.7	0.2	13.0	1.1	0.1	1.8	13.3	258.3	0.5	0.2	34.5	3.5
Activated Delayed Coke	0.0625	2155.2	3267.8	18.9	22.9	1.3	0.3	3.2	12.5	252.2	0.5	0.3	77.5	4.5
	5	1761.0	3604.5	29.1	12.9	0.8	1.5	7.2	7.5	240.9	0.6	0.3	8.5	3.7
Activated Fluid Coke	0.0625	2203.7	2762.8	14.6	22.7	1.4	0.2	3.4	14.7	270.0	0.5	0.3	73.8	4.4
	5	1710.0	3593.1	61.6	11.2	0.8	0.9	7.4	16.1	248.2	0.6	0.5	9.7	4.3

Table E-6: OSNA adsorption isotherm parameters for activated delayed and fluid coke and granular activated carbon (GAC).

Sample	**Carbon Mass (g/L)**	**Equilibrium Concentration (C_e) (mg/L)**	**X (C_i-C_e) (mg/L)**	**Q = X/M (mg/g)**	**Log (C_e)**	**Log (Q)**
Activated Delayed Coke	0.0625	32.63	32.21	515.36	1.51	2.71
	0.125	17.49	47.35	378.80	1.24	2.58
	2.5	5.44	59.40	23.76	0.74	1.38
	5	4.97	59.87	11.97	0.69	1.08
Activated Fluid Coke	0.0625	28.02	36.82	589.12	1.45	2.77
	0.125	13.70	51.14	409.12	1.14	2.61
	2.5	7.95	56.89	22.76	0.90	1.36
	5	4.98	59.86	11.92	0.69	1.08
GAC	0.0625	10.38	54.46	871.36	1.02	2.94
	0.125	5.95	58.89	471.12	0.77	2.67
	2.5	3.62	61.22	24.49	0.56	1.39
	5	3.28	61.56	12.31	0.52	1.09

C_i = 64.84 mg/L

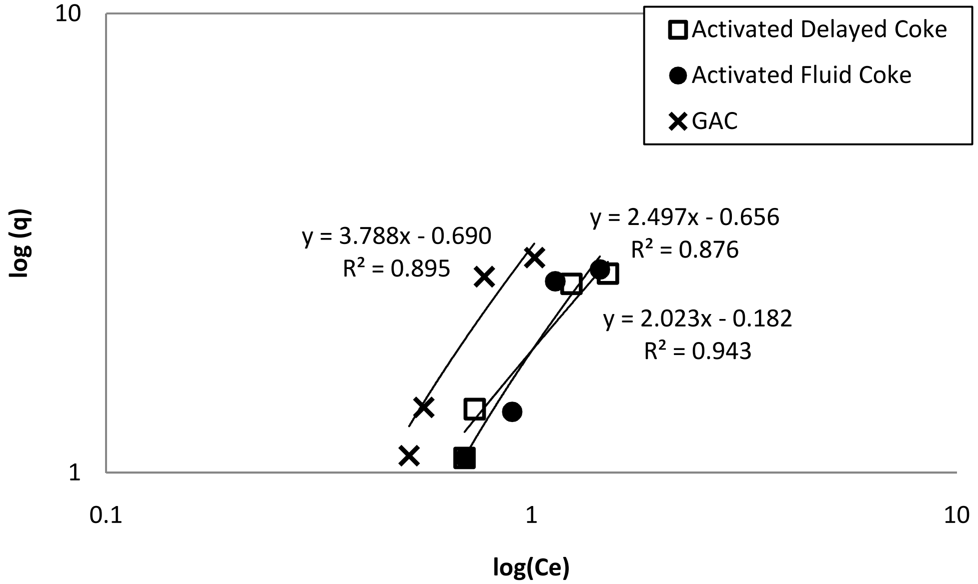

Figure E-1: Logarithmic adsorption isotherm for OSNAs indicating linear regression parameters.

Appendix F: Fluorescence Spectrometry Signatures Corrected with UV-VIS Absorption Data

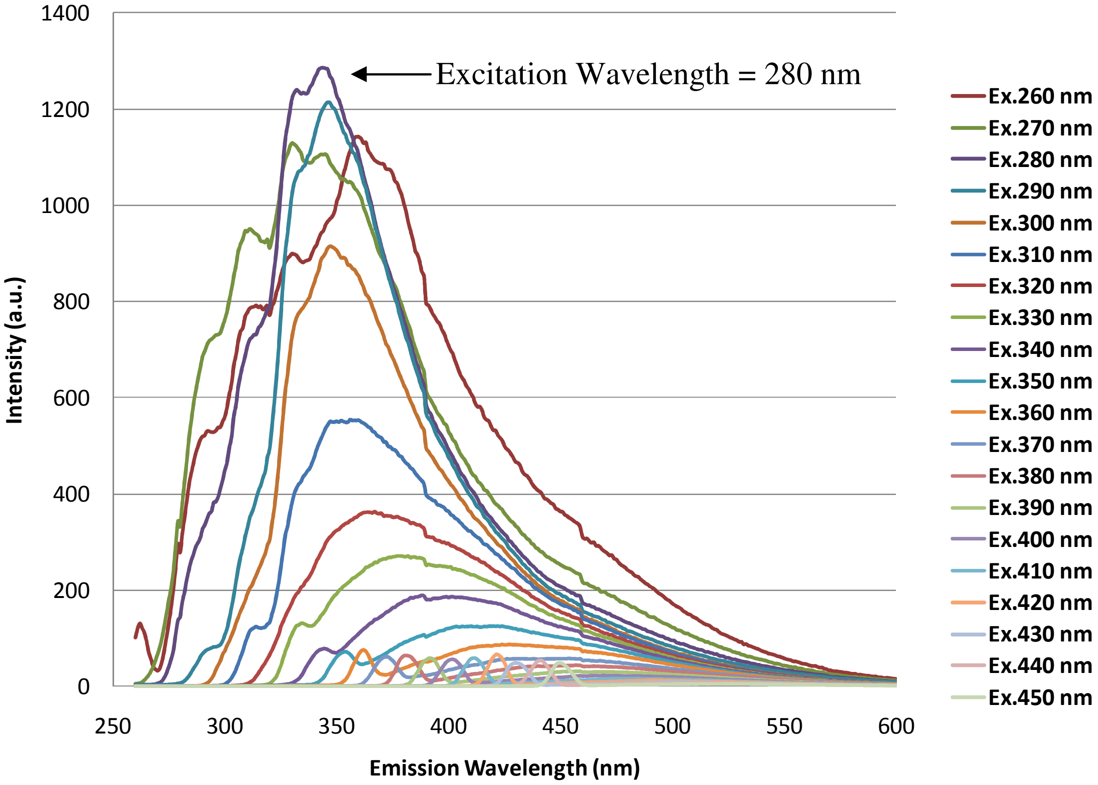

Figure F-1: Emission spectra of untreated process-affected water for excitation wavelengths from 260 to 450 nm. Measured through fluorescence spectrometry and corrected with UV-VIS spectrometry.

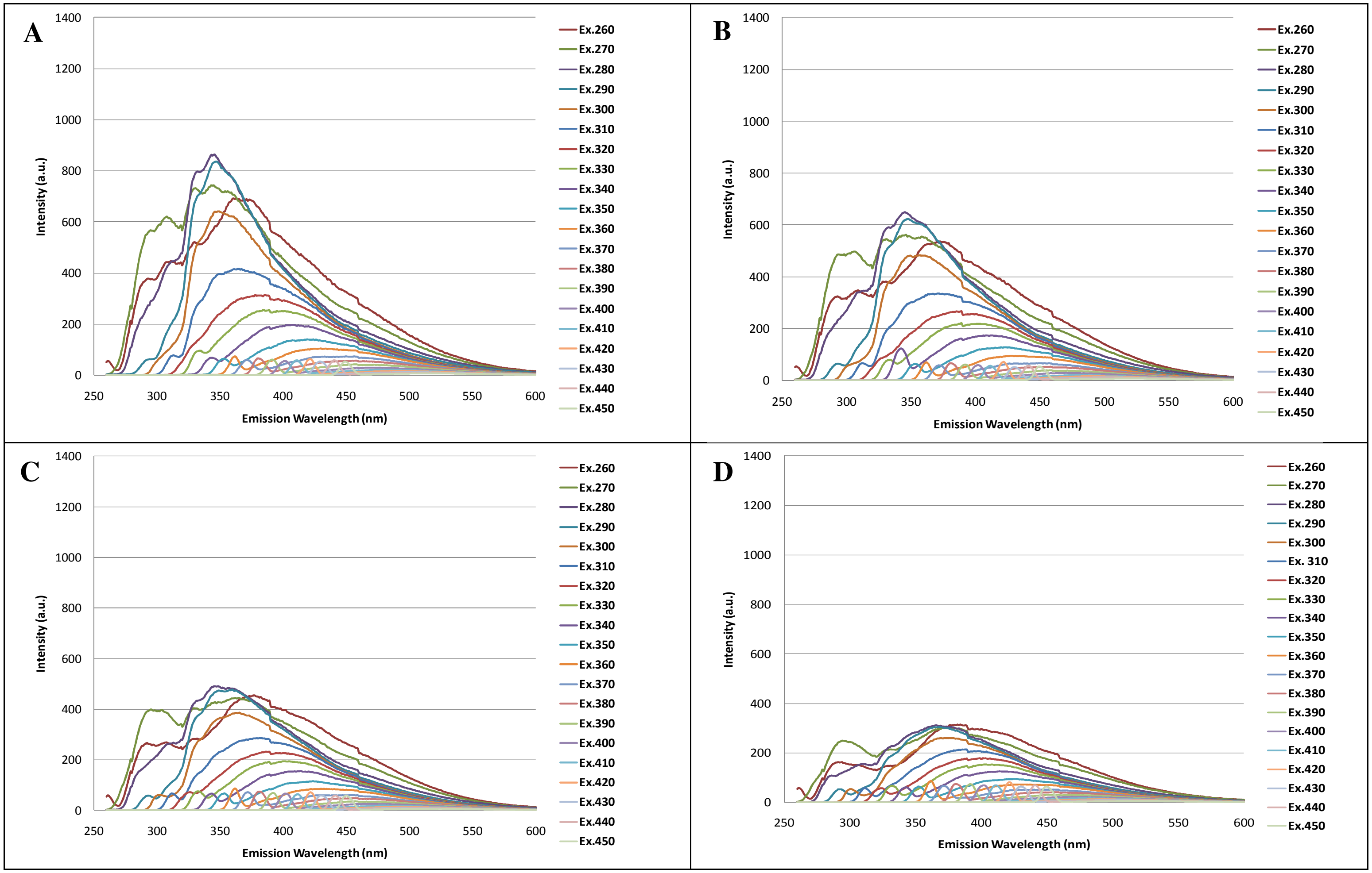

Figure F-2: Emission spectra for straight process-affected water treated with increasing weight additions of raw delayed coke; (A) 50 g/L, (B) 100 g/L, (C) 200 g/L, and (D) 300 g/L.

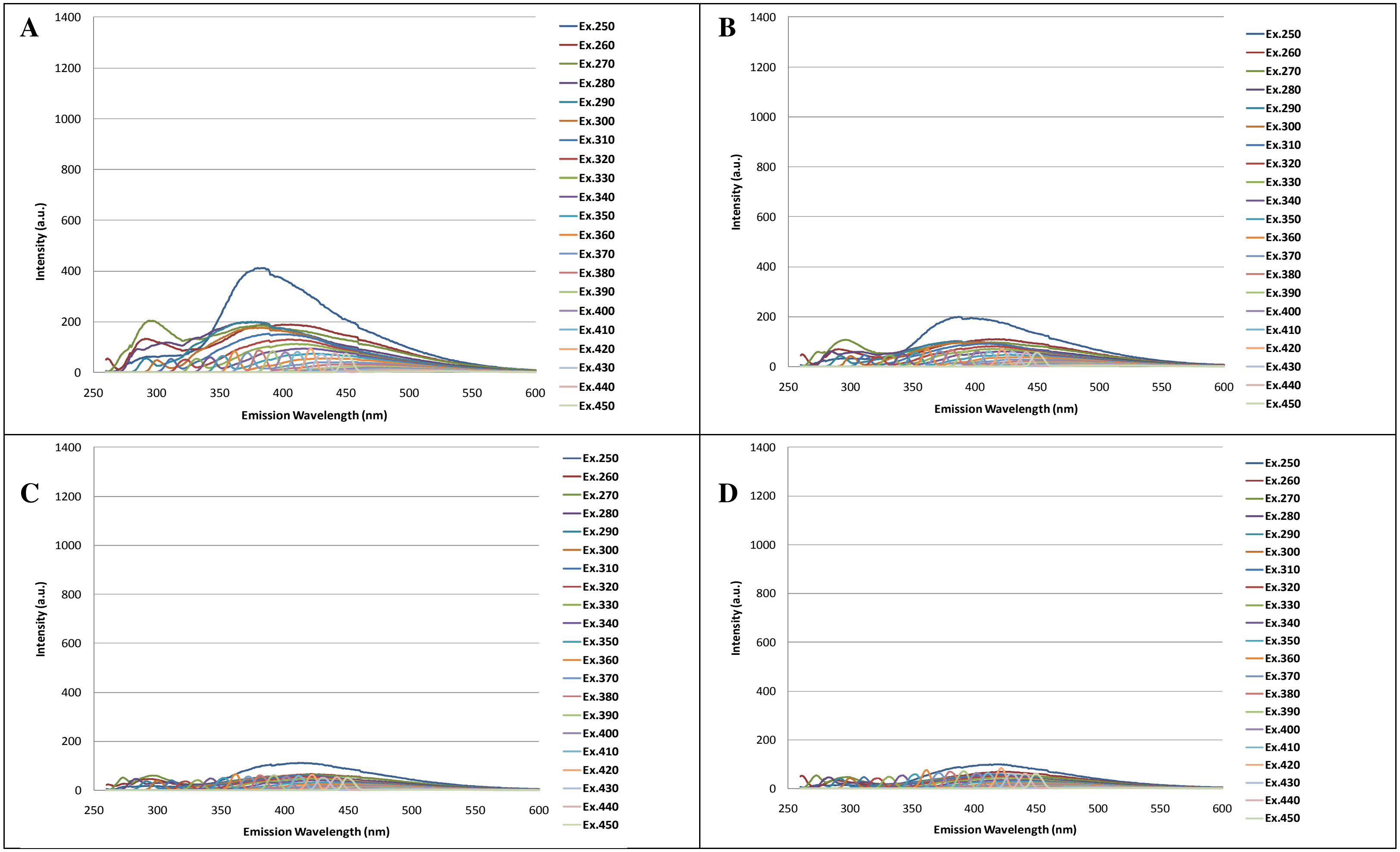

Figure F-3: Emission spectra for straight process-affected water treated with increasing weight additions of raw fluid coke; (A) 50 g/L, (B) 100 g/L, (C) 200 g/L, and (D) 300 g/L.

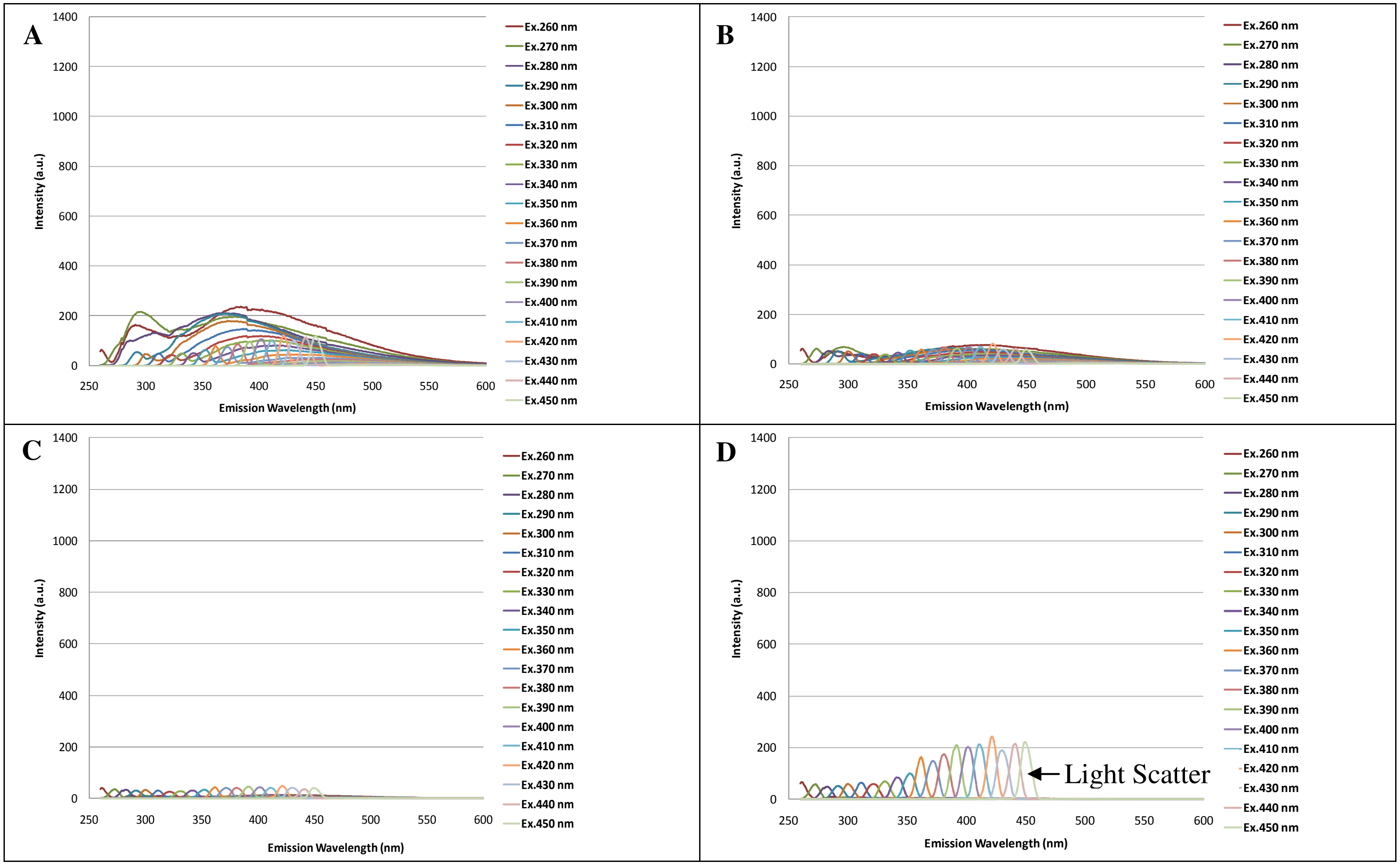

Figure F-4: Emission spectra for straight process-affected water treated with increasing weight additions of activated delayed coke; (A) 0.0625 g/L, (B) 0.125 g/L, (C) 2.5 g/L, and (D) 5 g/L.

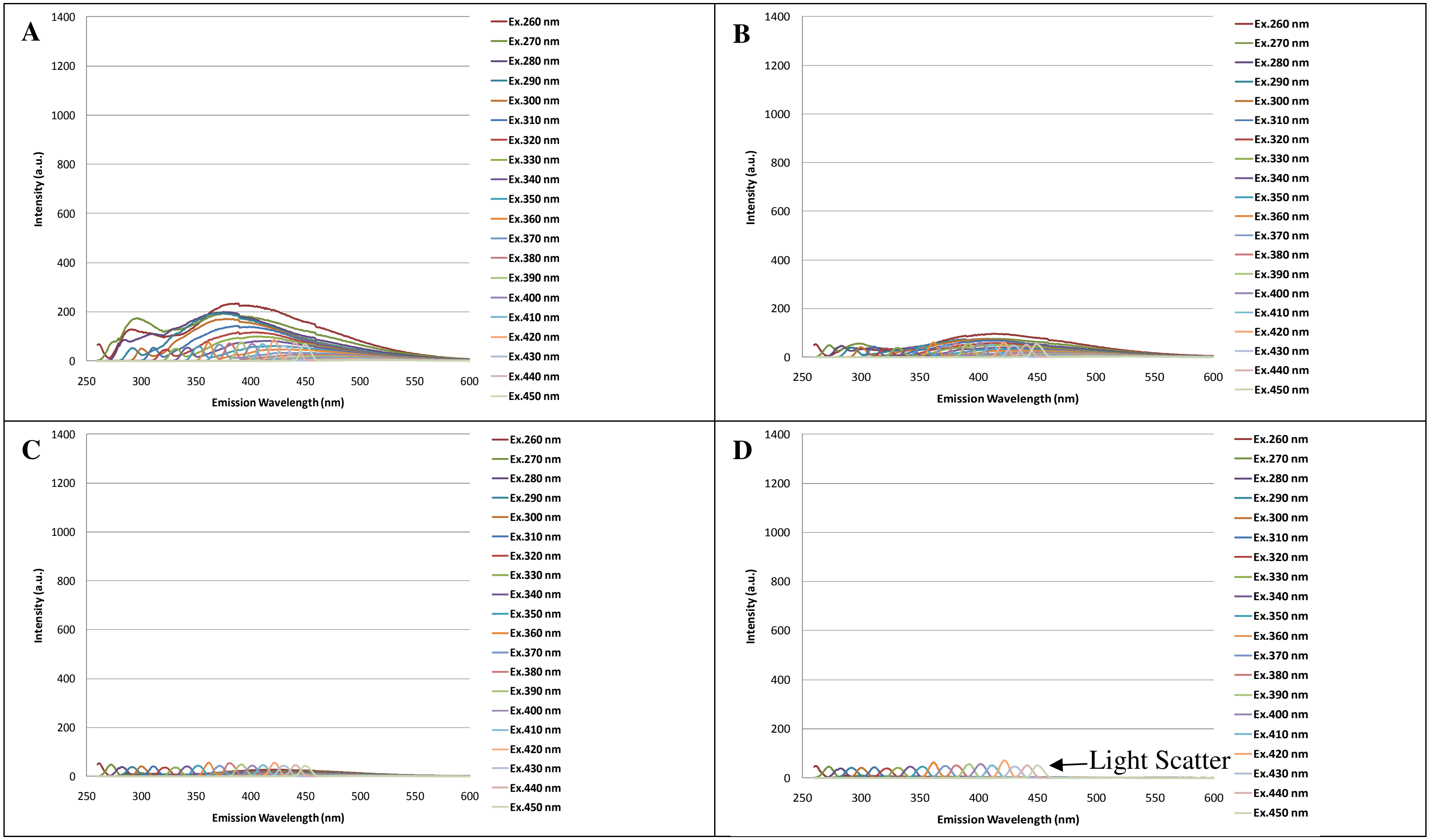

Figure F-5: Emission spectra for straight process-affected water treated with increasing weight additions of activated fluid coke; (A) 0.0625 g/L, (B) 0.125 g/L, (C) 2.5 g/L, and (D) 5 g/L.

Appendix G: FTIR Spectrometry Cell Construction and Instrument Theory

Cell Construction

The FT-IR spectrometer purchased was accompanied with a 0.1 mm KBr cell. More specifically, the lead spacer within the cell was 0.1 mm in thickness. Methodology for naphthenic acid detection specifies a path length of at least 3 mm in thickness. Consequently, the FT-IR spectrometer was unable to detect naphthenic acids within any sample tested. To trouble shoot whether the cell was appropriate for naphthenic acid detection, a concentrated sample of Sigma Aldrich derived naphthenic acids (NAs) were used in combination of dichloromethane (DCM) at 1g NA/ 6 g DCM as scanned by the instrument. At these high concentrations, irregular and unexpected peaks were observed indicating that there were direct problems with the cell. Experience has shown that the greater the path length of the sample cell, the greater the detection of peaks within a sample. More specifically, the greater path length may allow for a greater attenuation of light within a sample, permitting more changes in dipole moments (changes in vibrational and rotational status); and ultimately a greater degree of adsorption. With an increase in spacer thickness from 0.1 mm to 3 mm, an increase in naphthenic acid detection was expected.

To satisfy the path length requirement, a 3 mm variable cell was built by designing 3 mm Teflon spacers. Research proved that 3 mm spacers were not readily available on the market; spacers were created by the University of Alberta machine shop. Teflon was chosen for the spacer material instead of copper or lead because of the following reasons: (1) it is relatively non-reactive (inert); (2) it will not corrode over time; (3) it will have greater durability over time. Concerns revolved around sealing issues between the spacer and the KBr windows since an inefficient seal could lead to solvent evaporation (DCM has a high vapour pressure) leading to a change in naphthenic acid concentration within the cell. It was decided that the cell could be adequately sealed by pressure. The supplied casing of the original cell was preserved for the construction of the new cell. One KBr window was drilled with two holes to allow the solvent to reach the middle of the spacer, and the other was undrilled. The following figures outline the design of the new cell for the FT-IR spectrometer.

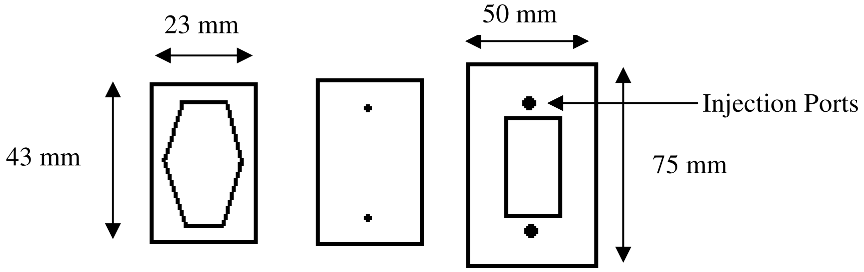

Figure G-1: Individual pieces of the cell including: Teflon spacer (left), drilled KBr window (middle), and provided metal casing from Perkin Elmer (right).

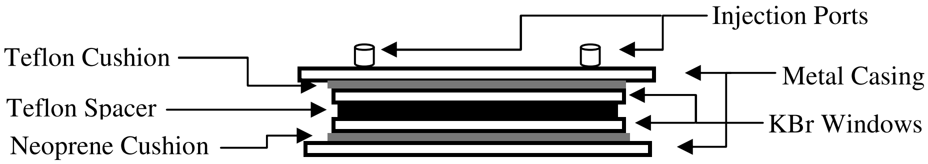

Figure G-2: Side view of the FT-IR cell showing the stacking arrangement of the different pieces.

Instrument Theory

Infrared light exists within the electromagnetic spectrum between visible light and microwaves, originating from a hot source thermal emission (Beekes et al., 2007). The infrared region can be split into three parts: near infrared, mid. infrared, and far infrared. Here, the wave numbers range from approximately 10-10 000 cm^{-1} (Beekes et al., 2007). The mid. infrared region (400- 4000 cm^{-1}) region is typically used in infrared spectrometry, as most materials respond to this range of light.

Infrared spectrometers generally provide results in terms of transmittance or absorbance. Transmittance relates the amount of measured light by a detector to the light absorbed by a material (or sample). For example, a 20% transmittance value describes that 20% of the incoming light reached the detector, and 80% of the light was absorbed by the sample. In contrast, absorbance values are a function of the transmittance and appear as an inverted transmittance spectral scan. The following formula is typically used to describe the relationship between absorption and transmittance:

$$A = \log_{10}\frac{1}{T} \qquad \textbf{(G-1)}$$

where A is the absorbance and T is the transmittance. As a result, 50% absorbance describes that 50% of the incoming infrared light was absorbed by the sample, and 50% of the incoming light reached the detector.

Fourier Transform Infrared (FT-IR) spectrometry differs from other spectrometers since it has the capacity to measure all of the wavelengths within the mid. infrared range at once. More specifically, the Fourier Transformation that occurs ‘behind the scenes’ is merely a mathematical means of extracting individual frequencies from the interferogram in order to produce a final representation of the infrared spectrum (Beekes et al., 2007). Within the FT-IR spectrometer, an infrared light source sends a beam of light to a beam splitter which directs one beam to a flat stationary mirror, and another to a flat rotating mirror. The velocity of the rotating mirror is constant and achieved through the automated monitoring of the mirror velocity with the wavelengths of the internal laser beam (IPTL, 2009). The two separated light beams are then reflected to an interferometer where they are merged and recombined; creating an interferogram (IPTL, 2009). After sample exposure, the interferogram contains the unique encoded sample information derived from each frequency in the mid. infrared light range; this information is gathered by a detector which measures the signal strength and encodes all of the sample information simultaneously (IPTL, 2009). The Fourier transform function converts the signal strength to an infrared light frequency. The FT-IR spectrometer requires an initial scan of a background solvent in order to set a baseline for the experiment. The solvent used is the solvent added to the sample during the sample runs. A beam of infrared light produces a signal which then undergoes a Fourier transformation to produce a frequency response for both the background solvent and the sample. The major peaks observed in the frequency response are typically due to the presence of water or carbon dioxide. The spectrometer then completes a point-by-point ratio between the sample and solvent to produce a plot of percent transmittance versus wavelength. This can then be converted to sample absorbance through using the absorbance/ transmittance relationship. The following Figure G-3 describes the FT-IR process, generated through experience with the equipment.

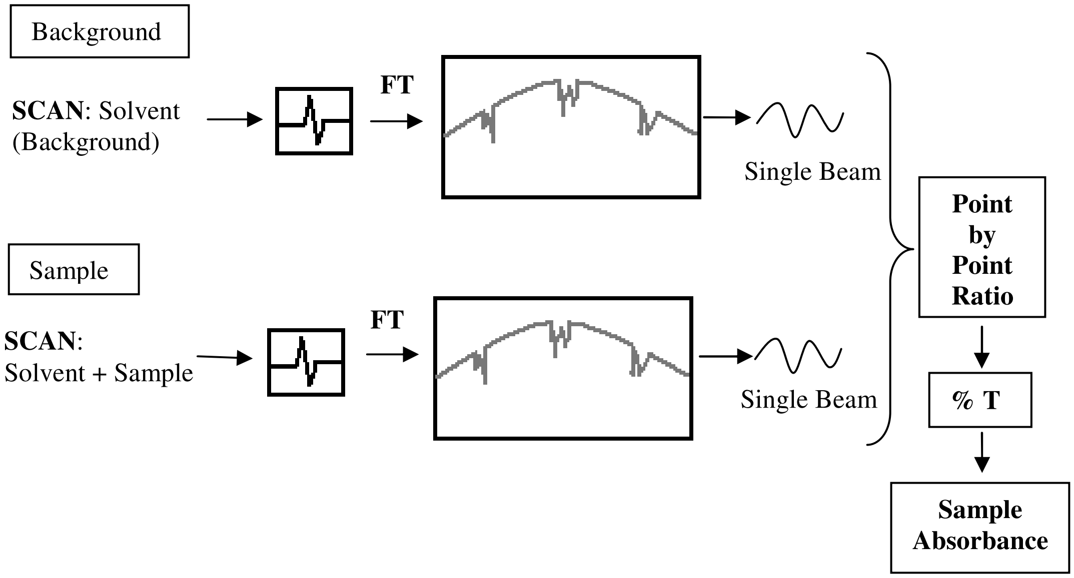

Figure G-3: Fourier Transform (FT) infrared spectrometry process.

APPENDIX G REFERENCES

Beekes, M., Lasch, P., and Naumann, D. 2007. Analytical Applications of Fourier Transform-Infrared (FT-IR) Spectroscopy in Microbiology and Prion Research. *Veterinary Microbiology*; 123: 305-319.

Intertek Plastics Technology Laboratories (IPTL). 2009. Fourier Transform Infrared Spectrometry (FTIR): How an FTIR Spectrometer Works. Available [Online]: <http://www.ptli.com/testlopedia/tests/FTIR-E168andE1252-more.asp#Spectrometer>. Accessed November 18, 2009.